AN INVESTIGATION OF THE DOUBLE VENTURI WIND TUNNEL

A THESIS

Presented to

the Faculty of the Division of Graduate Studies

Georgia Institute of Technology

In Partial Fulfillment

of the Requirements for the Degree

Master of Science in Aeronautical Engineering

by

Marvin Stockwell Mixon

December 1950

AN INVESTIGATION OF THE

DOUBLE VENTURI WIND TUNNEL

Approved:

Date Approved by Chairman Feb 6 1951

ACKNOWLEDGEMENTS

With the completion of this investigation, the author wishes to express his gratitude to Professor Alan Pope, not only for suggesting the topic, but also for his aid, guidance and constructive criticism throughout its prosecution. The author also wishes to thank Mr. W. C. Slocum for constructing several of the models used in this investigation.

PREFACE

Meaning of Symbols

A - cross-sectional area of tunnel

C_D - coefficient of drag of double Venturi, dimensionless

D - drag of double Venturi, pounds

F - temperature in degrees Fahrenheit

HP - horsepower

h - total head pressure increment, above or below atmospheric pressure, pounds per sq. foot

K_T - ratio of primary and secondary Venturi throats, dimensionless

ℓ - distance, exit of primary Venturi to throat of secondary Venturi, - upstream, + downstream, percentage of tunnel height (see page 27)

p - static pressure increment, above or below atmospheric pressure, pounds per sq. foot

q - dynamic pressure, pounds per sq. foot

R - temperature in degrees Rankine

SG - specific gravity

T - temperature, degrees

V - velocity, feet per second

δ_v - deflection of secondary Venturi

ρ - mass density, slugs per cubic foot

Superscripts

$()'$ - pressure as a column height on the manometer

Subscripts

$()_o$ - upstream of the double Venturi in the model tunnel

$()_1$ - test section, primary Venturi

$()_2$ - exit of primary Venturi

$()_3$ - throat of secondary Venturi

$()_4$ - downstream of the double Venturi in the model tunnel

$()_{at}$ - atmospheric

$()_s$ - sonic conditions

$()_{req}$ - required

TABLE OF CONTENTS

LIST OF FIGURES

AN INVESTIGATION OF THE DOUBLE VENTURI WIND TUNNEL

SUMMARY

In a thesis submitted by Alfred Ritter, titled "A Study of the Double Venturi Principle in its Application to High Speed Wind Tunnels", it was determined that this device could successfully be used to obtain a velocity increase in the neighborhood of 4 or 5 times that in the unaltered tunnel over a small part of its area. There was one objectional characteristic, however, and that was the length of the double Venturi due solely to the diffuser angle of the secondary Venturi. This investigation, intended as a continuation of Ritter's work, determines the maximum diffuser angle without excessive loss of energy due to separation. In addition, an attempt has been made to find the optimum configuration, i. e. relation of throat diameters, location of throats, shape of Venturis, etc.

The final data is presented in such a manner that the wind tunnel engineer, knowing the available horsepower for his tunnel, may calculate the additional power required for a certain increase in velocity over that in the unaltered tunnel.

INTRODUCTION

With the introduction of the new, more powerful methods of propulsion of aircraft, maximum speeds have steadily risen. The present maximum velocity for high speed military aircraft is slightly lower and, in extreme cases, slightly higher than a Mach number of unity. With this metamorphosis of aircraft characteristics, many wind tunnels have become obsolete or at the best, suitable only for limited cases.

The construction and operation of a high speed wind tunnel has been prohibitive in cost for most education institutions and research centers, which have consequently been limited in their scope of research. In view of these facts it has become increasingly desirable to obtain a high velocity, small test section wind tunnel at a comparatively low cost.

Various types and methods have been used. The blowdown and indraft principle has been used extensively. The blowdown tunnel exhausts compressed air through a properly designed test section, whereas the indraft uses a large evacuated tank to "suck" the air through the test section.[1,2] The test runs are intermittent with a duration of only 30 to 60 seconds, depending on the size of the storage tank.

---

[1]Bonney, E. Arthur, Engineering Supersonic Aerodynamics, New York: McGraw-Hill Book Co., 1950, p. 200

[2]Pope, Alan Y., Aerodynamics of Supersonic Flight, New York: Pitman Publishing Corp., 1950, pp. 107-109

The National Advisory Committee for Aeronautics at Langley Field, Virginia, successfully created high velocities by using the inductive action of compressed air exhausted through a narrow annular gap.[3] The annular nozzle was mounted aft of an eleven inch test section and compressed air (50-90 psi) was discharged on the downstream side. This high velocity, low pressure annular jet induced a uniform flow of air through the test section.

This same principle could be adapted to a system of Venturis. Two Venturis would be necessary, one of which is larger than the other. The larger plays the part of the annular nozzle. The exit cone of the smaller (primary) Venturi exhausts into the low pressure, high velocity region of the larger (secondary) Venturi. This induces an even higher velocity in the throat of the primary Venturi than would exist if it were in the air stream by itself. This combination is then placed in the test section of the wind tunnel with a consequent high velocity, small area, test section in contrast to the relatively large area, low velocity test section of the unaltered tunnel.

The increase in velocity is not obtained without payment existing in the form of an increase in power necessary

---

[3] Stack, John, "The NACA High Speed Wind Tunnel and Tests of Six Propeller Sections", National Advisory Committee for Aeronautics Technical Report No. 463, 1933

to drive the air through the tunnel. This increase in power is due to three types of drag: form, skin friction, and separation. Hunsaker and Rightmire[4] state that the losses due to separation are a minimum when the total included angle of divergence of the diffuser is between 6 and 9 degrees. However, this is for the single Venturi. With the low pressure region created by the secondary Venturi at the exit cone of the primary Venturi, somewhat higher divergent angles may be used in both.

In order to determine the optimum configuration as accurately as possible, a model of the double Venturi arrangement was desirable whose Venturis were easy to construct and simple to arrange in various combinations. A two-dimensional model tunnel was decided upon. The Venturis were nothing more than two short span airfoils placed opposite each other so as to form a converging and diverging passage. The data from this model could not be applied to the full-scale Venturi tunnel, but it would give an accurate indication of what to expect from the three-dimensional arrangement. In order to reproduce the full-scale Venturi tunnel an 8 inch duct was used with the three-dimensional double Venturi system placed inside. Results taken from the

---

[4] Hunsaker, J. C., and Rightmire, B. G., Engineering Applications of Fluid Mechanics, McGraw-Hill Book Company, New York, p. 151, 1947

two-dimensional tunnel were used to design Venturis for the three-dimensional tunnel. Both tunnels used the Georgia Tech 2-1/2 foot wind tunnel as a source of power.

APPARATUS

The two-dimensional model tunnel was constructed of wood in such a manner that a 3.2 inch by 8.45 inch channel was formed. In order to facilitate the changing of configurations of the double Venturi arrangement, a one-eighth inch plexiglass cover was attached to the legs of the channel with six bolts. The plexiglass cover also permitted tuft studies to be made of the different configurations, with the idea in mind of determining the type of flow of the air around the double Venturi.

The two-dimensional double Venturis were constructed of mahogany from aluminum templates. Essentially, they were two airfoil sections with a span of 3.2 inches placed in the model tunnel with their cambered surfaces facing each other. In order to insure the two sections of each Venturi being exactly alike, one section was constructed 6.4 inches in span and then cut in half to form the necessary two sections.

A nomenclature system was necessary so that each Venturi was readily distinguishable from the others. From a single designation a Venturi of any size may be constructed with the same proportions as the models tested in the model tunnel. An example is P-38-4.7-5.9-12. The letter P indicates that this particular section was used in the primary

Venturi. The first set of numerals (38) indicates the length of the chord of the Venturi section expressed as a percentage of the tunnel height. The second set (4.7) expresses the maximum thickness as a percentage of tunnel height, and the third set (5.9), the location of maximum thickness behind the leading edge of the Venturi section, again as a percentage of the tunnel height. The final number indicates the divergence angle for the Venturi section expressed in degrees. It should be noted that the divergence angle for a Venturi section is one-half the total diffuser angle for the assembled Venturi. If the designation is followed by the letter M (modified), the Venturi section also has a divergence on the outside surface (the surface not in the contracting, diverging passage). For all Venturi sections this value was 5^{o}. A summary of the two dimensional nomenclature system is presented below:

S-115-30.8-20.1-12-M

S - section used in the secondary Venturi

115 - length of chord of section, per cent of tunnel height

30.8 - maximum thickness, per cent of tunnel height

20.1 - location of maximum thickness behind the leading edge of the section, per cent of tunnel height

12 - divergence angle, degrees

M - modified section, outside divergence angle = 5^{o}

In addition to the Venturi sections designated by the above nomenclature system, various combinations employing a primary and secondary Venturi composed of thin, highly cambered sections were investigated. The results using these sections were poor; consequently no further investigation was made with these sections. The secondary Venturi was composed of sections having 3% camber, 3.6% thickness and a chord of 37%. The primary Venturi sections were 3.6% thick, had a camber of 3% and a chord of 48%. These sections will hereafter be referred to simply as "thin sections".

The three-dimensional Venturis, being circular in shape, were constructed in a much different and more difficult manner. Again they were constructed of mahogany (laminated), but turned on a lathe to the dimensions specified. The nomenclature system was somewhat simpler than that used with the two-dimensional Venturis. Since each Venturi could obviously have only one throat diameter, this dimension fixed the maximum thickness of the section used, holding the outside diameter constant. Also only one divergence angle was possible with each Venturi. Consequently, by giving the throat diameter, divergence angle, outside diameter, and stating whether or not the section employs the divergence on the outside of the Venturi (as indicated by "modified", two-dimensional Venturi), a three-dimensional Venturi may be reproduced with the same proportions as the model.

An example follows:

P-22-45-7-M5

P - Venturi used in the primary position

22 - throat diameter, per cent of tunnel diameter

45 - maximum outside diameter, per cent of tunnel diameter

7 - divergence angle

M5 - "modified", 5° outside divergence

The Venturis, both two and three-dimensional, were finished with four to six coats of clear lacquer to insure a smooth surface.

At this point, some attention should be directed to each part or portion peculiar to every Venturi. The Venturi consists of an entrance, throat and diffuser, with each demanding special consideration. The entrance increases the velocity of the air stream to a value somewhat higher than that before entering the Venturi. It performs with the highest efficiency when the velocity is increased uniformly with a corresponding uniform drop in static pressure. This process is often referred to as monotonic. If the velocity does not increase monotonically, an adverse pressure gradient is created, thereby causing separation in the boundary layer. The question now arises as to what shape entrance

will yield this type flow. M. S. Kisenko of the Central-Hydrodynamical Institute at Moscow, U.S.S.R., states[5]:

> "The only requirement for this part of the nozzle (entrance) is that it should be carefully rounded and that it should assure a smooth flow of gases. The smoothing curve is chosen on an intuitive basis."

His investigations were carried out at supersonic as well as subsonic velocities. Hsue-Shen Tsien[6], of the California Institute of Technology, has published a paper giving a method to design an entrance section with a monotonic velocity increase. Richard Smith and Chi-Teh Wang[7] in another paper have devised a design to give a uniform throat speed. The choice of designs would depend upon the velocities encountered and the device in which the entrance section is to be employed. In the case of the model Venturis, only low subsonic velocities were encountered; consequently Kisenko's advice was followed. However, in the full scale tunnel very high subsonic and low

---

[5]Kisenko, M. S., "Comparative Results of Tests on Several Different Types of Nozzles", National Advisory Committee for Aeronautics Technical Memorandum No. 1066, 1944, pp. 1,10

[6]Tsien, Hsue-Shen, "On the Design of the Contraction Cone for a Wind Tunnel", Journal of the Aeronautical Sciences, Vol. 10, February, 1943, pp. 68-70

[7]Smith, Richard H. and Chi-Teh Wang, "Contracting Cones Giving Uniform Throat Speeds", Journal of Aeronautical Sciences, October, 1944, p. 356

supersonic velocities could be encountered; thus one of the other more accurate designs should be applied.

The throats of the primary and secondary Venturis were treated separately. In the primary Venturi the throat or straight portion was the test section and was arbitrarily chosen to be the length of the diameter of the throat. Alfred Ritter[8] in his thesis investigated the Venturi tunnel employing a secondary Venturi with a straight portion. His opinion was that this portion offered an opportunity for the air stream leaving the primary Venturi to mix with that entering the secondary Venturi before the process of diffusion was begun. This portion increased the length of the tunnel, and in addition there is some doubt as to the necessity of the mixing of the two air streams before diffusion, other than that which is accomplished with a plain throat. On this basis this portion of the secondary Venturi was omitted.

The diffuser is perhaps the most difficult part to analyze, for if it is not correctly designed, a serious loss in energy will result, thereby increasing the amount of power required to drive the air through the tunnel. The diffuser of the Venturi transforms the dynamic pressure gained by increased velocity in the throat back to the static pressure of the free stream at the exit of the Venturi. The original

---

[8]Ritter, Alfred, A Study of the Double Venturi Principle in its Application to High Speed Wind Tunnels. Unpublished master's thesis, Georgia Institute of Technology, 1947

static pressure of the air stream before entering the Venturi cannot be entirely regained as a result of some of the kinetic energy being dissipated into unavailable thermal energy due to the viscosity of the air. Part of this thermal energy is a result of the friction between the wall of the diffuser and the air. The majority, however, is due to the boundary layer separating from the wall creating vortices or eddies. The magnitude of these vortices is proportional to the angle of divergence. Tests have been carried out by Gibson[9] on conic diffusers, with the results expressed as a proportion of the loss by

$$h_L = K_L \frac{(V_1 - V_2)^2}{2g}$$

where K_L is primarily dependent upon the divergent angle, but is also a function of the area ratio. He determined that the combined effects of friction and vortices were a minimum with a total diffuser angle of 7° (divergent angle, 3.5°). However, Vedernikoff[10], at the Central Aero-Hydrodynamical Institute, through investigations with a flat broadening channel, concluded that these losses were a minimum when the total diffuser angle was 14° (divergent angle, 7°). He

---

[9] Gibson, A. H., Hydraulics and Its Application, Fourth Edition, New York: D. Van Nostrand Co., 1930, p. 93

[10] Vedernikoff, A. N., An Experimental Investigation of the Flow of Air in a Flat Broadening Channel, National Advisory Committee for Aeronautics Technical Memorandum No. 1059, 1944

expressed the quality X of the diffuser by a ratio

$$X = \frac{V_1^2}{2g} \div (1 + \delta_2)\frac{V_2^2}{2g}$$

where δ_2 is the loss coefficient in the diffuser. Then 1/X is the total loss, and a plot of this curve indicates a minimum at 14°. The difference between these two investigations lies in the fact that Gibson's experiments were conducted with conical diffusers and Vedernikoff's investigation was with a flat, rectangular-sectioned diffuser. If the diffuser in the tunnel is conic, then Gibson's results should be used. For the rectangular diffuser, Vedernikoff's analysis is recommended.

In order to reproduce the conditions existing in a full scale tunnel, an 8 inch duct, 36 inches in length, was mounted in the jet of the Georgia Tech small wind tunnel. Within this duct, the three-dimensional model Venturi tunnels were placed and data was recorded from various pressure measuring instruments.

In both the two and three-dimensional model tunnels, total head tubes were placed near the exit. For the two-dimensional tunnel, 8 tubes were spaced 1 inch apart. The three-dimensional tunnel had 7 tubes placed 1 inch apart. Close to the entrance of the model tunnels was installed a pitot-static tube which could be raised or lowered, effectively surveying the section of the tunnel ahead of the double Venturi. Located in the geometric center of the

test section in the primary Venturi was a static pressure orifice flush with the surface.

All pressures were measured with conventional manometers. For the pitot-static tube a micro-manometer was employed. A multiple tube manometer measured the total head pressures behind the double Venturi. Due to the low pressures encountered in the test section, a glass tube was mounted on a meter stick and placed on a base. The reservoir for a micro-manometer served the same purpose for this manometer. The arrangement was satisfactory for the purpose for which it was intended.

As was stated before, the Georgia Tech small wind tunnel was the source of power to drive the air through the Venturi tunnel.

PROCEDURE

Investigations of double Venturi arrangements were conducted in two and three-dimensional model tunnels. Since both tunnels were similar and all measurements were taken in the same manner using the same instruments, a general description of the procedure will be given at this time. It should be understood that it applies to investigations conducted in both tunnels.

With each specific configuration, the final information was to include the velocity in the model tunnel ahead of the double Venturi, the velocity in the test section of

the primary Venturi, and the total drag of the double Venturi. This data was to be presented in such a manner that a wind tunnel engineer could, for a given velocity increase, readily determine the power increase required for his tunnel. Dimensionless coefficients appeared to be the most convenient solution.

With the aid of the pitot-static tube ahead of the double Venturi, it was no trouble to determine the velocity at that point. The micro-manometer was used to record the pressure in millimeters of alcohol. The velocity in the test section was, however, not so simple a matter. It would have been desirable to place a pitot-static tube in the test section, but it was feared that this object, when placed within the small passage of the test section, would have a choking effect. The next best solution was followed. An assumption was made that the losses in the entrance of the primary Venturi were small and could be neglected. Using Bernoulli's theorem and this assumption, the velocity in the test section could be determined. A derivation of Bernoulli's theorem as applied in this case, is presented in the Appendix.

The velocities encountered were low; consequently the mass density of the air was assumed to be approximately constant throughout the model tunnel. Specifically, the total head pressure ahead of the double Venturi and the

static pressure in the test section were necessary to compute the velocity within the test section. To determine the first of these items (total head pressure ahead of the double Venturi), the static pressure tube was disconnected from the pitot-static tube. This pressure was then recorded on the micro-manometer in millimeters of alcohol. From the orifice flush with the surface in the test section, the static pressure was recorded on the manometer, which was constructed of a glass tube attached to a meter stick. The pressure was then measured in centimeters of alcohol.

To determine the total drag of the double Venturi, a total head integration across sections of the tunnel both ahead of and behind the double Venturi was necessary. To obtain the integration across the section ahead of the double Venturi, the pitot-static tube was used with only the total head pressure lead connected. It should be recalled that the tunnel was constructed allowing the pitot-static tube to be raised or lowered through the height of the tunnel. However, it was found that the total head across this section of the tunnel varied only 2% even for the most adverse configurations. The pitot-static tube was then set $\frac{1}{2}$ inch below the top of the tunnel and the value recorded on the micro-manometer was then taken as constant across the tunnel section. The total head tubes spaced 1 inch apart across the tunnel section behind the double Venturi were used to

determine the total head integration at this section of the model tunnel. The pressures from these tubes were recorded on a multiple manometer in inches of alcohol.

To be reasonably sure that the flow in the model tunnels was not excessively turbulent or irregular, several dynamic pressure surveys were made at different sections of the tunnel without the double Venturi installed. One such survey was conducted approximately 4 inches behind the entrance of the model tunnel with the pitot-static tube located at this point. Measurements were taken on both center lines of the tunnel cross section at every inch. The pressures, as measured on the micro-manometer, varied only 2% at the most. A similar survey was conducted in the section of the tunnel 4 inches from the exit. The pressures in this section of the tunnel similarly varied only a small amount, but were somewhat higher. Due to the growth of the boundary layer towards the exit of the tunnel, the effective area became smaller, and by the law of continuity, it can easily be surmised that the velocity at this point would be higher.

In order to reduce the number of variables involved, the Venturi models were investigated for only one size of test section. The two-dimensional models all had a test section of 10 to 1, i. e. 1/10 of the model tunnel height (0.845 inches). The three-dimensional models had a test section 4.55 to 1 or 1/4.55 of the model tunnel height (1.76 inches).

RESULTS AND DISCUSSION

It is a well known fact that a low pressure region exists in the vicinity of the maximum thickness of an airfoil section. As the angle of attack relative to the air stream is increased, the velocity increases (static pressure decreases) in this region.

At this point it should be remembered that the purpose of the secondary Venturi is to create a low pressure, high velocity region into which the primary Venturi may exhaust. In a conventional Venturi this region is created simply by contracting a passage; thus, by the law of continuity, a decrease in area through which the stream passes is accompanied by an increase in velocity. Since a two-dimensional Venturi is composed of two sections resembling airfoil sections, an additional gain in velocity could be obtained by installing the sections of the secondary Venturi so that the angle of attack (deflection angle) could be varied. As the deflection angle is increased, the total drag is also increased due to the increase in separation within the diffuser.

Investigations were initiated using the sections P-38-4.7-5.9-12, S-49-6.5-11.2-div. angle. The position of the secondary Venturi was moved about in an attempt to determine the optimum configuration, i. e., highest velocity increase for the lowest drag.

Final results using these sections are presented in Figures 7, 8 and 9. Plots of the total head pressures against tunnel station are shown in Figures 16 through 35. Extensive tuft studies were made with both Venturis. With the aid of these studies and analysis of the total head pressure plots, it was decided that the total drag at a divergence angle of 12° was the result of separation in both Venturis, in addition to the always present skin friction and diffusion losses. The coefficient of drag, C_D, hovered around 0.21 for all configurations except $K_T = 2.5$ and $\ell = 0\%$. The tuft studies indicated that an insufficient quantity of air was passing through the slot between the primary and secondary Venturi. This had the effect of stalling the secondary Venturi sections. Figure 24 clearly demonstrates this point.

As the divergence angle is increased, separation becomes predominant and the total drag increases rapidly. Figure 7 is a plot of the coefficient of drag vs. divergence angle. The curves in this figure were plotted from data obtained from each configuration, i. e., ratio of throats, K_T, and location of primary Venturi, ℓ. Attention should be directed to the similarity between these curves and the parabolic shape of corresponding curves for airfoil sections. This figure also brings out the fact that a benefit was realized from the high velocity region of the secondary Venturi section close to the leading edge. The drag curves are

parabolic up to a divergence angle of 14.5° to 17°. However, at this point there is a distinct leveling off due to the velocity increasing and moving forward. Figure 8 is a plot of velocity ratio, V_R, against the same abcissa as Figure 7. Again there is a distinct leveling off, but it is not as pronounced as in the drag curves. The ordinates in Figures 7 and 8 are plotted against each other in Figure 9. The curves of the latter figure would be most useful to the wind tunnel engineer. Since he would know the additional power available at any velocity in the unaltered tunnel test section, the maximum value of C_D could be easily calculated. Then from Figure 9, the maximum velocity increase could be determined for each configuration. From either Figure 7 or 8, the divergence angle could be found for the corresponding configuration. For an example, assume that the engineer has determined the maximum C_D to be 0.35 for a velocity of 200 mph, then from Figure 9, a maximum velocity ratio of 2.53 corresponds to $C_D = 0.35$. The configuration is $K_T = 2.5$ and $\ell = 7.7\%$. From Figure 7, for $C_D = 0.35$ and the configuration as found above, the divergence angle is 16.6°. A velocity in the test section of 2.53 x 200 = 560 mph. could be expected.

The fact having been definitely established that the circulation about a Venturi section could be used to an advantage, it was decided to investigate sections known to possess circulation of greater magnitude than that of the previous sections. Highly cambered airfoils have this quality, but are

also accompanied by increased drag. In order to offset the latter characteristic, a thin section was employed. The results, however, did not materialize as anticipated. Figures 36 through 41 are plots of the total head pressures. Tuft studies indicated that separation had begun in the diffuser of the primary Venturi for values of the deflection angle greater than 0°. As the deflection angle was increased the drag rose sharply. For deflection angles above 2.5°, the drag was very high and the flow unstable as a result of vortices created in the primary Venturi. Reliable data could not be gathered under these conditions; consequently, it was deemed inadvisable to attempt to present data similar to Figures 7, 8 and 9 for these sections.

Up to this point the sections P-38-4.7-5.9-12, S-49-6.5-11.2-12 had given the best results. In an attempt to reduce the losses due to separation, the diffuser angle of the primary Venturi was reduced to 14° (divergence angle for each section 7°). The problem that confronted Ritter, i. e., the prohibitive length of the double Venturi, was now becoming evident in this investigation. In order to shorten the length, yet still incorporate a small divergence angle, a similar divergence was placed on the outside of each section. With the velocity increasing over the outside of the primary Venturi due to the effect of the secondary Venturi, no adverse pressure gradient could develop. A primary Venturi

composed of sections with these characteristics (P-40-5.6-5.9-7-M) was constructed and investigated with the secondary Venturi used in previous experiments (S-49-6.5-11.2-12). The modified primary Venturi had approximately the same dimensions as the previous one; consequently, the data from the two could be compared and the advantage, if any, of this section could be determined. Figures 42 through 45 are plots of the total head pressures. Analysis of these figures indicated that the diffusion losses had been reduced as noted by the increased total head pressures in the center of the tunnel. The velocity ratios were also increased appreciably (approximately 15% over the unmodified section). Tufts were placed on the outside surfaces of the modified section in order to determine the type of flow over this portion. As was anticipated, no separation was involved.

Since the total drag had been reduced by reducing the diffuser angle of the primary Venturi, it was felt that a similar reduction would result from a smaller diffuser angle in the secondary Venturi. Again the problem of excessive length was encountered. To reduce this dimension, a divergence was also placed on the outside of the Venturi. The section S-76-11.4-17.8-7-M was constructed with these characteristics and investigated with the modified primary Venturi P-40-5.6-5.9-7-M. From the plot of total head pressures, Figure 46, it is noticed that the drag has again been reduced. However, the tufts on the outside surface of the

secondary Venturi indicated that some separation was occuring, i. e., the 5° divergence angle resulted in too rapid an expansion.

Two points should be stressed at this time: (1) an advantage is gained from the circulation about a Venturi section at the higher deflection angles, but it is also accompanied by a rapidly increasing drag due to separation, (2) the modified section gives less drag due to separation as a result of smaller diffuser angles.

From the results of investigations with the previous Venturis, it appeared necessary to increase the contraction ratio in order to obtain higher velocity ratios. Sections were constructed for new Venturis with greater thickness and the same characteristics of the modified sections (P-76-11.4-17.8-7-M, S-115-30.8-20.1-7-M). Investigations with these sections were rather extensive and included a determination of the effects of varying the secondary throat height, enlarging the diffuser angle from 14 to 24 degrees and varying the position of the primary Venturi horizontally. The results are plotted in Figures 10 through 12 and 47 through 64. Analysis of the total head pressure plots indicated that for a narrow slot between the primary and secondary Venturis, (small K_T), insufficient air is allowed to pass and the separation from both diffusers is bad, as shown in Figures 47, 48, 53, etc. As the diffuser angle is increased from 14 to 19 degrees, the drag, hence the separation,

remains fairly constant, but upon increasing the angle further, the drag increases rather rapidly (Figure 10). To the contrary, (Figure 11), as the diffuser angle is increased from 14 to 18 degrees, the velocity ratio decreases, but increases beyond this point. Figure 12 is a plot of C_D versus V_R and would be of most value to the tunnel engineer. Figures 10, 11 and 12 are similar to 7, 8 and 9 and could be used in a similar manner. An interesting development noticed in Figure 12 is that at 7° divergence, (14° diffuser angle), a value of l = 6% gave the best results. As the divergence angle was increased, however, the best value of l became smaller.

During the early stages of this investigation, it was felt that Venturis composed of thin, highly cambered sections would yield satisfactory, if not superior results; consequently, construction was begun on three-dimensional Venturis employing this type of section. After investigations with the two-dimensional models, however, it became evident that this section would produce disappointing results. Construction had progressed so far that it was decided to complete them. Investigations, however, confirmed suspicions that the three-dimensional models would produce no better results than the two-dimensional Venturis. Separation, was so extensive that it was difficult to collect data. Pressures on all manometers fluctuated profusely. Since the accuracy of the data collected from these Venturis

was questionable, the results of these experiments are not presented.

As was stated previously, the results obtained with the two-dimensional models would be used to design the three-dimensional models. Figures 7, 8, and 9 could be used to design Venturis to yield a velocity ratio between 2.5 and 3.0. For higher values figures 10, 11, and 12 must be used.

In the design of a three-dimensional double Venturi, the contraction ratio, throat diameter ratio, and the diffuser angle are the most important parameters. Obviously, the largest contraction ratio possible is desirable without the overall length becoming excessive. From figure 12, the lowest drag occurs at a velocity ratio of approximately 3.58, the configuration being $K_T = 3.5$ and $\ell = 3.5\%$. From figure 11, for a velocity ratio of 3.58, the divergence angle for the section was 10.15°. The primary Venturi in all instances employed a diffuser angle of 14°. From this information and the knowledge that a 5° outside divergence on the secondary Venturi was excessive, the three-dimensional double Venturi was designed. When the new Venturis were completed (P-22-45-7-M5, S-37.5-75-10-M3), the only parameter that could be varied was the position of the primary Venturi relative to the secondary. Figures 65 through 69 present the total head pressure vs. tunnel diameter, and figures 13, 14, and 15 are plots of the dimensionless coefficients C_D and V_R against ℓ.

Analysis of the total pressure plots indicates that there was no separation in the diffuser of the primary Venturi. To determine the amount of total drag due to separation in the secondary Venturi, the drag due to skin friction was calculated from formulae and charts presented by Binder[12]. To be on the conservative side, skin friction coefficients for turbulent flow were chosen. Average velocities over each surface of both Venturis were used in calculating Reynolds Number. The final figure indicated that approximately 40% of the total drag was due to skin friction.

The results of the previous experiments have been presented without regard to the effects of Reynolds Number or compressibility. The effects of compressibility have been neglected due to the low velocities encountered (from 50 mph to 220 mph). Within this range this assumption is valid; however, in the full scale tunnel the velocities may approach a Mach number of unity. Its effect on the drag of the system will be negligible, but it is hard to predict what the effect on the velocity ratio would be.

In order for the data from a model to be accurately applied to the full scale object, the flow about both must be dynamically similar. The criterion for this situation is Reynolds Number, which is a ratio of the mass forces to the

---

[12] Binder, R. C., Fluid Mechanics, New York: Prentice-Hall, Inc., 1943, pp. 138, 139.

viscous forces. At low Reynolds Number the viscous forces are predominate, and at high Reynolds Number, the mass forces. From this discussion it can be seen that Reynolds Number would have only a small effect on the velocity ratio, but a large effect on the total drag. Jacobs and Sherman[13] made an extensive investigation in the NACA Variable Density Wind Tunnel on airfoil sections with the view in mind of determining the effects of this criterion on the different performance parameters. Using the values of Reynolds Number for the models (100,000) and the full scale Venturi (4,000,000), the drag for various airfoil sections as presented by Jacobs and Sherman was reduced 50% to 65%. No indication was given as to the extent of separation. The drag caused by this factor is not as severely affected by an increase in Reynolds Number as skin friction drag. A reasonable assumption would then be that the skin friction drag, as calculated by suitable formulae, is reduced 60% and the remaining drag (separation and diffusion) is reduced 20%.

---

[13] Jacobs, E. N., and A. Sherman, "Airfoil Section Characteristics as Affected by Variation of the Reynolds Number," National Advisory Committee for Aeronautics Technical Report No. 586, 1936.

THEORY

With the large number of variables involved in a double Venturi system, it would be difficult to present a complete analytical analysis of the system. To reduce this number of variables, several phases of the process may be isolated.

The engineer interested in the double Venturi wind tunnel would know the velocity increase desired. Starting at the test section, the volume through the test section is A_1V_1, and that at the exit of the primary Venturi is

$$V_2 = \frac{A_1}{A_2} V_1 \qquad (1)$$

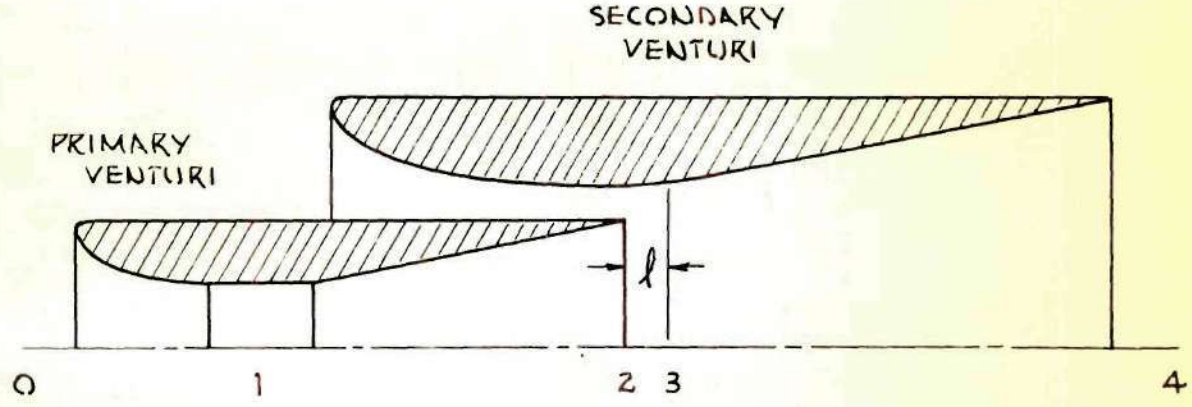

The loss through the primary Venturi appears at the exit of the primary Venturi as a drop in static pressure,

i.e. the static pressure recovery at the exit is somewhat lower than that expected if there were no losses. In order for the primary Venturi to produce the required velocity increase, the secondary Venturi must produce a drop in static pressure equal to the total losses through the primary Venturi. This is accomplished by an increase in velocity.

The losses in the entrance and test section have been considered negligible. The losses in the diffuser, if there is no separation, are found from[14],

$$\Delta p = q_1 \left[\frac{\lambda}{8 \tan \frac{\alpha}{2}} + 0.6 \tan \frac{\alpha}{2} \right] \left[1 - \frac{D_1^4}{D_2^4} \right] \qquad (3)$$

where,

Δp = drop in static pressure

q_1 = dynamic pressure in the test section

α = total diffuser angle

D_1 = diameter of test section

D_2 = diameter of exit

λ = skin friction coefficient.

Using Bernoulli's Theorem, the pressure necessary at the exit to produce the required velocity increase is,

---

14 Pope, Alan Y., Wind Tunnel Testing, New York: John Wiley and Sons, Inc., 1947, pp. 62-67

$$P_1 + \frac{\rho}{2} V_1^2 = P_2 + \frac{\rho}{2} V_2^2 + \text{LOSSES}$$

$$(P_{at} + P_1) + \frac{\rho}{2} V_1^2 = (P_{at} + P_2) + \frac{\rho}{2} V_2^2 + \Delta P$$

$$P_2 = -\Delta P + P_1 - \frac{\rho}{2} (V_2^2 - V_1^2) \qquad (4)$$

Since p_2 is the pressure necessary at the exit, then it is also the pressure that the secondary Venturi must produce; therefore

$$P_2 = P_3 .$$

Assuming no losses in the entrance of the secondary Venturi,

$$(P_{at} + P_o) + \frac{\rho}{2} V_o^2 = (P_{at} + P_3) + \frac{\rho}{2} V_3^2 ,$$

but since

$$(P_{at} + P_o) + \frac{\rho}{2} V_o^2 = (P_{at} + h_o)$$

$$(P_{at} + P_3) + \frac{\rho}{2} V_3^2 = (P_{at} + h_o)$$

$$V_3 = \sqrt{\frac{2 (h_o - P_3)}{\rho}} \qquad (5)$$

and substituting $p_2 = p_3$, and equation (4),

$$V_3 = \sqrt{\frac{2 [h_o + \Delta P - P_1 + \rho/2 (V_2^2 - V_1^2)]}{\rho}}$$

$$= \sqrt{\frac{2 (h_o - P_1) + \rho (V_2^2 - V_1^2) + 2\Delta P}{\rho}} \qquad . \quad (6)$$

The velocity V_3 is composed of several components which makes it a rather complex quantity to compute. The blocking effect, i.e. the constriction of area through which the air stream may pass, produces an increase. The secondary Venturi section resembles an airfoil section; consequently circulation has a sizeable effect. The vortex (circulation) center of the primary Venturi sections is located a relatively large distance from the point in question; therefore its effect may be neglected. The velocity at the minimum section of the secondary Venturi is then,

$$V_3 = \frac{V_a A}{A - A_B} + V_\Gamma \quad , \qquad (7)$$

where

A_B = blocking area of secondary Venturi

V_Γ = induced velocity resulting from circulation about the secondary Venturi section.

The quantity V_Γ is a function of the dimensions of the Venturi system,

$$V_\Gamma = K\Gamma \quad . \qquad (8)$$

The circulation Γ may be found using the expression

$$\Gamma = \frac{c\, C_\ell\, (V_a + V_B)}{2} \qquad (9)$$

where

c = chord of the section

C_ℓ = section lift coefficient

V_s = velocity due to blocking alone.

The lift coefficient C_ℓ may be evaluated by thin airfoil theory and assuming the slope of the lift curve to be 2π. This last assumption of course is not entirely correct and the amount of error will have to be determined by further investigations.

The factor K must be evaluated by use of the Biot-Savart law, i.e. the induced velocity due to a line vortex is,

$$V_r = \frac{\Gamma}{4\pi h}\left(\cos\theta_1 + \cos\theta_2\right) . \qquad (10)$$

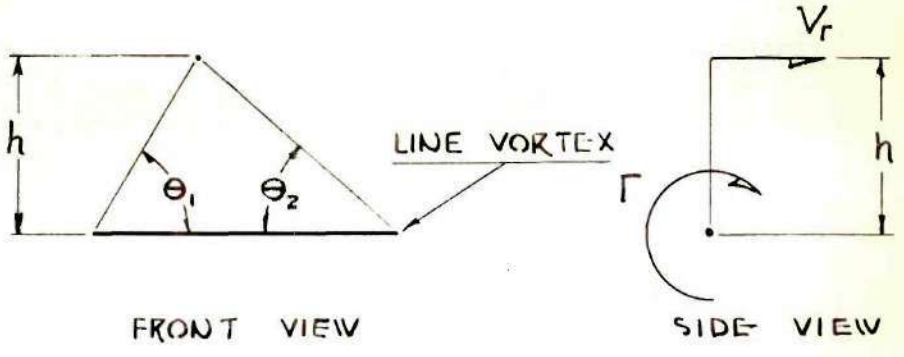

Therefore the quantity K is,

$$K = \frac{1}{4\pi h}\left(\cos\theta_1 + \cos\theta_2\right) . \qquad (11)$$

The method of computing K is different for the two and three dimensional cases. An explanation of each follows.

Two Dimensions

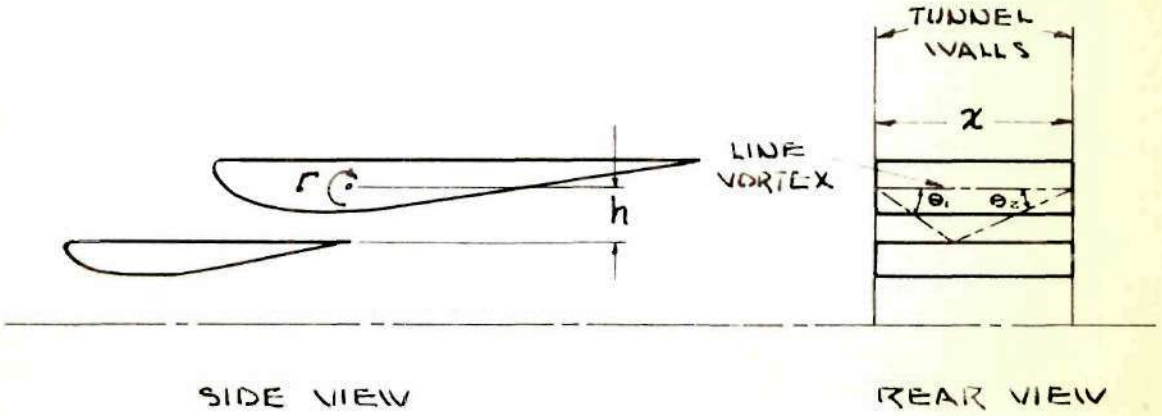

SIDE VIEW REAR VIEW

The vortex center is placed at the point of maximum thickness which is approximately the quarter chord point. The point in question is located at the exit of the primary Venturi. It can be seen that K will vary across χ. The maximum value will occur at the center and and the mimimum will be at the walls. An average of the two values is a reasonable solution.

Three Dimensions

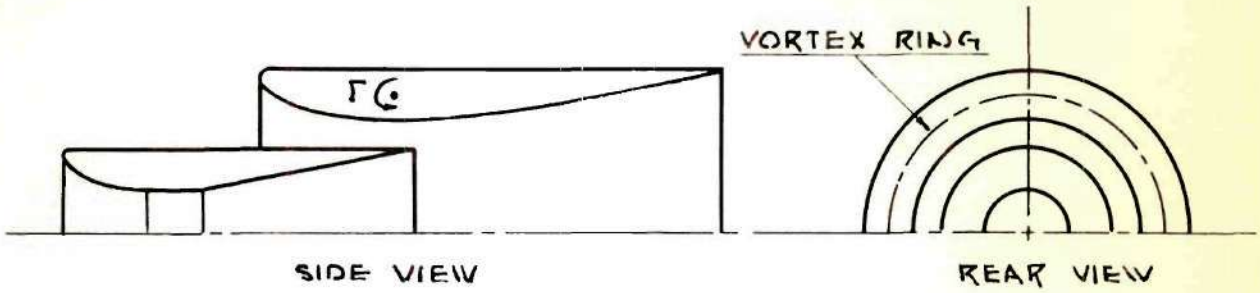

The exact solution for the effect of a vortex ring is complicated and arduous in solution. An approximate solution is to replace the vortex ring with a series of vortex lines. The greater number of vortex lines, the greater will be the accuracy of the answer. A hexagon will suffice in our case.

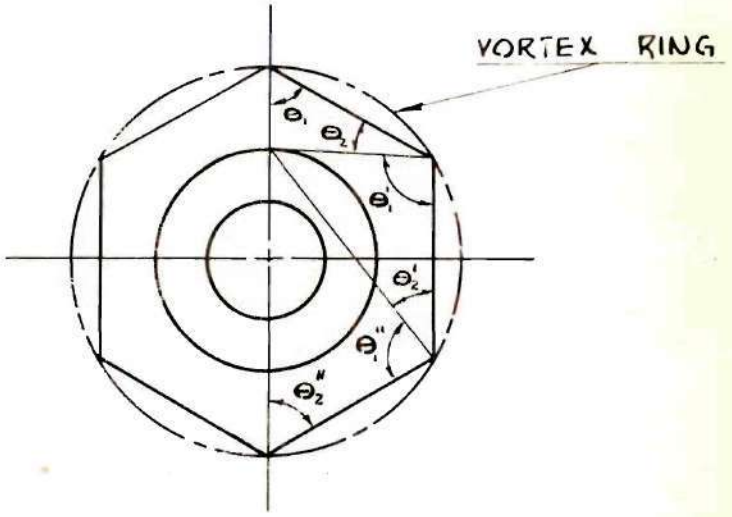

The effect of each segment of the hexagon may be found by use of the Biot-Savart law. The effect of the

hexagon is then the sum of the effects of the segments. The total effect at only one point need be found as it is the same at any point on any one circle.

For clarification of the analysis, an example is presented and compared with data taken from the three dimensional model double Venturi.

Primary Venturi

The various physical and air stream characteristics associated with the primary Venturi are:

4 = contraction ratio

14° = diffuser angle, α

.0135 = skin friction coefficient, λ

77.9 = free stream velocity, V_o , ft./sec.

.0717 = area of entrance, A_o, sq. ft.

.0169 = area of test section, A_1 , sq. ft.

.0341 = area of exit, A_2 , sq. ft.

2.79 = static pressure at entrance, above atmospheric pressure, p_o , #/sq. ft.

9.45 = free stream total head pressure, above atmospheric pressure, h_o , #/sq. ft.

The desired velocity in the test section is,

$$V_1 = 329.0 \text{ FT/sec} .$$

From equation (2), the velocity at the exit of the primary Venturi is,

$$V_2 = \frac{A_1 V_1}{A_2} = \frac{(0.0169)(329.0)}{(0.0341)}$$

$$= 163.0 \text{ FT./SEC.} \quad .$$

The losses in the diffuser are, from equation (3),

$$\Delta p = q_1 \left[\frac{\lambda}{8 \tan \frac{\alpha}{2}} + 0.6 \tan \frac{\alpha}{2}\right]\left[1 - \frac{D_1^4}{D_2^4}\right]$$

$$= 7.94 \text{ LB./SQ. FT.} \quad .$$

The pressure at the exit neccessary to produce the desired velocity increase is from equation (4),

$$p_2 = -\Delta p + p_1 - \frac{\rho}{2}(V_2^2 - V_1^2)$$

$$= -7.94 + p_1 - \frac{(0.0022)}{2}\left[(163.0)^2 - (329.0)^2\right]$$

$$= p_1 + 81.66$$

The assumption that no losses occur in the entrance of the primary Venturi and Bernoulli's Theorem may be used to compute p_1,

$$(p_{at} + p_0) + \frac{\rho}{2} V_0^2 = (p_{at} + p_1) + \frac{\rho}{2} V_1^2$$

$$p_1 = p_0 - \frac{\rho}{2}(V_1^2 - V_0^2)$$

$$= -109.41 \text{ LB./SQ. FT.} \quad .$$

From the equation for p_2 and this value of p_1, the value of p_2 is,

$$p_2 = p_1 + 81.66$$

$$= -27.75 \text{ LB./SQ. FT.} \quad .$$

Since $p_2 = p_3$, this is the pressure the secondary Venturi must produce. The velocity V_3 is then found from

equation (5),

$$V_3 = \sqrt{\frac{2(h_0 - p_3)}{\rho}}$$

$$= \sqrt{\frac{2(9.45 + 27.75)}{0.0022}}$$

$$= 184.0 \text{ ft./sec.}$$

At this point, the problem is to design a secondary Venturi that will develop this velocity in the throat. There is no direct method of designing such a Venturi. The process involves the choice of a configuration and working through the computations to find if that configuration gives the necessary velocity. If not, then the procedure is repeated until the correct configuration is found. The general procedure is as shown below.

Secondary Venturi

The velocity increase due to blocking may easily be computed from the projected area of the Venturi normal to the air stream,

$$A_B = \frac{\pi}{4} D_0^2 - \frac{\pi}{4} D_T^2 = 0.103 \text{ sq. ft.}$$

where, D_0 = outside diameter of secondary Venturi

D_T = throat diameter of secondary Venturi

therefore,

$$(V_B + V_0) = \frac{A V_0}{A - A_B} = 110.0 \text{ ft./sec.}$$

The component of V_3 due to circulation about the secondary Venturi, V_r , is computed by use of the Biot-

Savart law.

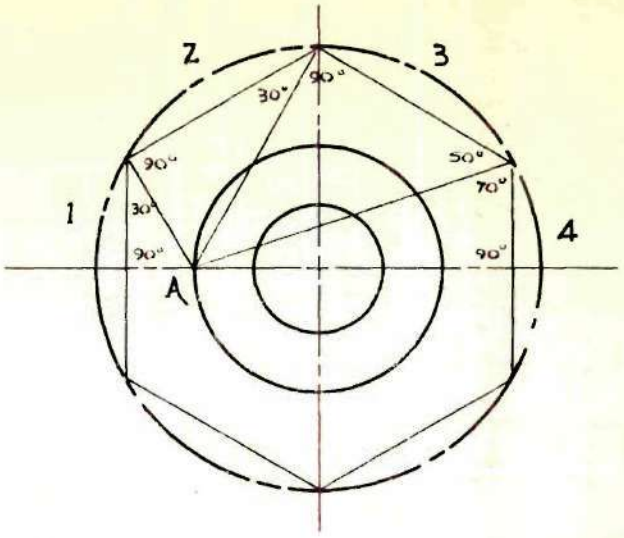

The vortex ring is broken down into a hexagon as discussed previously and the effect of each segment is determined. In as much as the hexagon is symmetrical, the effect of only half the figure need be found. The total effect at a point A is then twice this value. Sample calculations of the effect of a vortex ring are shown below.

Segment 1: $\theta_1 = 90°$

$\theta_2 = 30°$

$h = 0.62$ in.

Substituting these values in the proper equation, the value of K for this segment may be determined.

$$K = \frac{1}{4\pi h}(\cos\theta_1 + \cos\theta_2)$$

$$= 1.336$$

Following the same procedure, the effects of the remaining segments are:

Segment 2: $K = 0.661$

Segment 3: $K = 0.245$

Segment 4: $K = 0.0947$

Then the total K would be,

$$\text{TOTAL } K = 2 \text{ (SUM OF } K\text{'s)}$$
$$= 2 (2.337)$$
$$= 4.674 .$$

In order to compute the magnitude of the circulation, the section lift coefficient, C_l, must be determined. This is accomplished with the aid of thin airfoil theory. The procedure is lengthy and will not be shown. For our section the value of C_l is 0.4. The circulation is then from equation (9),

$$\Gamma = \frac{c C_l (V_0 + V_B)}{2}$$
$$= 15.1 \text{ SQ FT/SEC} .$$

The component due to circulation is then,

$$V_\Gamma = K_{TOTAL} \Gamma$$
$$= 70.6 \text{ FT/SEC} .$$

The total velocity produced by the secondary Venturi at the exit of the primary Venturi is,

$$V_3 = (V_0 + V_B) + V_\Gamma$$
$$= 180.6 \text{ FT/SEC} .$$

This value is slightly less than necessary (184.0 ft./sec.); consequently the velocity in the test section should be lower than expected. A comparison of values found using this theory and those found from investigations with the three dimensional models brings this point out.

Theory	Models
$V_0 = 77.9$ ft./sec.	$V_0 = 77.9$ ft./sec.
$V_1 = 329.0$ ft./sec.	$V_1 = 321.6$ ft./sec.
$V_2 = 163.0$ ft./sec.	$V_2 = 160.5$ ft./sec.
$V_3 = 184.0$ ft./sec.	$V_3 = 180.6$ ft./sec.

This theory is valid only if no separation is present in the diffuser of the primary Venturi. The slot between the exit of the primary Venturi and the throat of the secondary Venturi must be sufficiently large enough to permit the diffuser of the secondary Venturi to function properly. The minimum value for this characteristic is not known at the present time and can only be determined through further investigation.

CONCLUSIONS

Unless specifically specified, conclusions apply to both two and three-dimensional Venturis.

(1) The double Venturi wind tunnel may be employed successfully without an excessive increase in power required.

(2) A velocity increase of 3 to 3.5 may be expected from a two-dimensional double Venturi and 4 to 4.5 from the three-dimensional double Venturi.

(3) The diffuser of the two-dimensional primary Venturi may be a maximum of 14° without creating separation.

(4) The diffuser of the three-dimensional primary Venturi should be 14° for no separation, but it is possible to approach 20° without the resulting drag becoming excessive.

(5) Divergence on the outside of both Venturis is permissible, preferably 5° for the primary and 3° for the secondary.

(6) The exit of the primary Venturi should be slightly forward of the throat of the secondary Venturi.

(7) As the ratio of throats, K_T, decreases, the velocity ratio, V_R, increases up to the point where insufficient air is allowed to pass through the slot to keep the secondary Venturi from stalling.

(8) The increase in Reynolds Number with the full scale tunnel would reduce the drag due to skin friction by approximately 60% and that due to diffusion and separation by 20%.

BIBLIOGRAPHY

Bailey, A. and Wood, S. A., "Development of a High Speed Induced Wind Tunnel", Aeronautical Research Committee Reports and Memoranda, No. 1468, 1933

_____, "Development of a High Speed Induced Wind Tunnel of Rectangular Cross Section", Aeronautical Research Committee Reports and Memoranda, No. 1791, 1937

Binder, R. C., Fluid Mechanics, New York: Prentice-Hall, Inc., 1943, pp. 63-67

Bond, W. N., "Viscosity in Orifice Flows", Proceedings of the Physical Society, London, Vol. 33, 1921, pp. 225-230

Bonney, E. Arthur, Engineering Supersonic Aerodynamics, New York: McGraw-Hill Book Co., 1950, p. 200

Coleman, E. P., "The Flow of Fluids in a Venturi Tube", Transactions of the American Society of Mechanical Engineers, Vol. 28, 1907, pp. 483-507

Dryden, Munaghan, and Bateman, Hydrodynamics, Washington, D. C.: Bulletin of the National Research Council No. 84, 1932, pp. 477-481

Gibson, Hydraulics and Its Applications, Fourth Edition, New York: D. Van Nostrand Co., 1930, p. 93

Herchel, C., "The Venturi Water Meter", Transactions of the American Society of Civil Engineers, Vol. 17, 1887, pp. 228-258

Hunsaker, J. C. and Rightmire, B. G., Engineering Applications of Fluid Mechanics, New York: McGraw-Hill Book Co., 1947, p. 151

Jacobs, E. U. and Sherman, Albert, "Airfoil Section Characteristics as Affected by Variations of the Reynolds Number", National Advisory Committee for Aeronautics Technical Report No. 586, 1937

Kisenko, M. S., "Comparative Results of Tests on Several Different Types of Nozzles", National Advisory Committee for Aeronautics Technical Memorandum No. 1066, 1944, pp. 1, 10

Ledoux, J. W., "Venturi Tube Characteristics", Transactions of the American Society for Civil Engineers, Vol. 91, 1927, pp. 565-574

Piercy, N. A. V., and Miner, R., "On the Immersed Venturi with Special Reference to Its Use on Aircraft for Purposes of Power Transmission", Aeronautical Research Committee Reports and Memoranda, No. 664, 1919, 1920, p. 641

Pope, Alan Y., Aerodynamics of Supersonic Flight, New York: Pitman Publishing Corp., 1950, pp. 107-109

_____, Wind Tunnel Testing, New York: John Wiley and Sons, Inc., 1947, pp. 62-67

Reynolds, J. L. and Ling, H. J., "The Flow of Air Through Nozzles and Orifices", Journal of the American Society of Mechanical Engineers, Vol. 39, 1917, pp. 250-252

Ritter, Alfred, A Study of the Double Venturi Principle in Its Application to High Speed Wind Tunnels, Unpublished Master's Thesis, Georgia Institute of Technology, 1947

Smith, Richard H. and Chi-Teh Wang, "Contracting Cones Giving Uniform Throat Speeds", Journal of the Aeronautical Sciences, October, 1944, p. 356

Stack, John, "The NACA High Speed Wind Tunnel and Tests of Six Propeller Sections", National Advisory Committee for Aeronautics Technical Report No. 463, 1933

Tsien, Hsue-Shen, "On the Design of the Contraction Cone For a Wind Tunnel", Journal of the Aeronautical Sciences, Vol. 10, February, 1943, pp. 68-76

Vedernikoff, A. N., "An Experimental Investigation of the Flow of Air in a Flat Broadening Channel", National Advisory Committee for Aeronautics Technical Memorandum No. 1059, 1944

Vennard, John K., Elementary Fluid Mechanics, First Edition, New York: John Wiley and Sons, 1940, p. 246

APPENDIX

FORMULAE AND SAMPLE CALCULATIONS

Velocity in Model Tunnel Ahead of the Double Venturi

$$q_o = \frac{1}{2} \rho_o V_o^2$$

$$V_o = \sqrt{\frac{2 q_o}{\rho_o}} = \sqrt{\frac{2 q_o}{\rho}} \quad ; \rho_o = \rho_1 = \rho$$

$$= \sqrt{\frac{2q' \times \text{SG of alcohol} \times 62.4 \text{ lb/ft}^3}{\rho \times 25.4 \text{ mm/in} \times 12 \text{ in/ft}}}$$

Velocity in Test Section of Primary Venturi

Bernoulli's Theorem,

$$p_o + \frac{1}{2} \rho_o V_o^2 = p_1 + \frac{1}{2} \rho_1 V_1^2 = \text{constant}$$

$$p_o + q_o = p_1 + q_1$$

as applied to the double Venturi arrangement is,

$$(p_{et} + h_o) = (p_{et} + p_1) + \frac{1}{2} \rho V_1^2$$

$$\frac{1}{2} \rho V_1^2 = (p_{et} + h_o) - (p_{et} + p_1)$$

$$= h_o - p_1$$

$$= \sqrt{\frac{2 (h_o - p_1)}{\rho}}$$

Drag of the Double Venturi

$$\int h_o \, dA - \int h_2 \, dA = D$$

Graphic integration of the above quantities is the simplest of solutions. The procedure of de-

termining the drag is as follows:

> Plot the values of total head pressures vs. tunnel height for sections $(\ )_o$ and $(\ )_2$. Using a planimeter, integrate the two curves. The difference of the two values multiplied by the tunnel width gives the drag in pounds.

$$h = \frac{h' \times \text{Sg of alcohol} \times 62.4\ \text{lb/ft}^3}{25.4\ \text{mm/in} \times 12\ \text{in/ft}}$$

Dimensionless Coefficients

V_R = velocity ratio $\frac{V_1}{V_o}$

C_D = coefficient of drag of double Venturi

$$= \frac{D}{\frac{1}{2}\rho V_o^2 A}$$

Calculation of Power Required for Double Venturi

Calculations will be based on the dimensions of the nine foot wind tunnel at the Georgia Institute of Technology. Results from the three-dimensional investigation will be utilized.

Primary Venturi, P-22-45-7-M5:

throat diameter = (.22)(9ft.) = 2 ft.

maximum outside diameter = (.45)(9ft.) = 4.05 ft.

diffuser angle = $2(7^\circ) = 14^\circ$

outside divergence angle = 5°

Secondary Venturi, S-37.5-75-10-M3:

throat diameter = (.375)(9ft.) = 3.8 ft.

maximum outside diameter = (.75) (9ft.)
= 6.75 ft.

diffuser angle = $2(10^{\circ}) = 20^{\circ}$

outside divergence angle = 3°

In most instances, the wind tunnel engineer will want the highest possible velocity ratio, V_R. This of course, will depend on the amount of power available in his tunnel. For our purposes, we will assume that a velocity ratio of 4 is desired.

From Figure 14, the location of the primary Venturi is l=6%.

From Figure 13, the coefficient of drag C_D, is 0.344 for l=6%. From,

$$D = C_D \frac{\rho}{2} V_o^2 A$$

where,

C_D = 0.344

ρ = 0.0022, average Atlanta density

V_o = 150 mph, maximum velocity of the 9 foot wind tunnel

A = 63.6 $ft.^2$, cross-sectional area of wind tunnel,

the drag of the double Venturi may be calculated.

Substituting the correct values in the drag equation,

$$D = 1165 \text{ lbs.} \quad \therefore HP_{req} = \frac{DV_o}{550 \text{ ft-lbs/sec}} = 466$$

The velocity in the test section is,

$$V_1 = V_R V_0 = 4.0 \times 150 \text{ mph} = 600 \text{ mph}$$

The Mach number in the test section is found using,

$$P_1 = P_0 \left[1 - \frac{V_1^2 - V_0^2}{2} \cdot \frac{\gamma - 1}{\gamma} \cdot \frac{\rho_0}{P_0} \right]^{\frac{\gamma}{\gamma - 1}}$$

assuming that,

$$P_0 = 2000 \text{ lbs./ft}^2$$
$$\gamma = 1.4$$
$$\rho_0 = 0.0022 \text{ slugs/ft}^3$$

and inserting known values,

$$P_1 = 1650 \text{ lbs/ft}^2$$
$$\frac{P_0}{P_1} = \left[\frac{T_0}{T_1} \right]^{\gamma/\gamma - 1}$$
$$\therefore T_1 = \frac{T_0}{\left(\frac{P_0}{P_1} \right)^{\gamma/\gamma - 1}}$$

Again inserting known values,

$$T_1 = 55^\circ F = 515^\circ R$$
$$V_S = 33.42 \sqrt{^\circ R} = 33.42 \sqrt{515^\circ R}$$
$$= 758 \text{ mph}$$
$$\therefore M_1 = \frac{V_1}{V_S} = \frac{600 \text{ mph}}{758 \text{ mph}} = 0.792$$

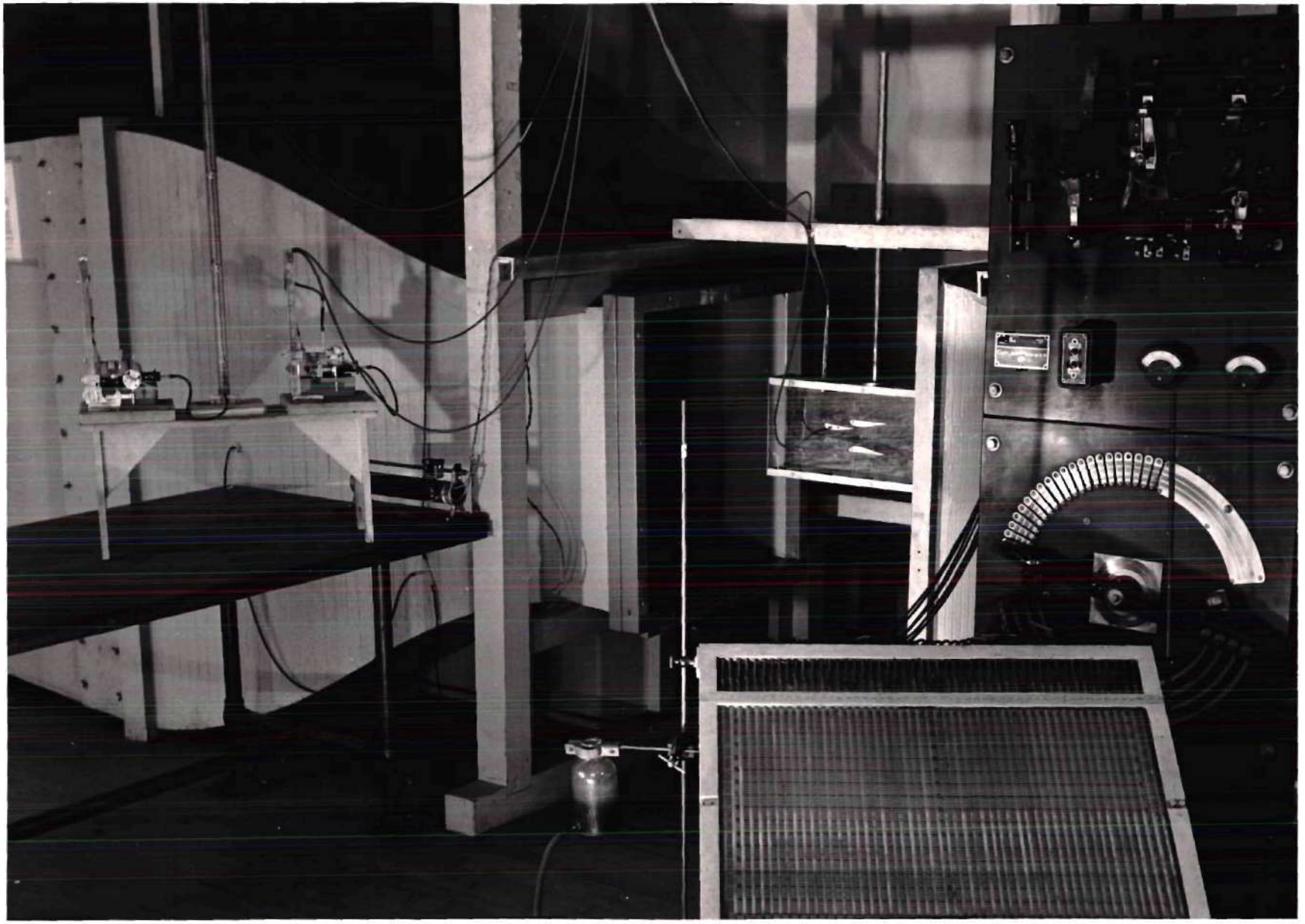

FIG. I PRESSURE MEASURING INSTRUMENTS

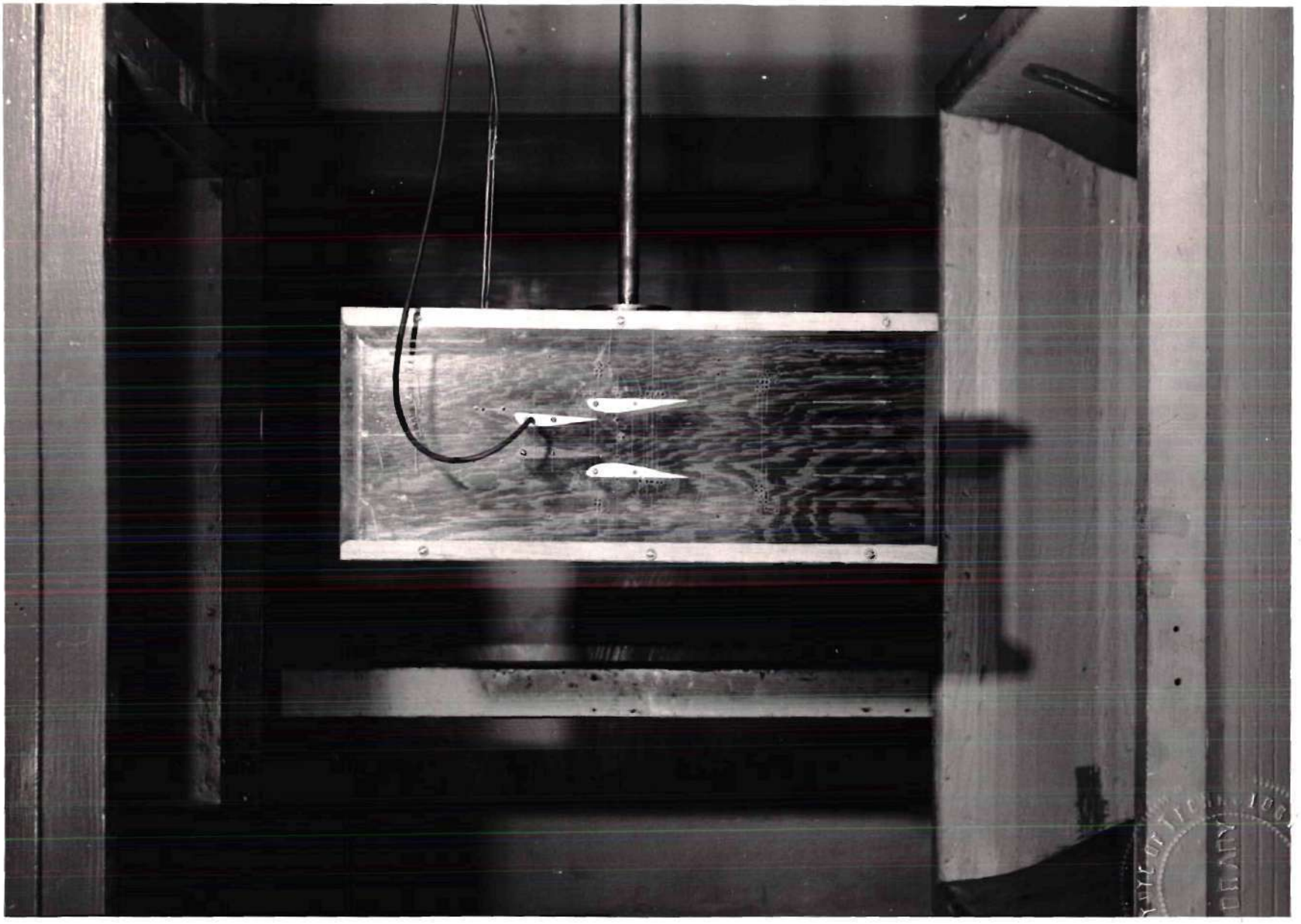

FIG. 2 TWO DIMENSIONAL MODEL TUNNEL

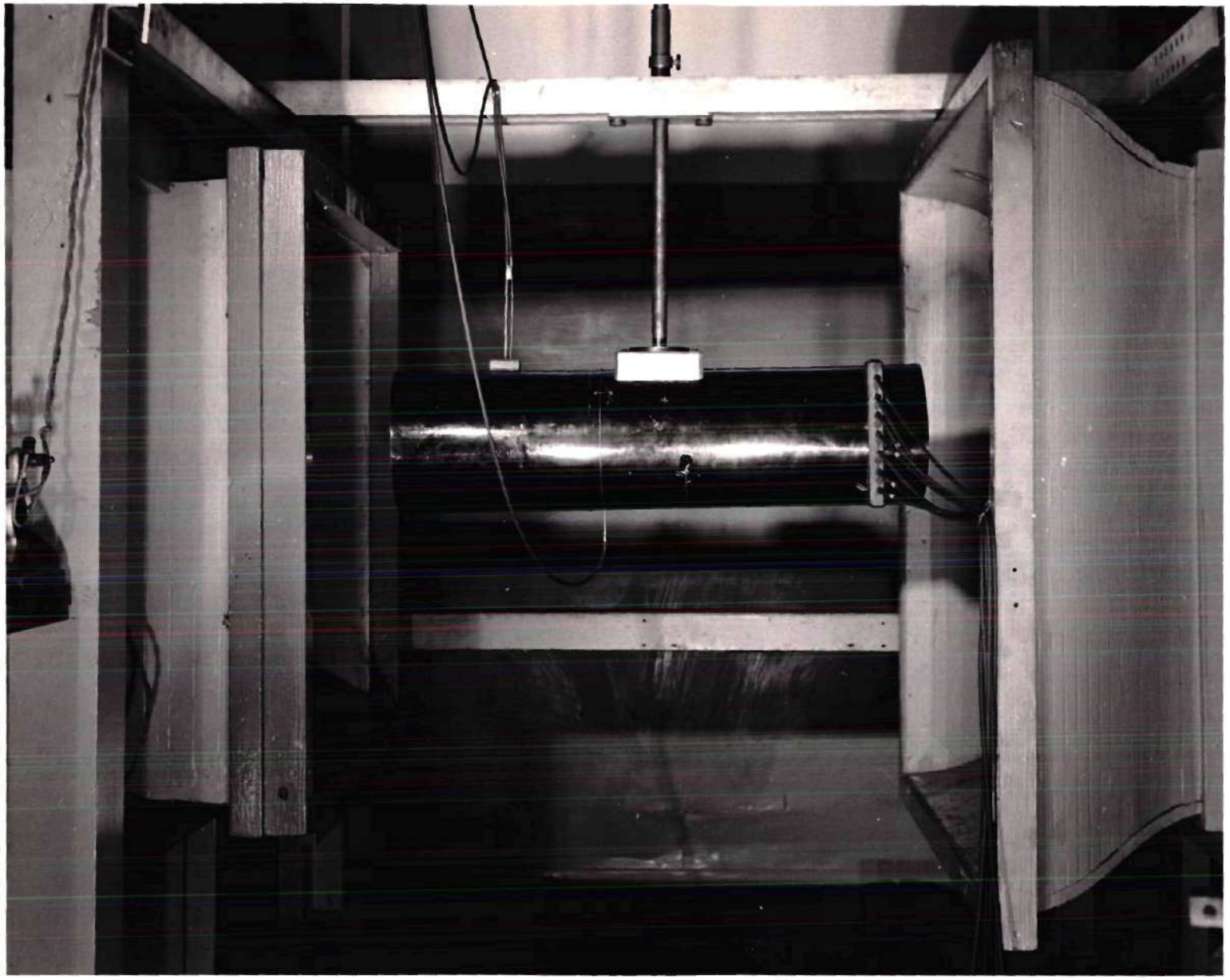

FIG.3 THREE DIMENSIONAL MODEL TUNNEL

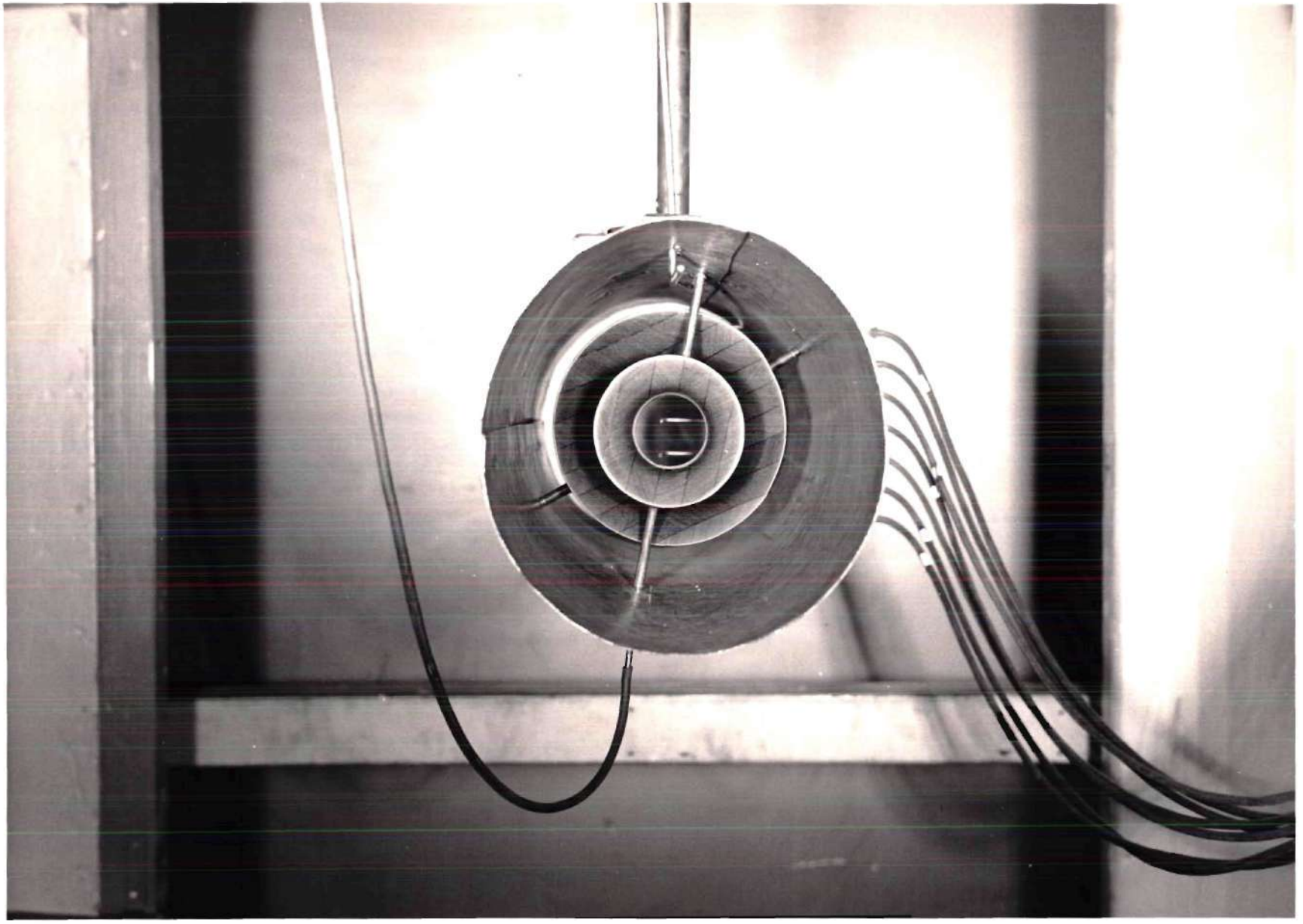

FIG.4 THREE DIMENSIONAL DOUBLE VENTURI INSTALLATION

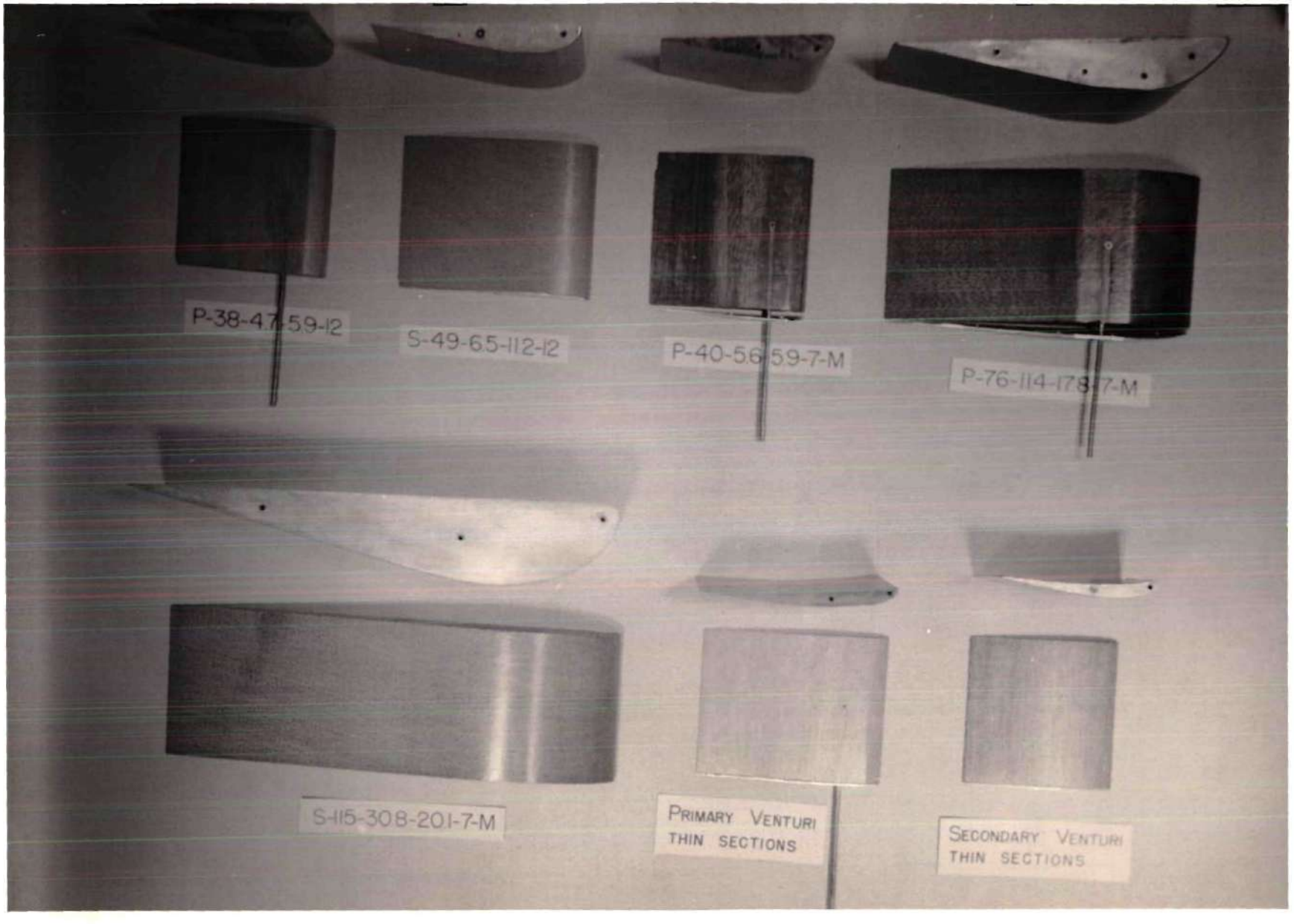

FIG. 5 TWO DIMENSIONAL VENTURIS

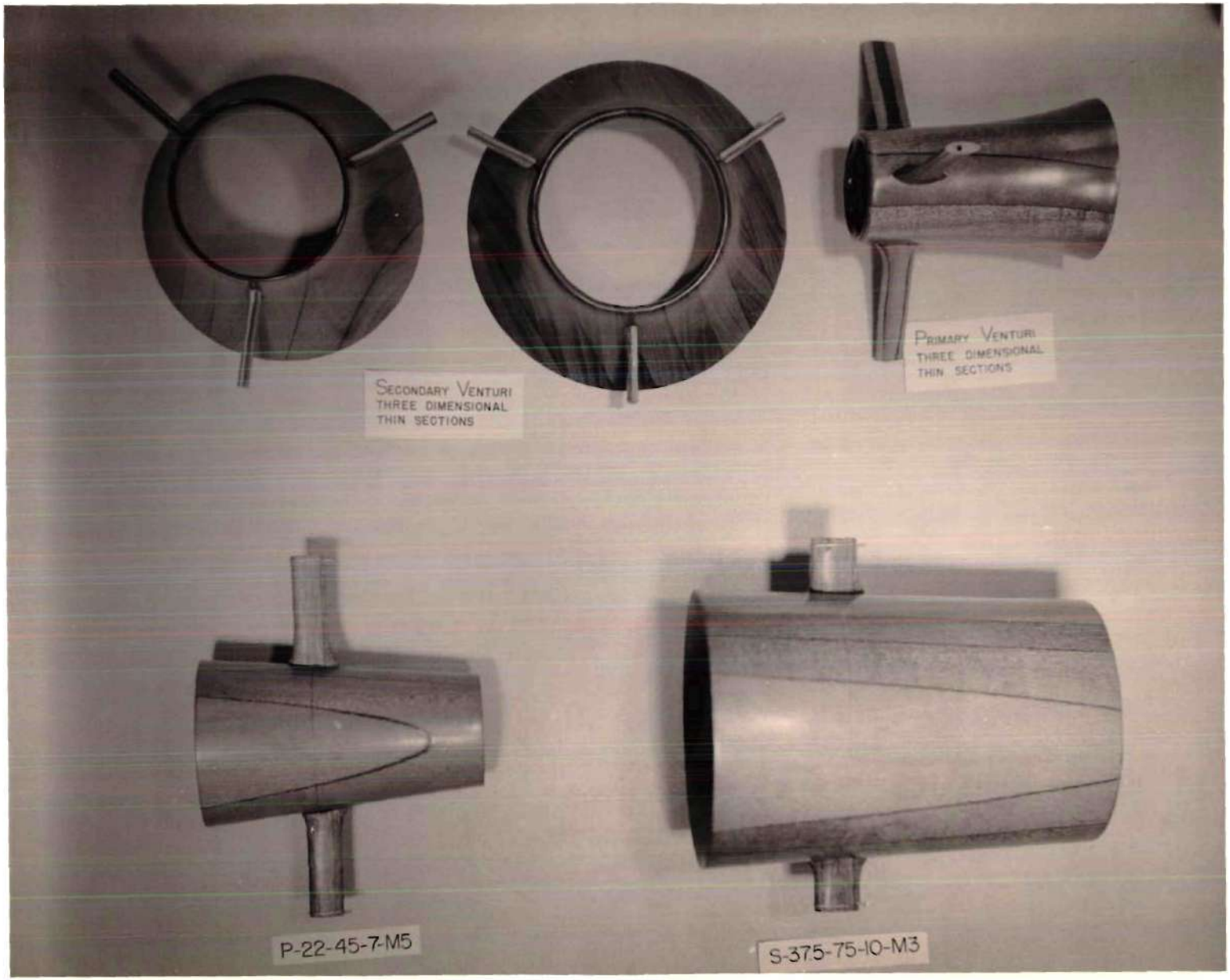

FIG. 6 THREE DIMENSIONAL VENTURIS

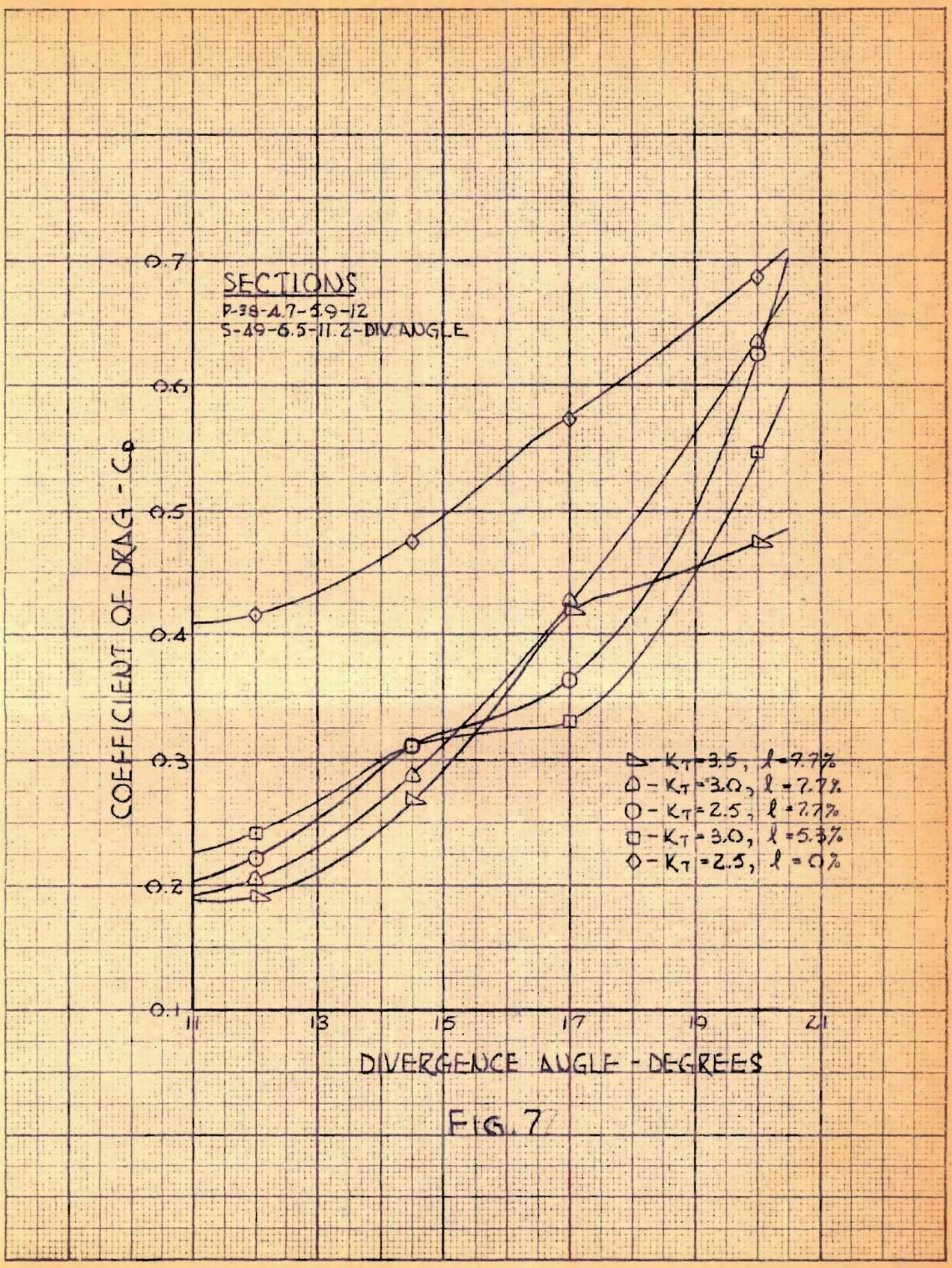
SECTIONS
P-38-4.7-5.9-12
5-49-6.5-11.2-DIV. ANGLE
COEFFICIENT OF DRAG - C_D
0.7
0.6
0.5
0.4
0.3
0.2
0.1
11
13
15
17
19
21
DIVERGENCE ANGLE - DEGREES
△ - K_T = 3.5, ℓ = 7.7%
△ - K_T = 3.0, ℓ = 7.7%
○ - K_T = 2.5, ℓ = 7.7%
□ - K_T = 3.0, ℓ = 5.3%
◇ - K_T = 2.5, ℓ = 0%

Fig. 7

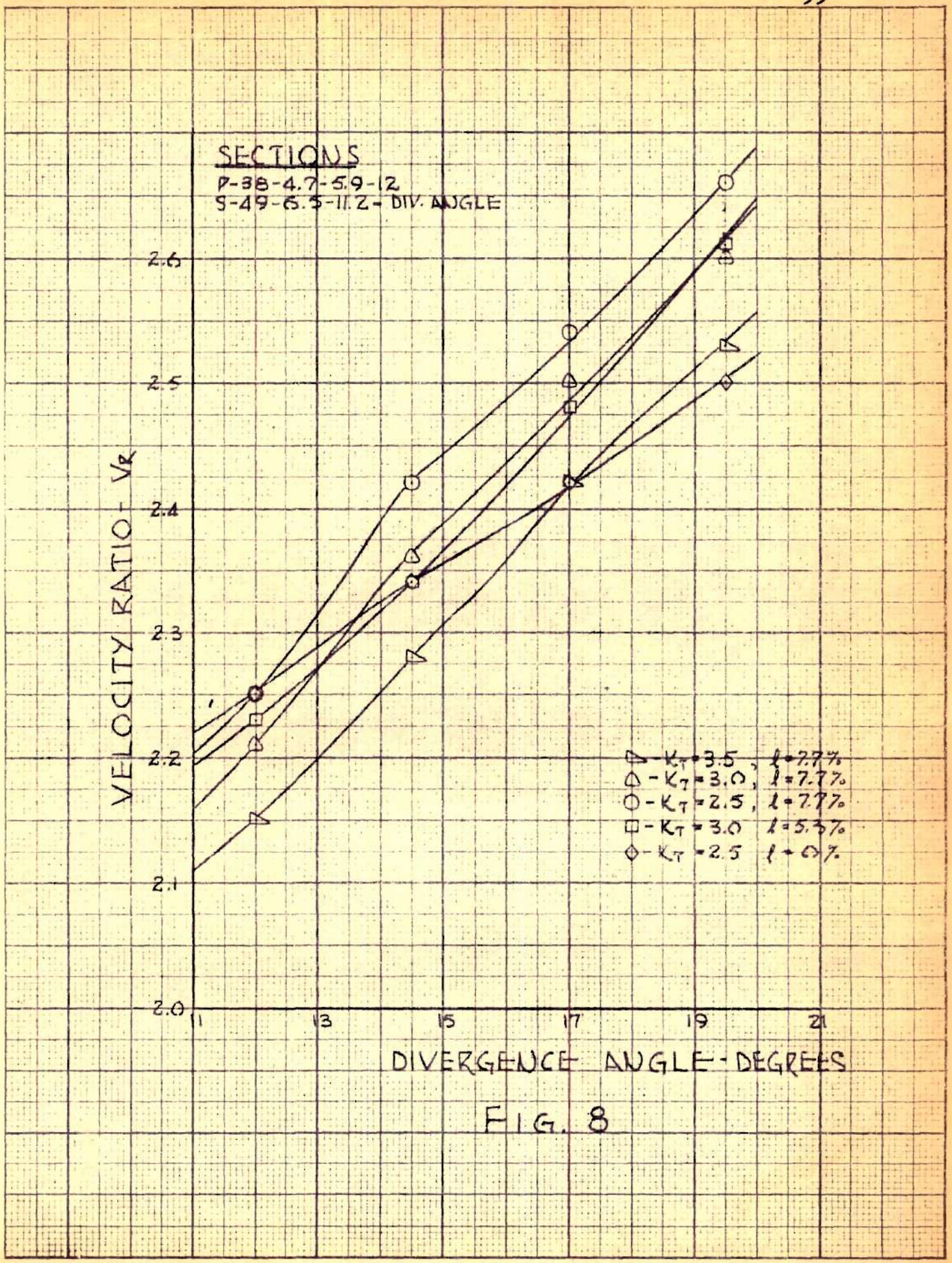
SECTIONS
P-38-4.7-5.9-12
S-49-6.5-11.2 - DIV. ANGLE
VELOCITY RATIO - V_R
2.6
2.5
2.4
2.3
2.2
2.1
2.0
1
13
15
17
19
21
DIVERGENCE ANGLE - DEGREES
K_T = 3.5, l = 7.7%
K_T = 3.0, l = 7.7%
K_T = 2.5, l = 7.7%
K_T = 3.0 l = 5.3%
K_T = 2.5 l = 0%

FIG. 8

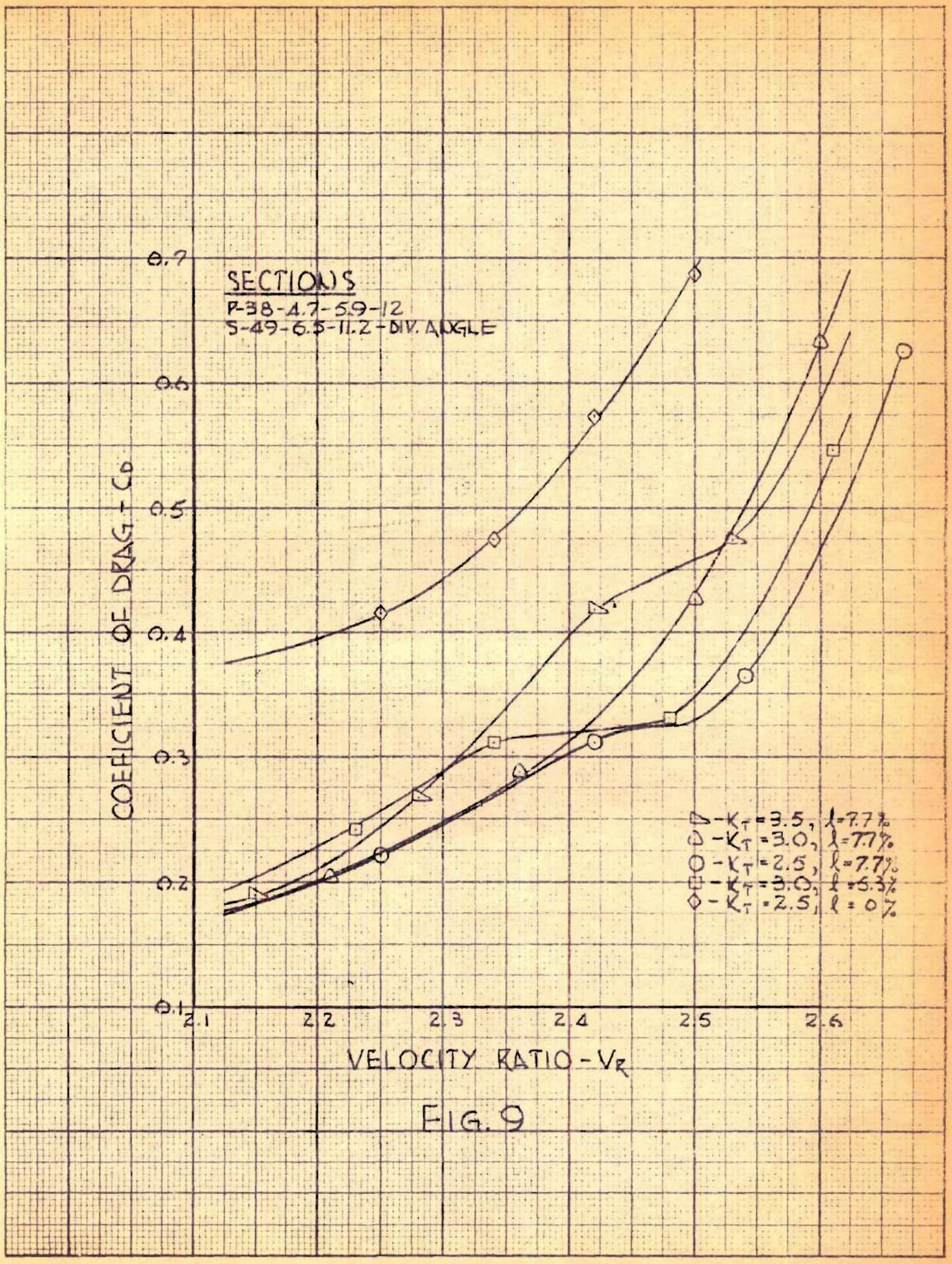
SECTIONS
P-38-4.7-5.9-12
S-49-6.5-11.2-DIV. ANGLE
COEFICIENT OF DRAG - C_D
0.7
0.6
0.5
0.4
0.3
0.2
0.1
2.1
2.2
2.3
2.4
2.5
2.6
VELOCITY RATIO - V_R
△ - K_T = 3.5, l = 7.7%
△ - K_T = 3.0, l = 7.7%
○ - K_T = 2.5, l = 7.7%
□ - K_T = 3.0, l = 5.3%
◇ - K_T = 2.5, l = 0%

FIG. 9

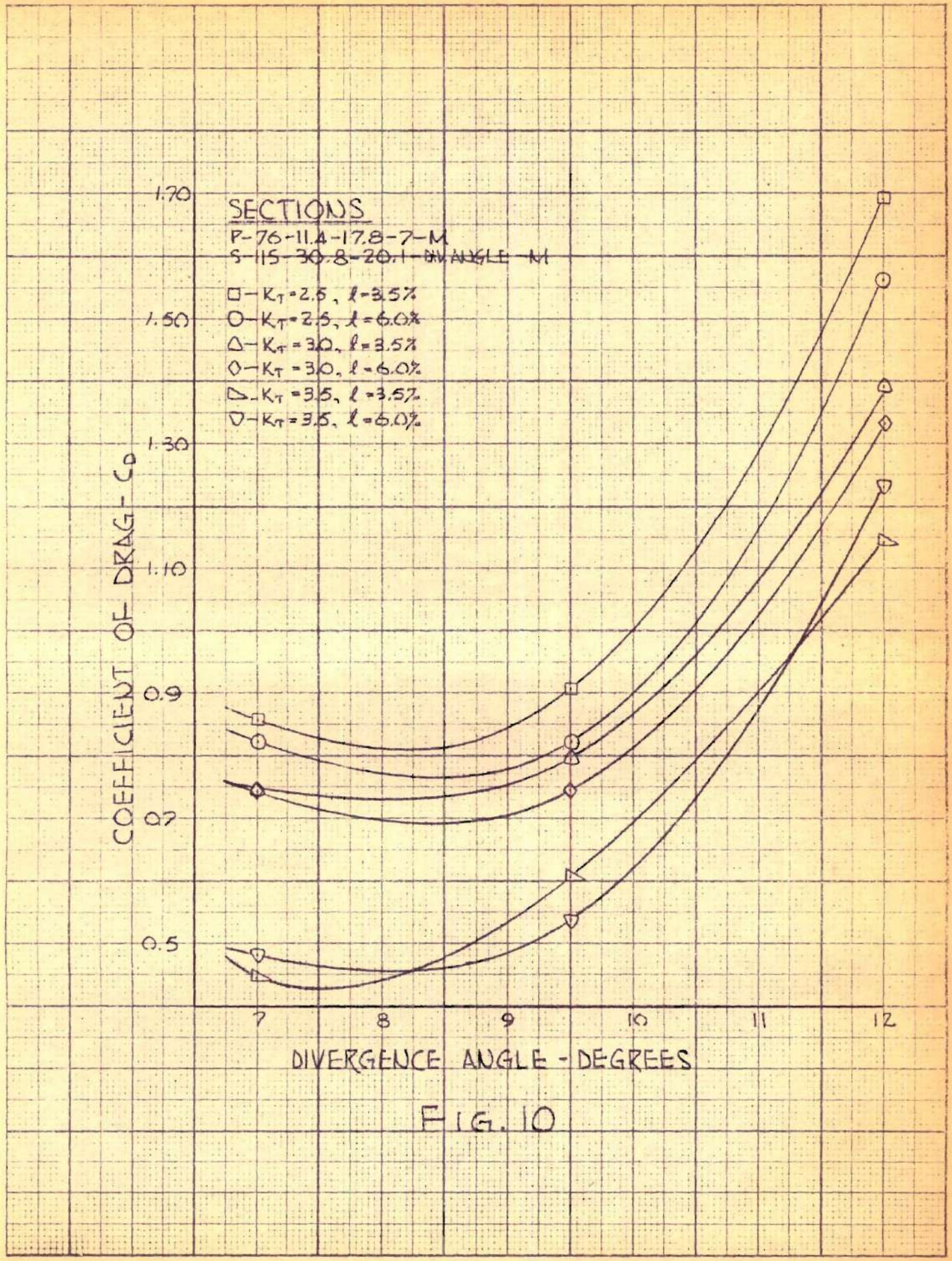
SECTIONS
P-76-11.4-17.8-7-M
S-15-30.8-20.1-DIV.ANGLE-M
□ - K_T = 2.5, ℓ = 3.5%
○ - K_T = 2.5, ℓ = 6.0%
△ - K_T = 3.0, ℓ = 3.5%
◇ - K_T = 3.0, ℓ = 6.0%
▷ - K_T = 3.5, ℓ = 3.5%
▽ - K_T = 3.5, ℓ = 6.0%
COEFFICIENT OF DRAG - C_D
1.70
1.50
1.30
1.10
0.9
0.7
0.5
7
8
9
10
11
12
DIVERGENCE ANGLE - DEGREES

FIG. 10

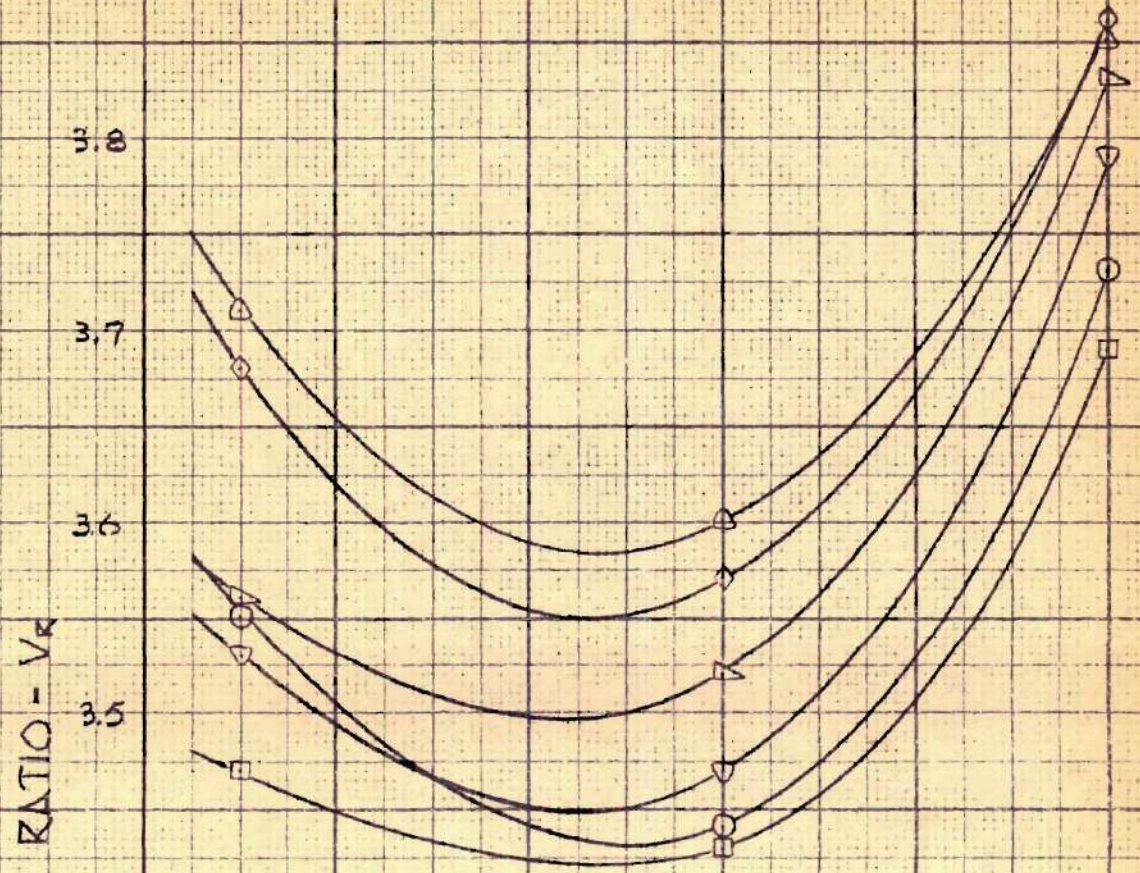

FIG. 11

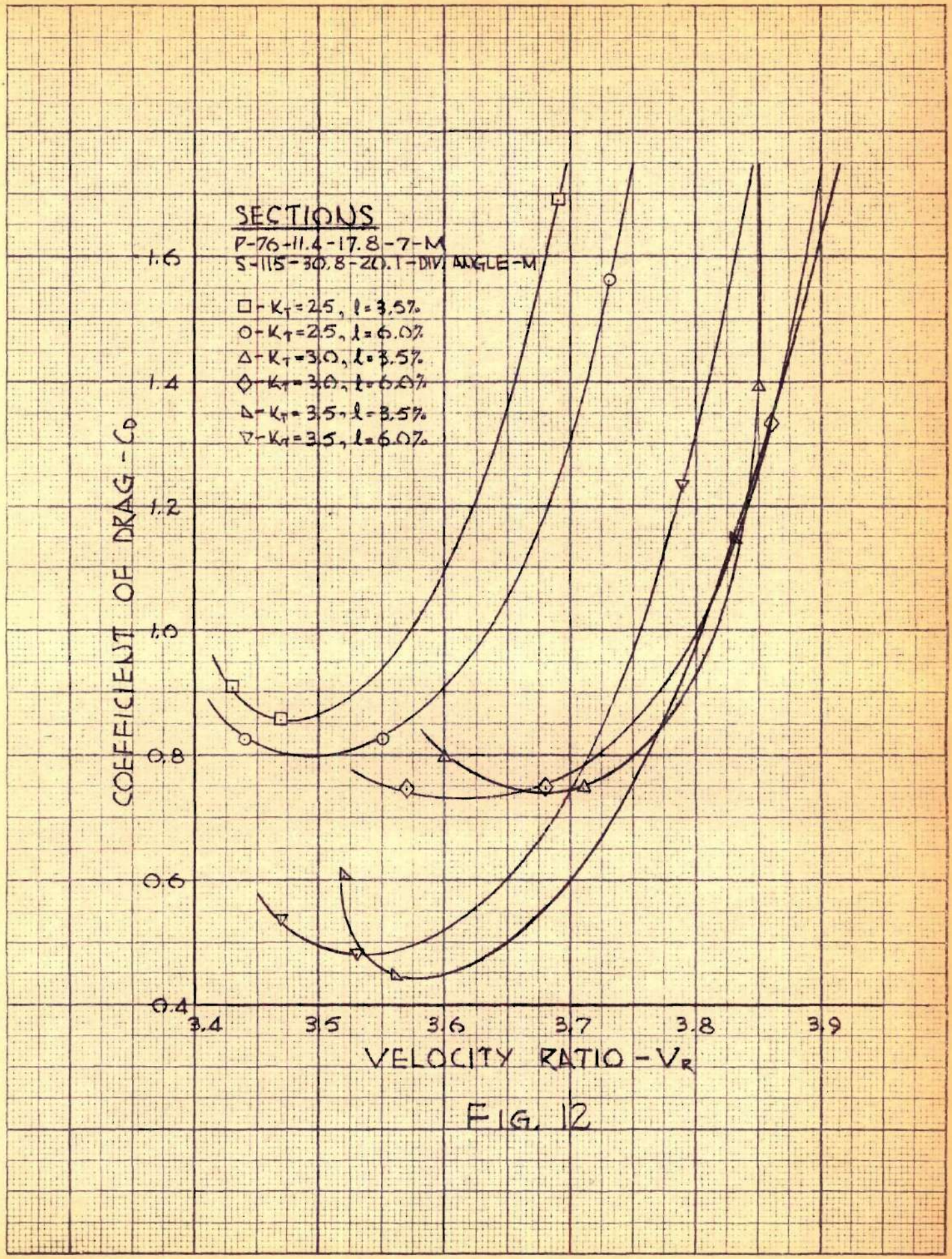
SECTIONS
P-76-11.4-17.8-7-M
S-115-30.8-20.1-DIV. ANGLE-M
□ - K_T = 2.5, ℓ = 3.5%
○ - K_T = 2.5, ℓ = 6.0%
△ - K_T = 3.0, ℓ = 3.5%
◇ - K_T = 3.0, ℓ = 6.0%
△ - K_T = 3.5, ℓ = 3.5%
▽ - K_T = 3.5, ℓ = 6.0%
COEFFICIENT OF DRAG - C_D
1.6
1.4
1.2
1.0
0.8
0.6
0.4
3.4
3.5
3.6
3.7
3.8
3.9
VELOCITY RATIO - V_R

FIG. 12

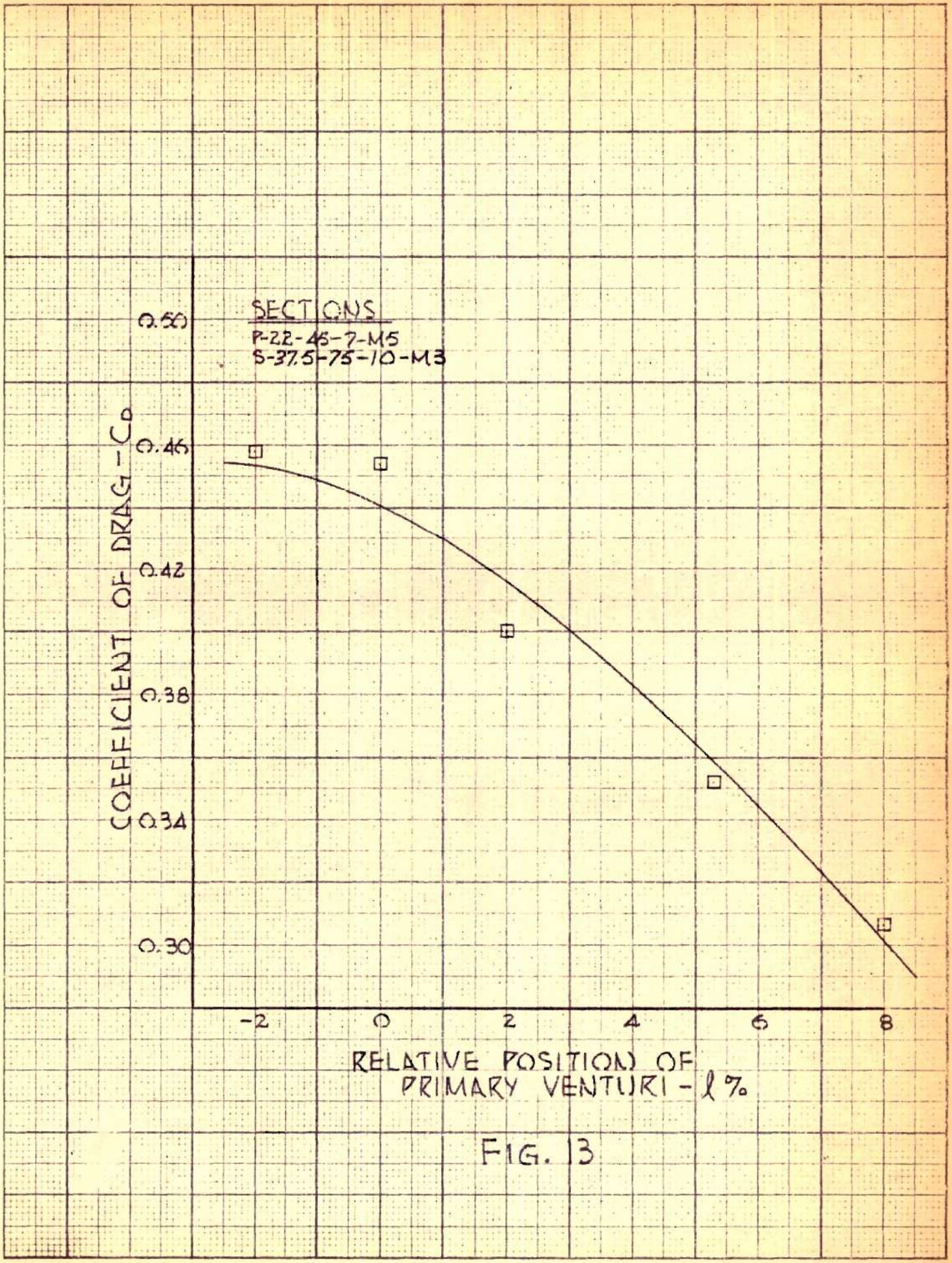
SECTIONS
P-22-46-7-M5
S-37.5-75-10-M3
0.50
0.46
0.42
0.38
0.34
0.30
COEFFICIENT OF DRAG - C_D
-2
0
2
4
6
8
RELATIVE POSITION OF PRIMARY VENTURI - l %

FIG. 13

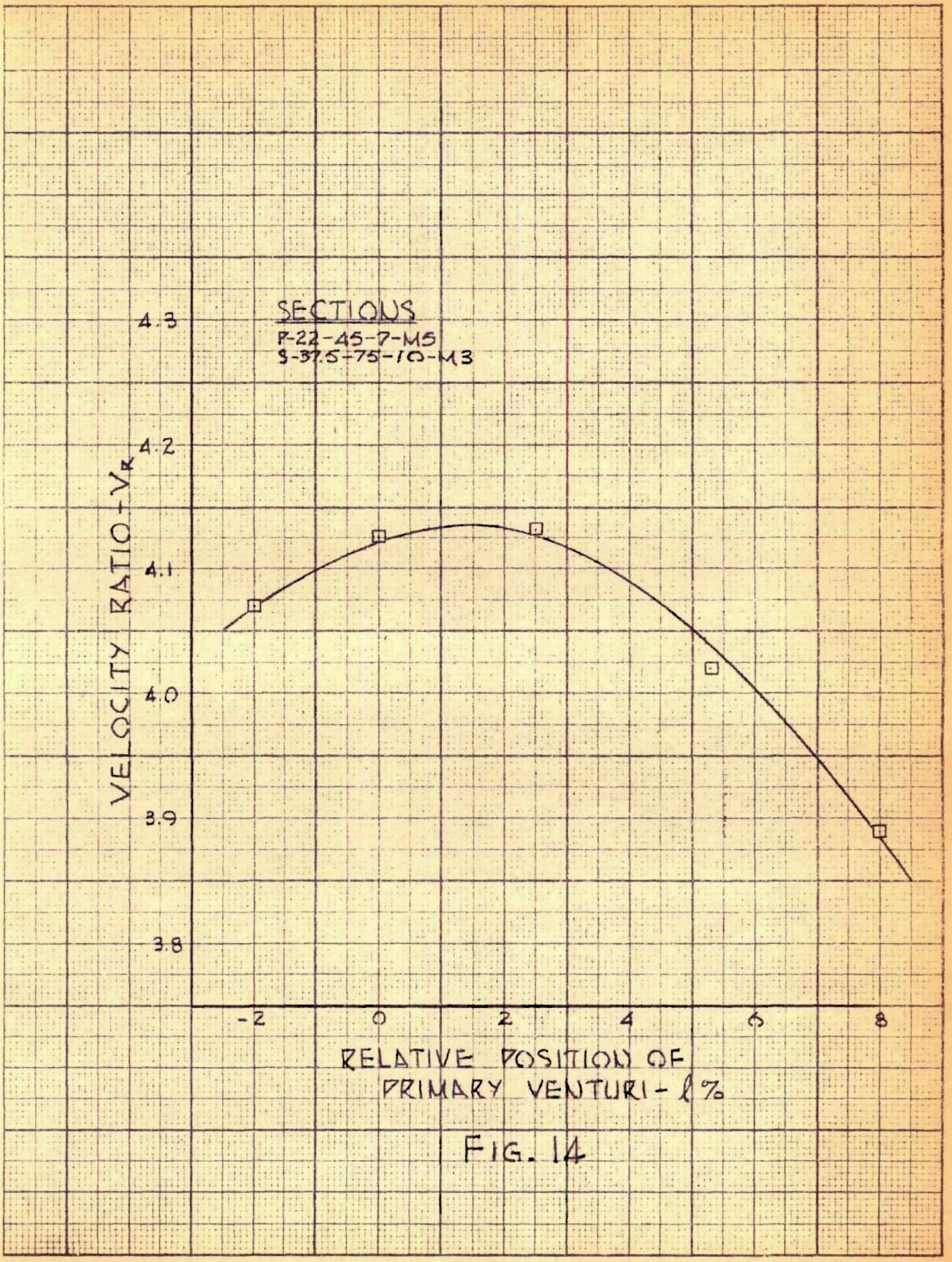

FIG. 14

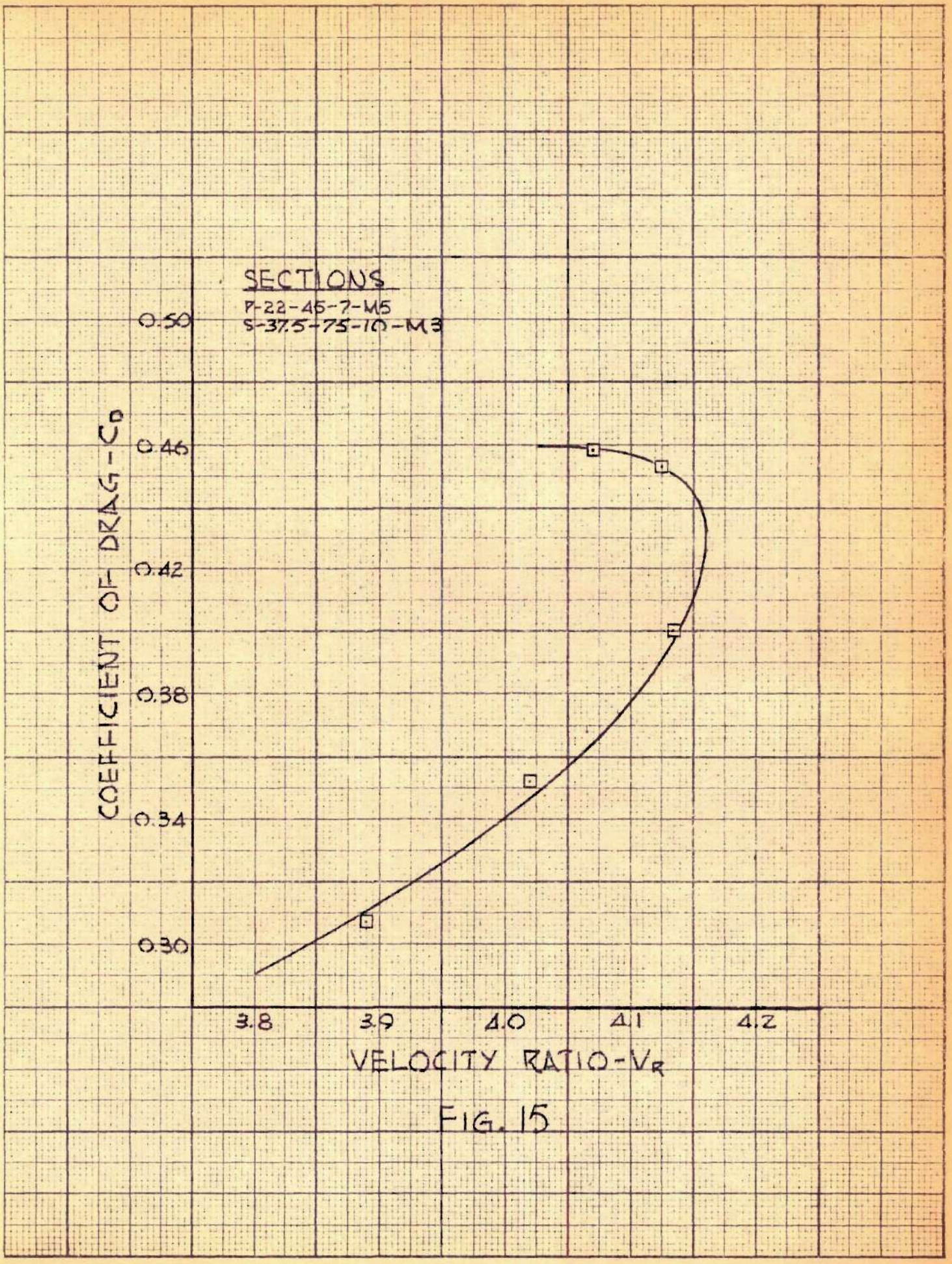
SECTIONS
P-22-45-7-M5
S-37.5-75-10-M3
0.50
0.46
0.42
0.38
0.34
0.30
COEFFICIENT OF DRAG - C_D
3.8
3.9
4.0
4.1
4.2
VELOCITY RATIO - V_R

FIG. 15

TOTAL HEAD PRESSURES

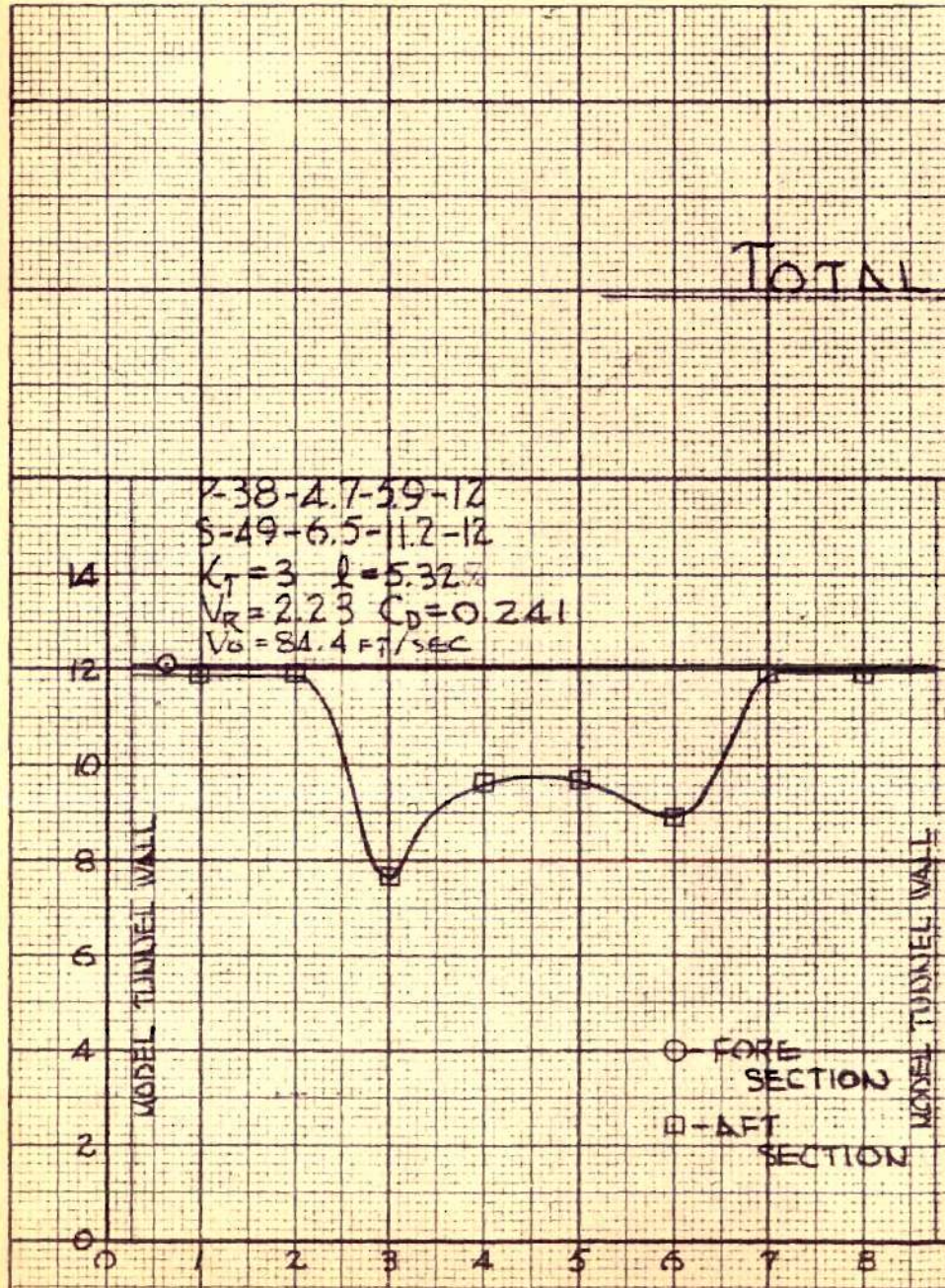

FIG. 16

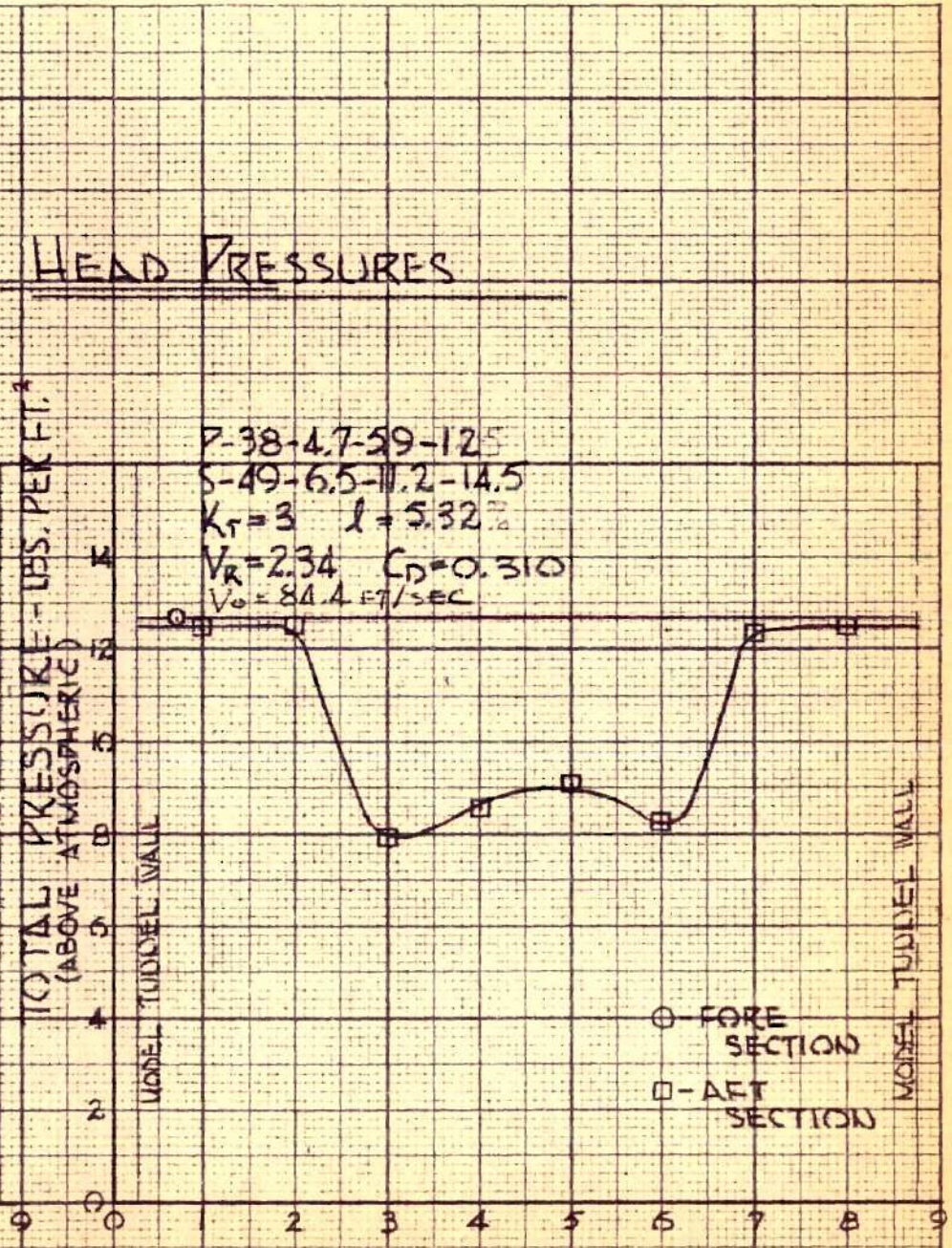

FIG. 17

TOTAL HEAD PRESSURES

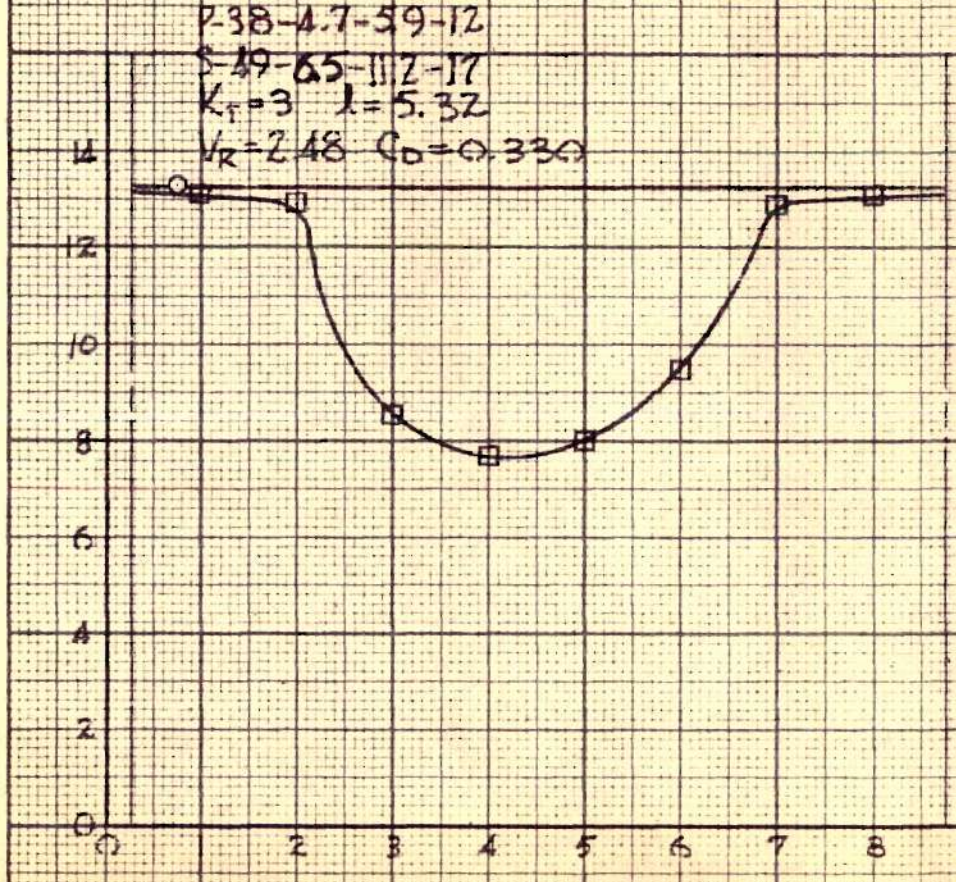

FIG. 18

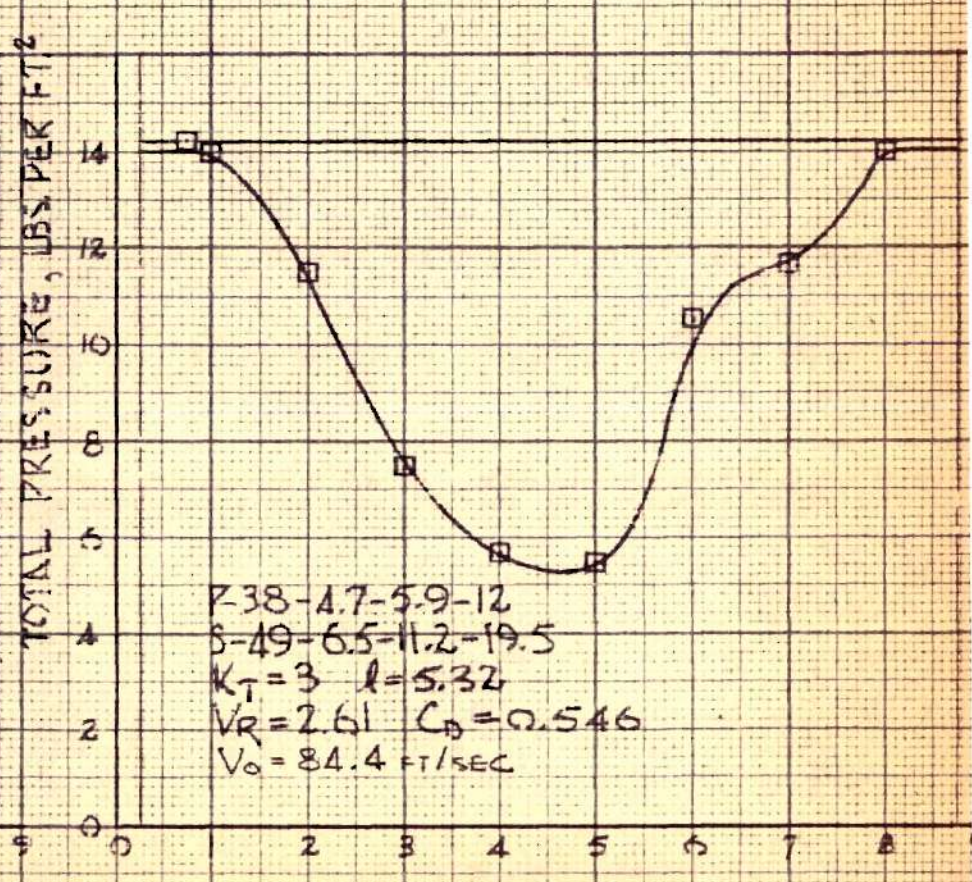

FIG. 19

TOTAL HEAD PRESSURES

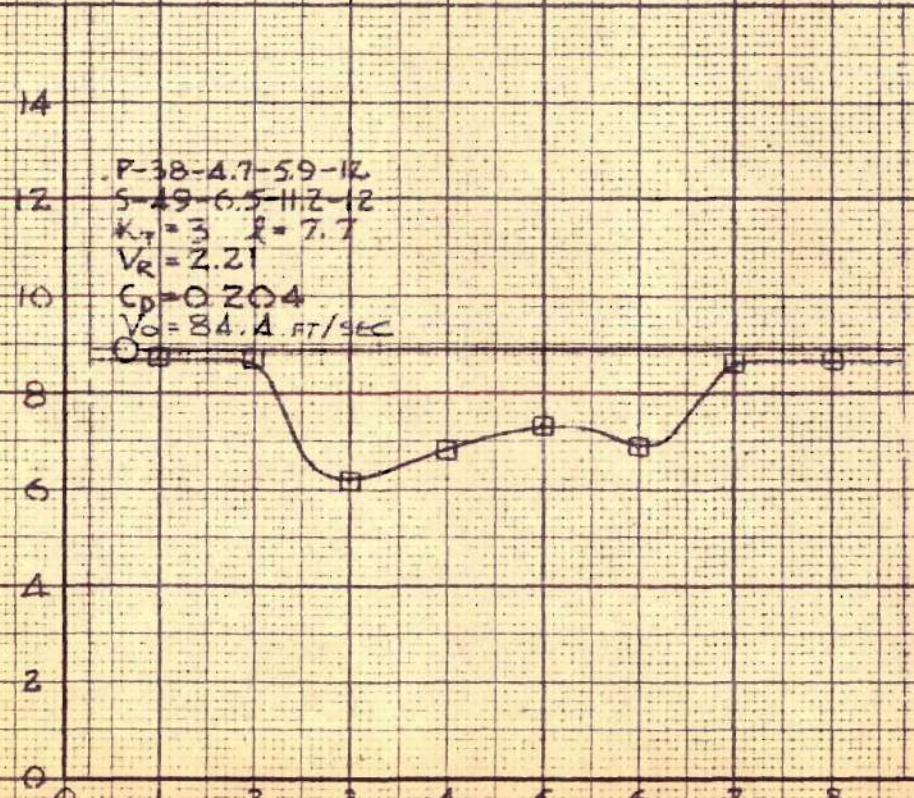

FIG. 20

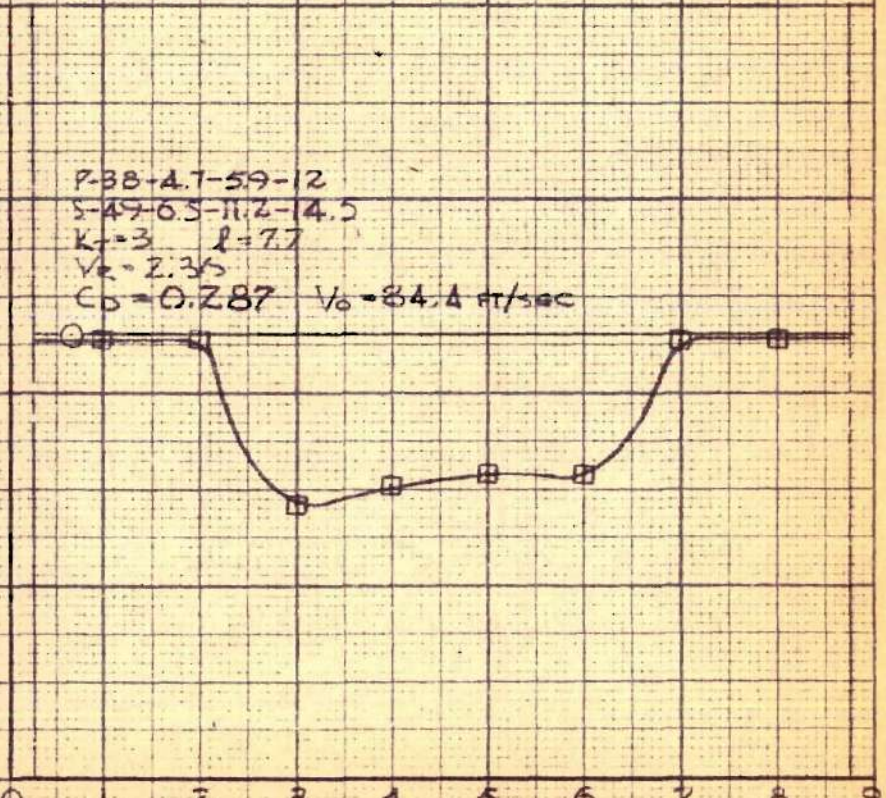

TUNNEL STATION, FORE & AFT SECTIONS

FIG. 21

TOTAL HEAD PRESSURES

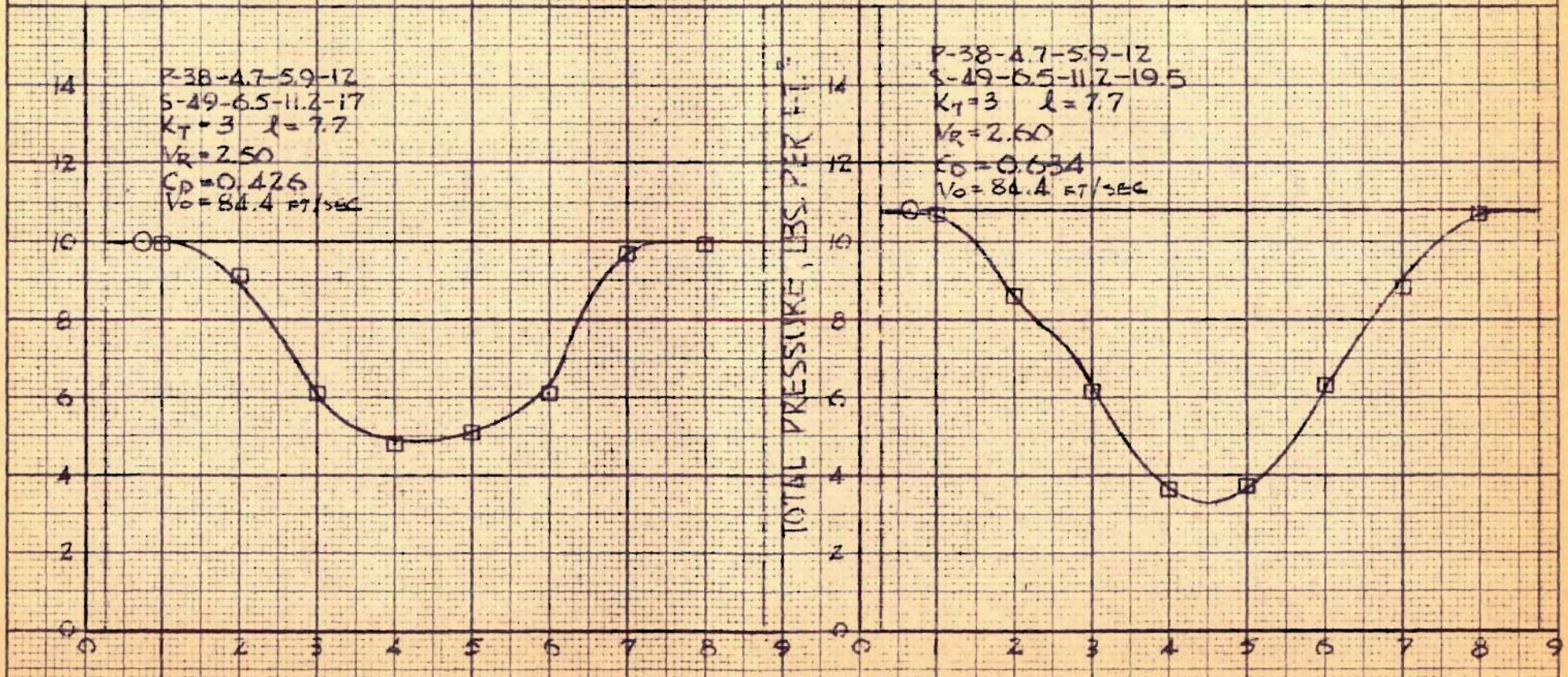

TUNNEL STATION, FORE & AFT SECTIONS

FIG. 22

FIG. 23

TOTAL HEAD PRESSURES

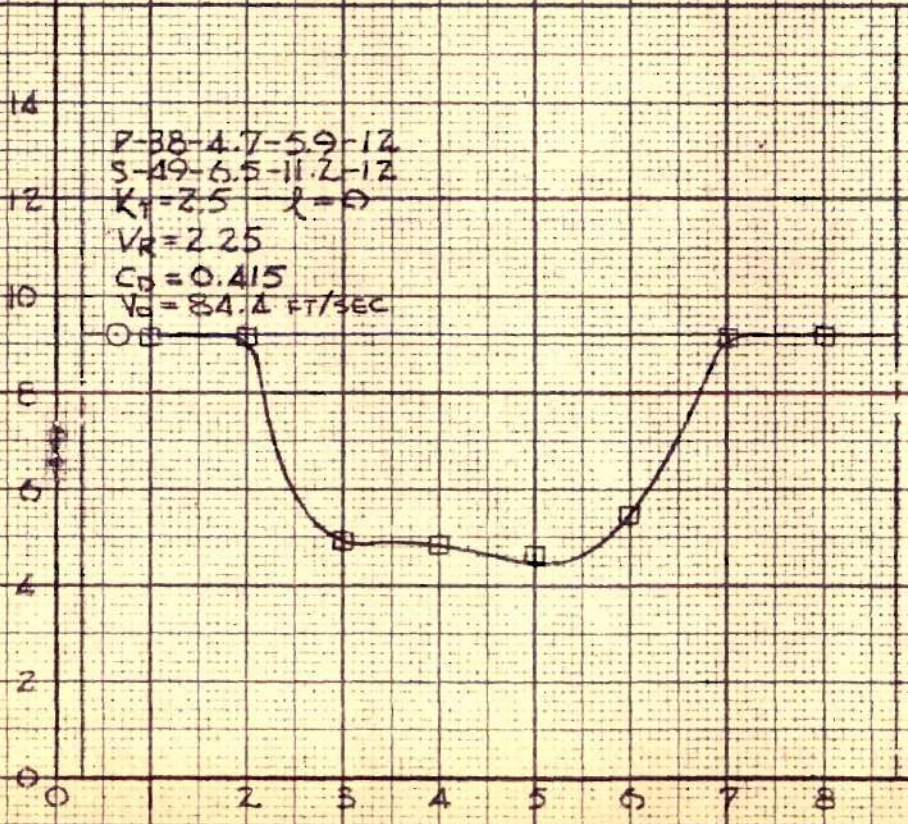

TUNNEL STATION, FORE & AFT SECTIONS

FIG. 24

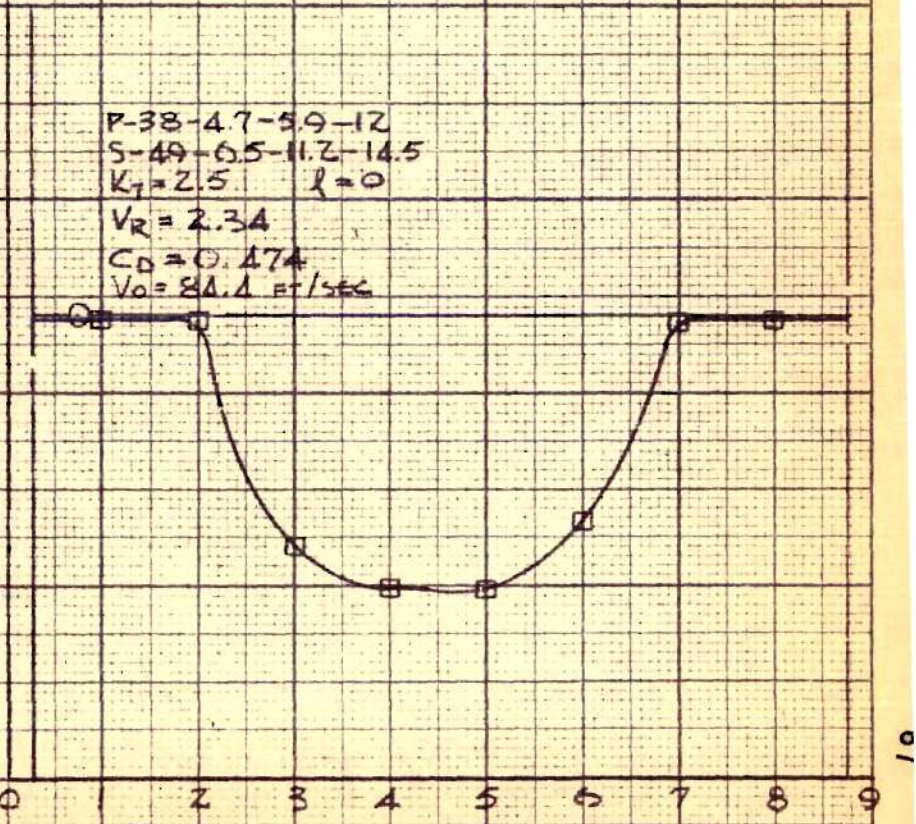

FIG. 25

TOTAL HEAD PRESSURES

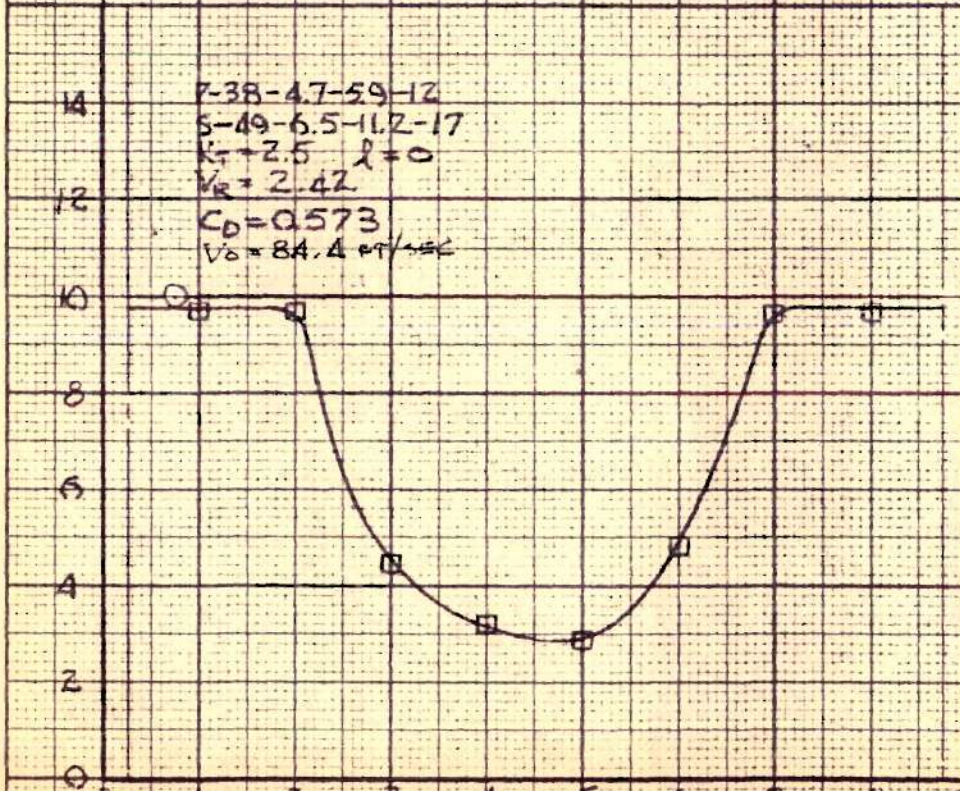

FIG. 26

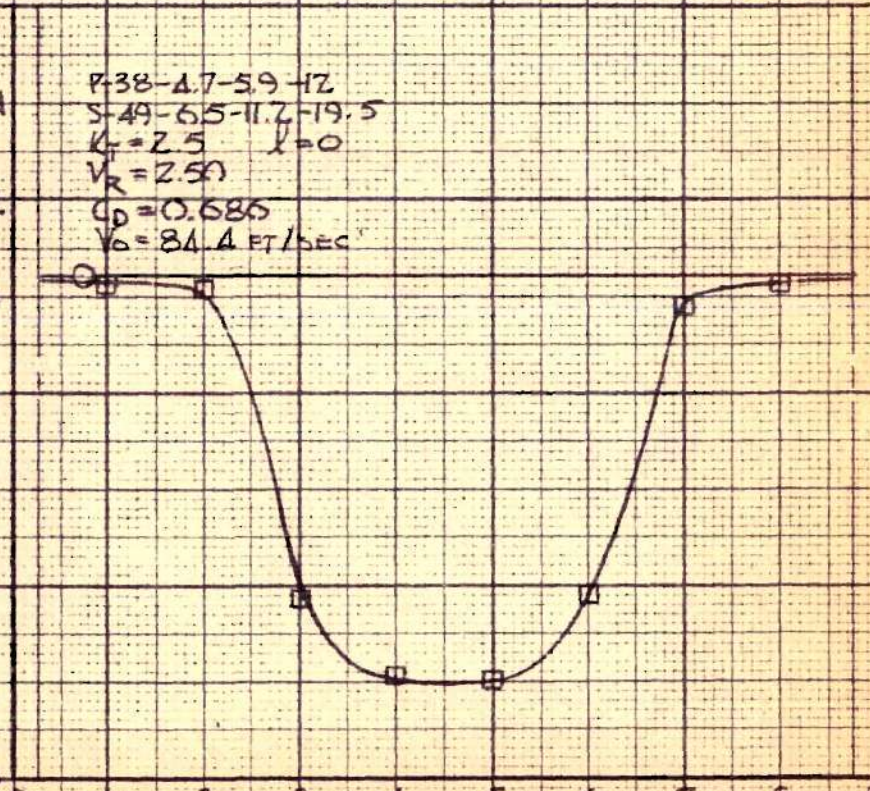

FIG. 27

TOTAL HEAD PRESSURES

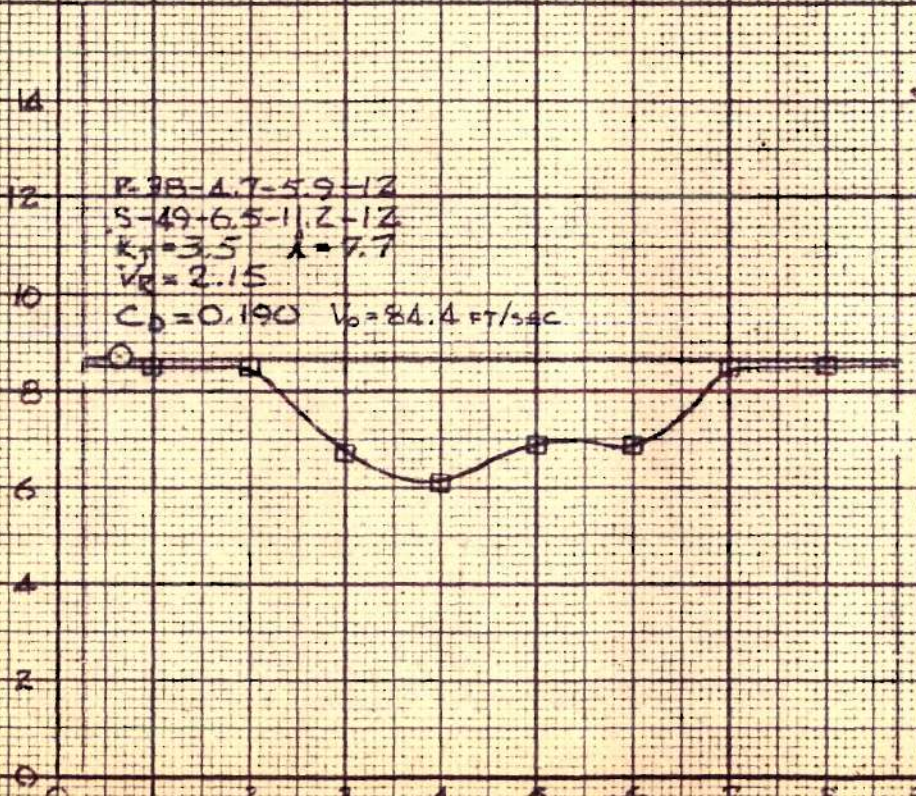

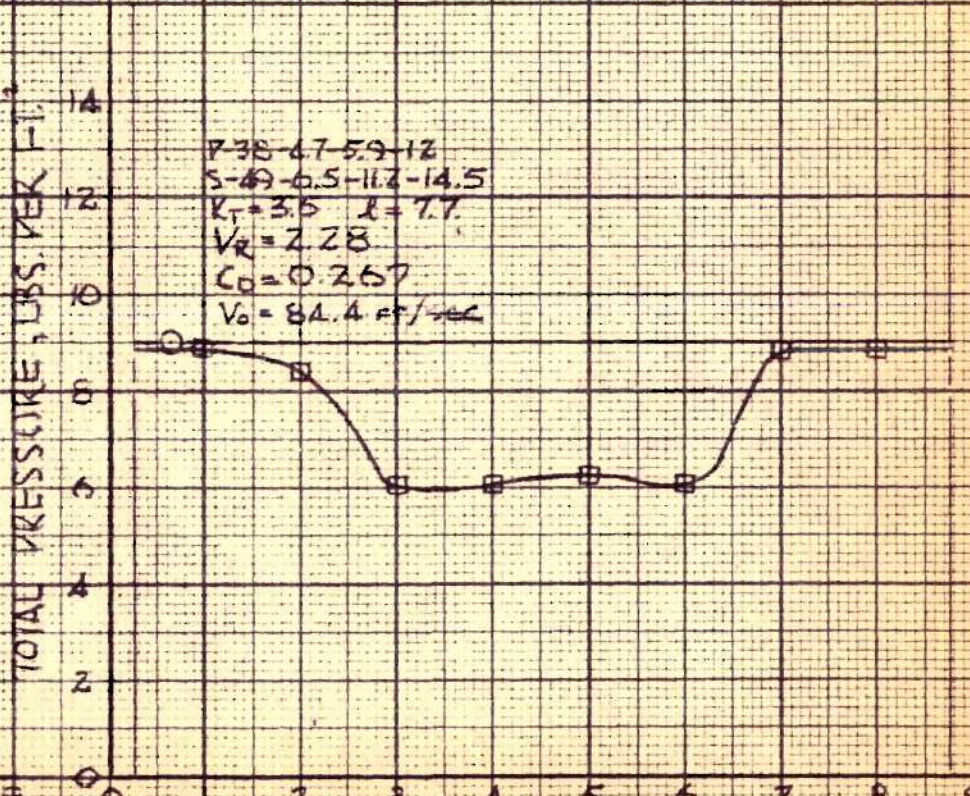

TOTAL PRESSURE, LBS PER FT²

TUNDEL STATION, FORE & AFT SECTIONS

FIG. 28 FIG. 29

TOTAL HEAD PRESSURES

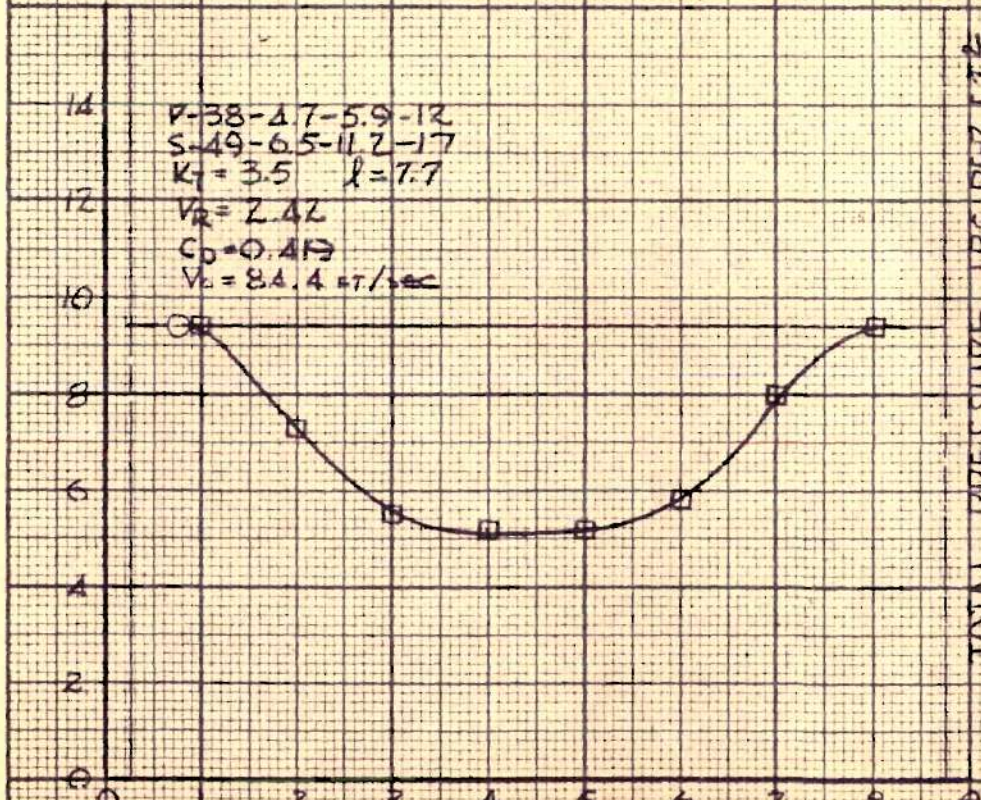

FIG. 30

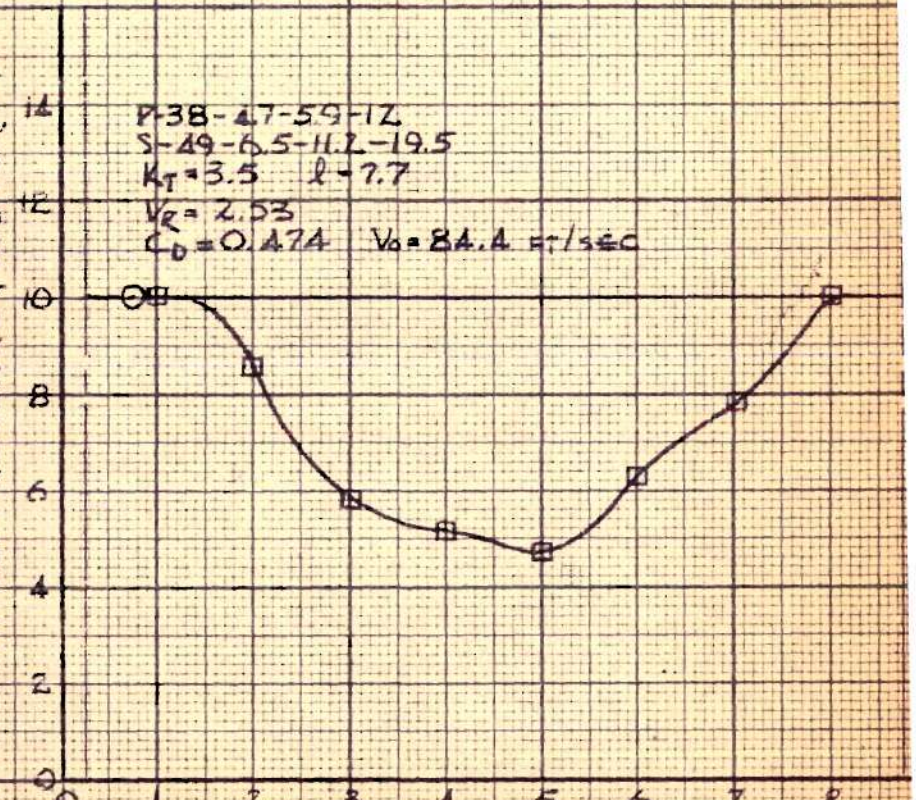

FIG. 31

TOTAL PRESSURE, LBS. PER FT.²

TUNNEL STATION, FORE & AFT SECTIONS

TOTAL HEAD PRESSURES

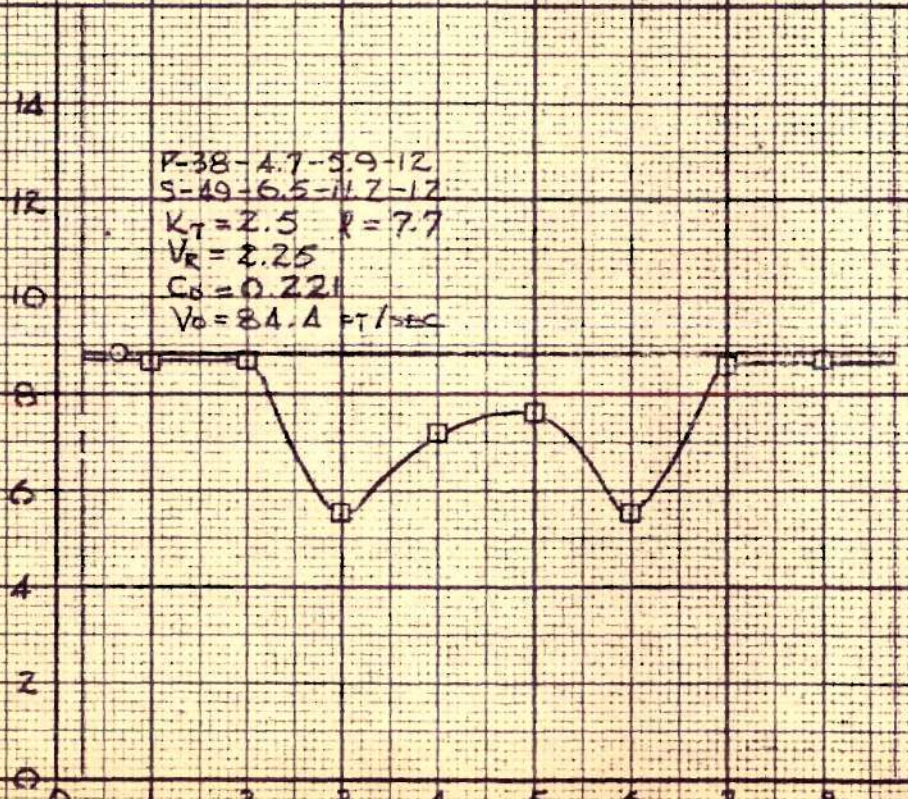

FIG. 32

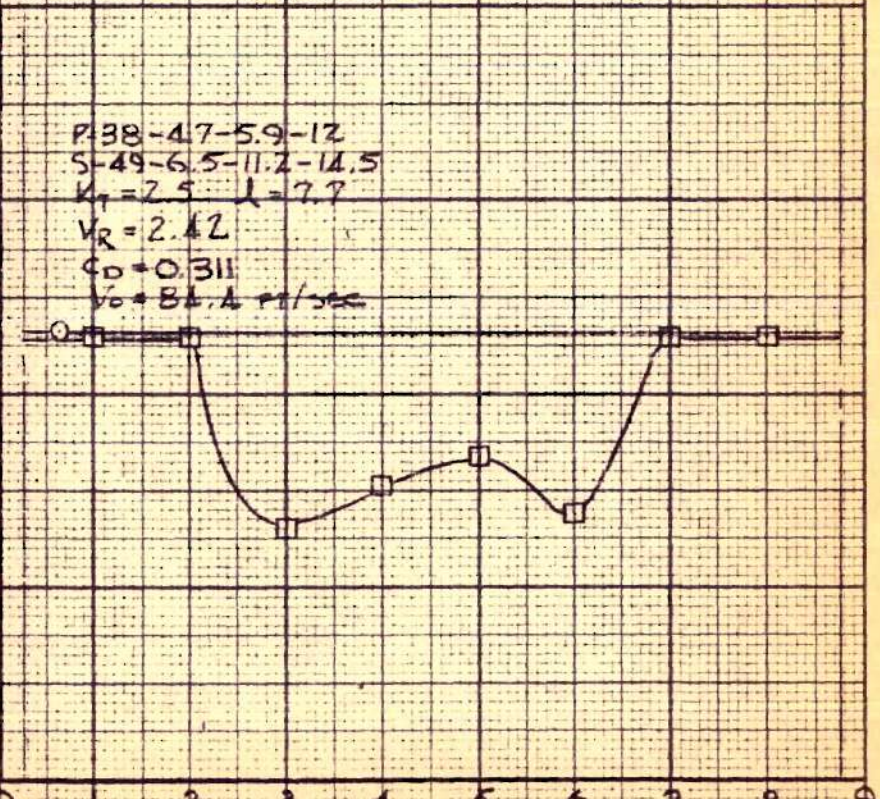

TUNNEL STATION, FORE & AFT SECTIONS

FIG. 33

TOTAL HEAD PRESSURES

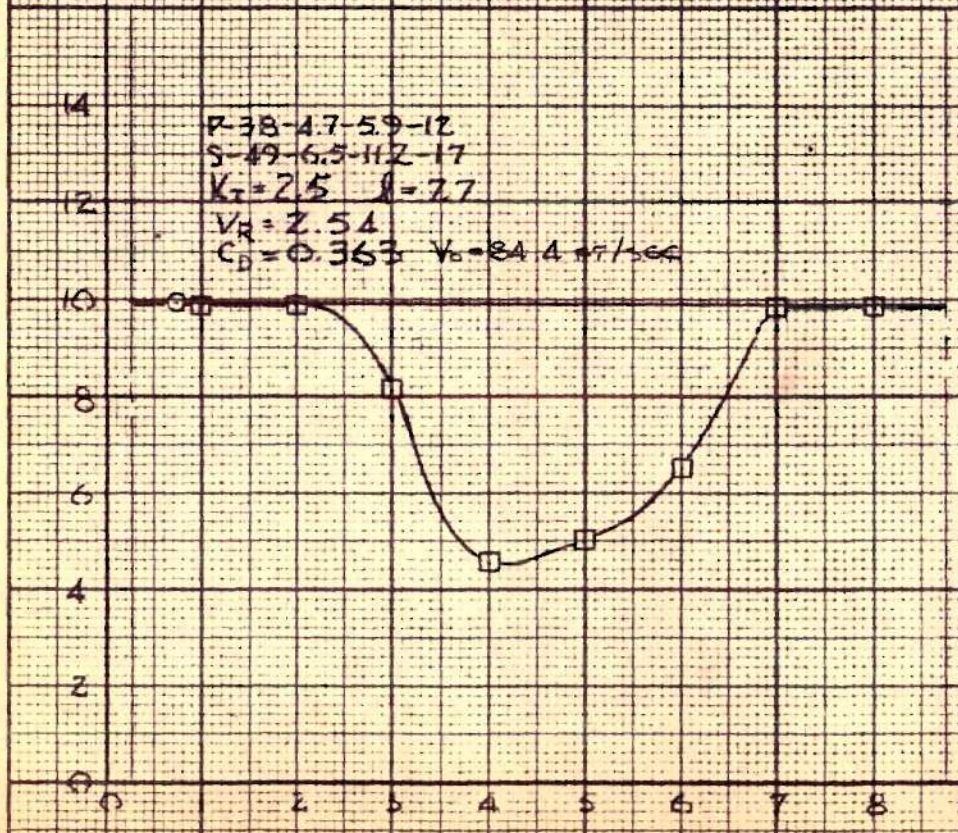

TUNDEL STATION, FORE & AFT SECTIONS

FIG. 34

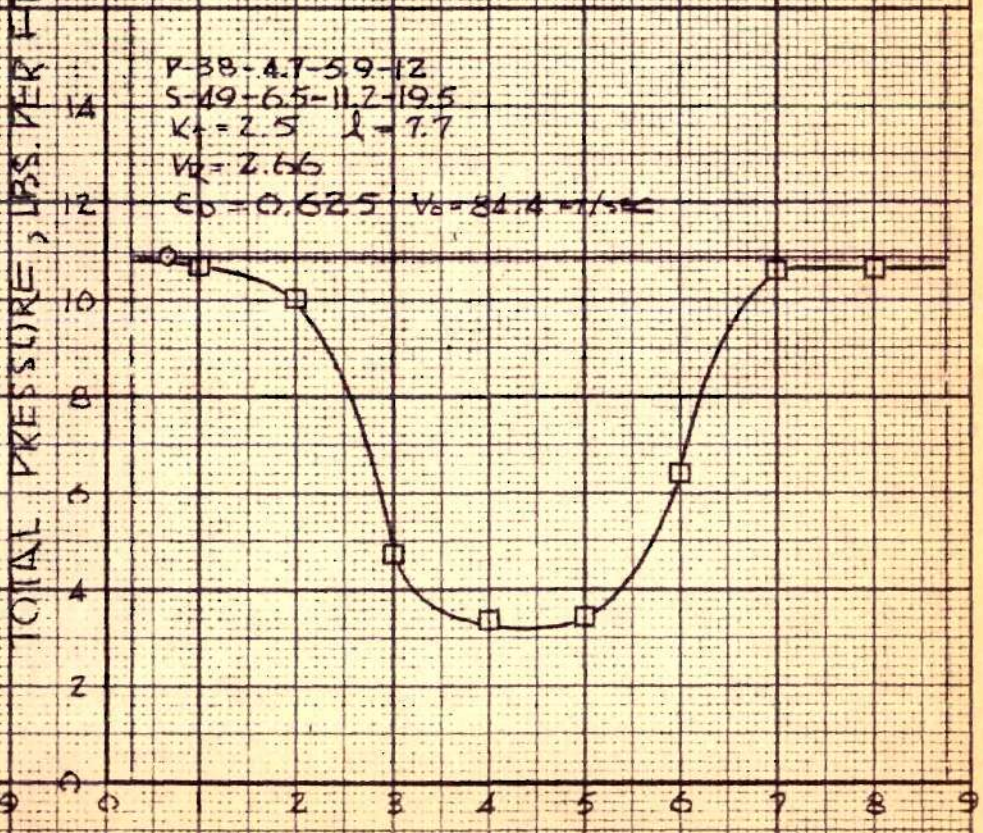

FIG. 35

TOTAL HEAD PRESSURES

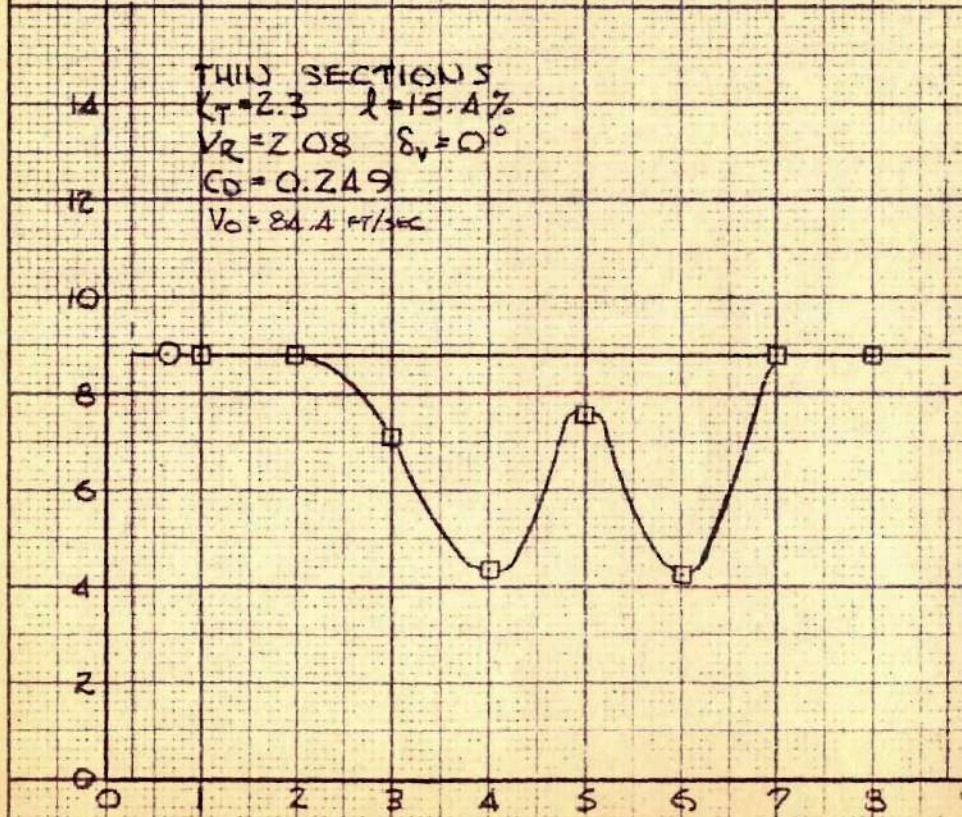

FIG. 36

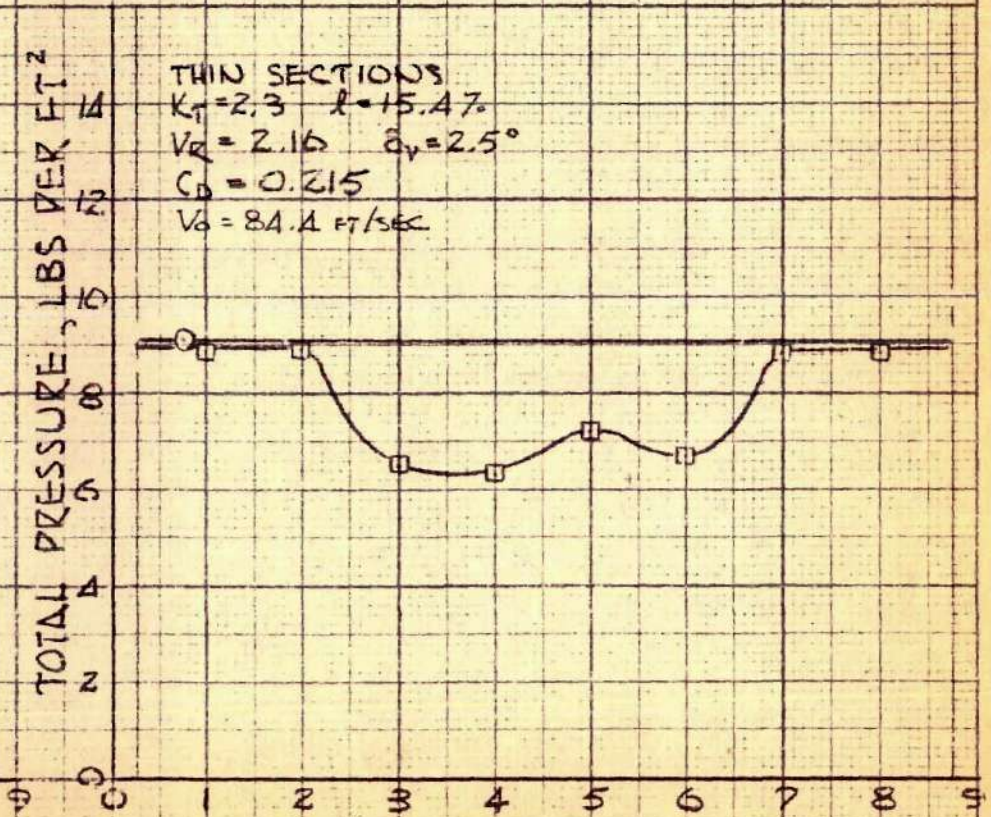

TUNNEL STATION, FORE & AFT SECTIONS

FIG. 37

TOTAL HEAD PRESSURES

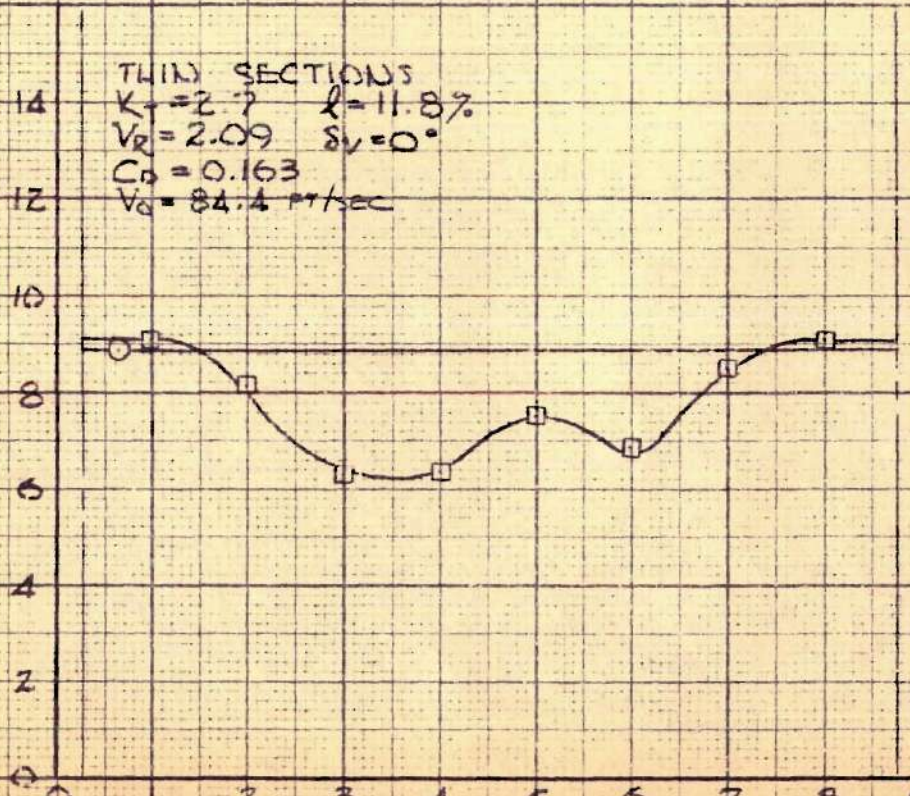

FIG. 38

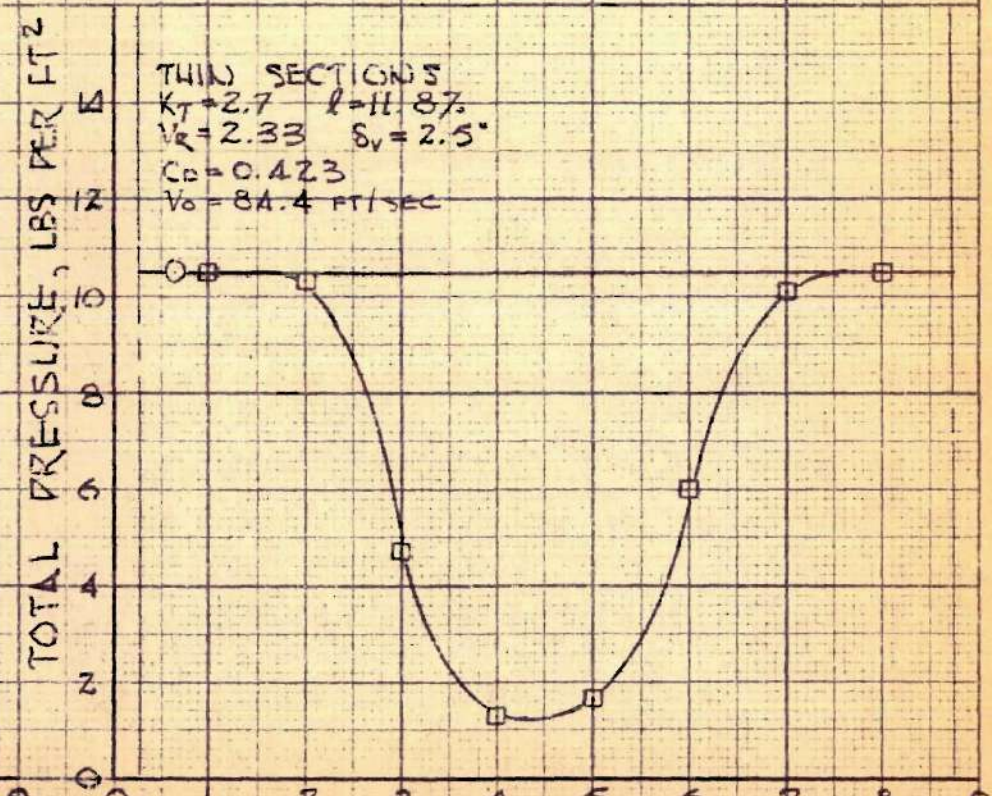

FIG. 39

TOTAL HEAD PRESSURES

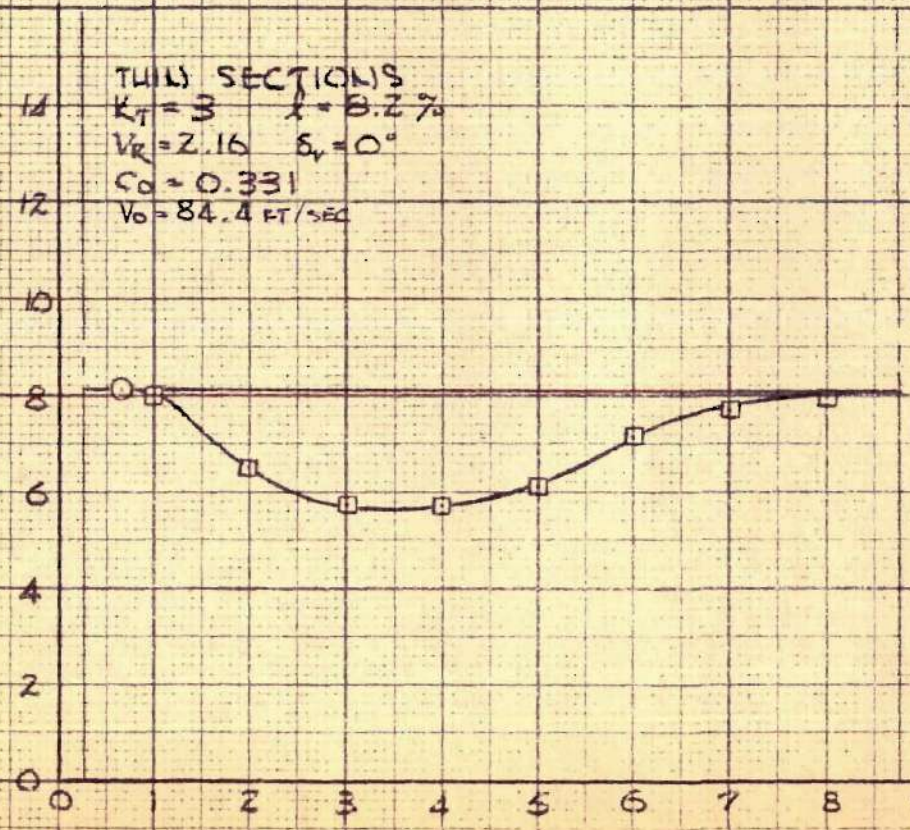

FIG. 40

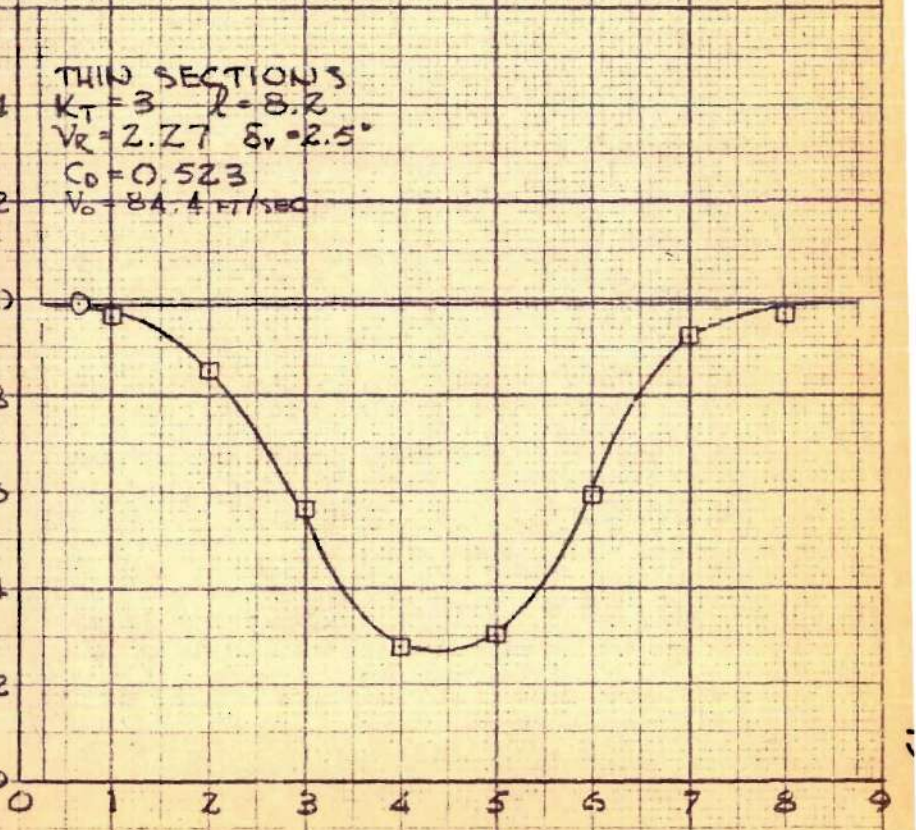

FIG. 41

TOTAL PRESSURE, LBS PER FT^2

TUNNEL STATION, FORE & AFT SECTIONS

TOTAL HEAD PRESSURES

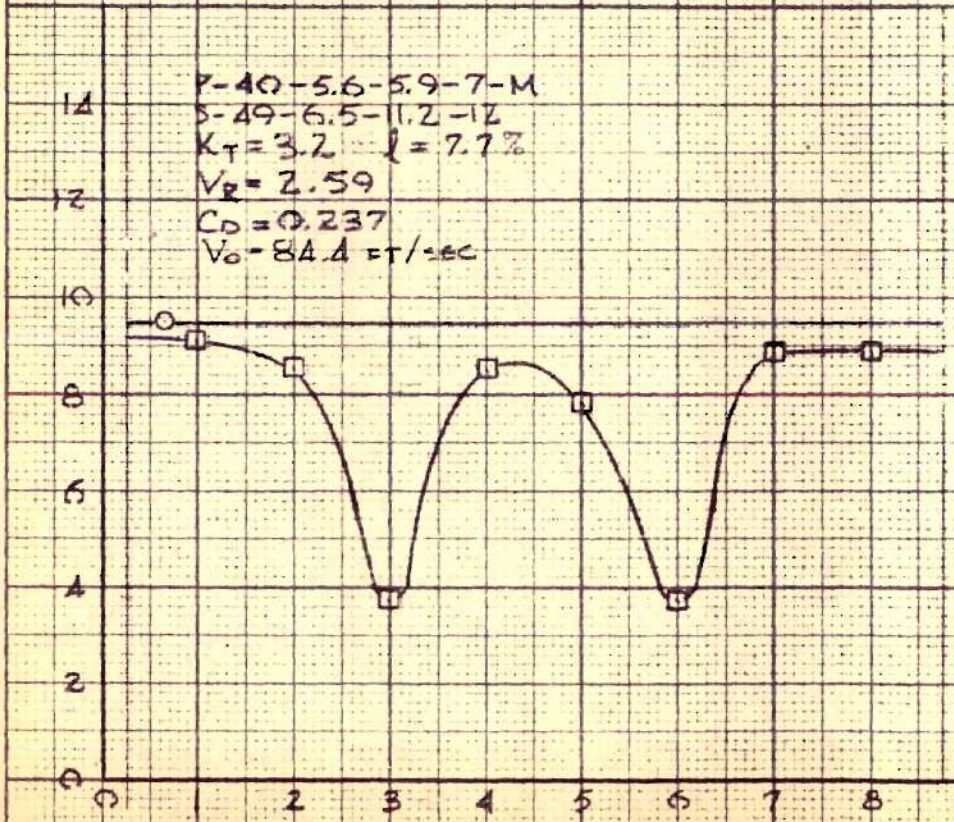

TUNNEL STATION, FORE & AFT SECTIONS

FIG. 42

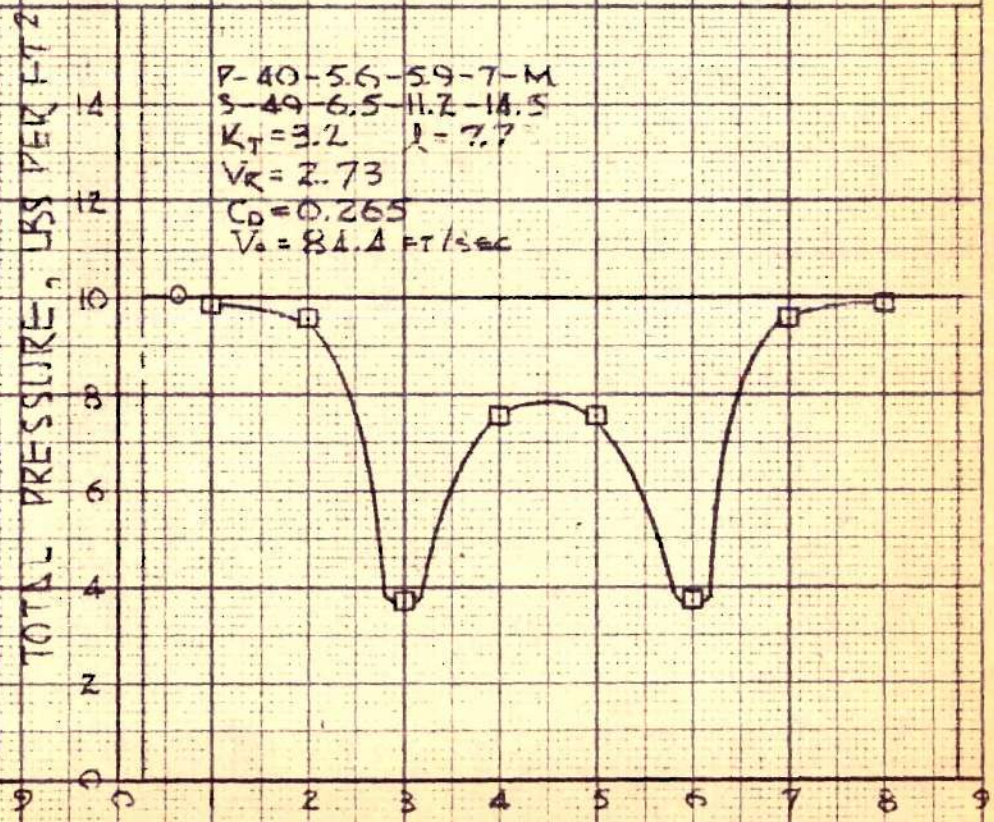

FIG. 43

TOTAL HEAD PRESSURES

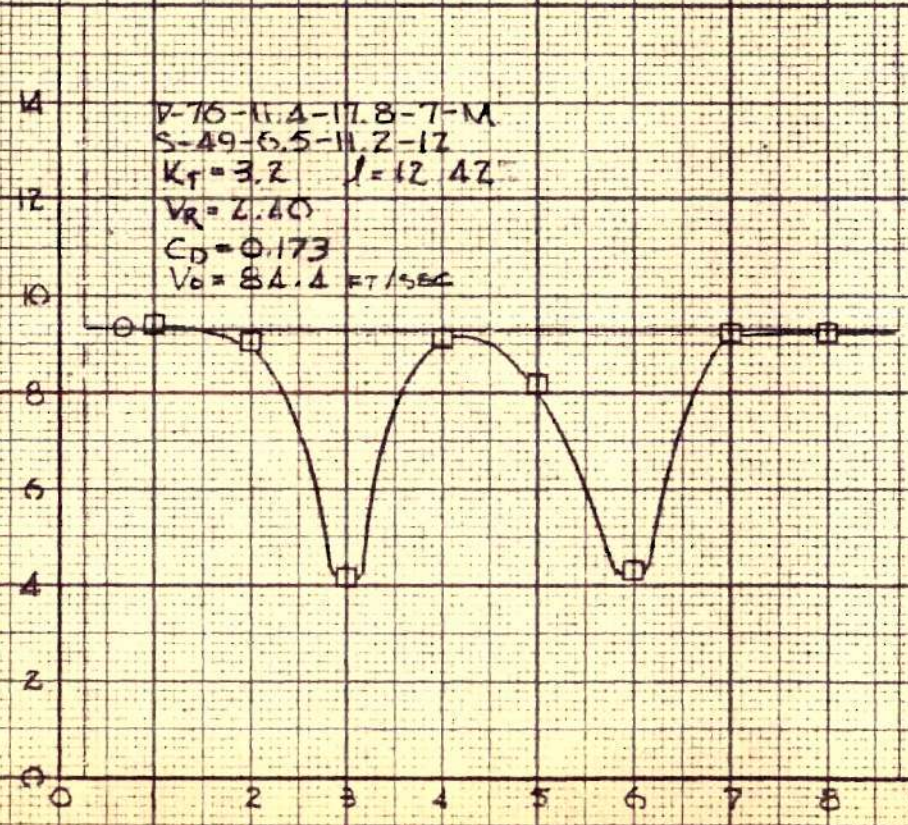

FIG. 44

TOTAL PRESSURES, LBS PER FT²

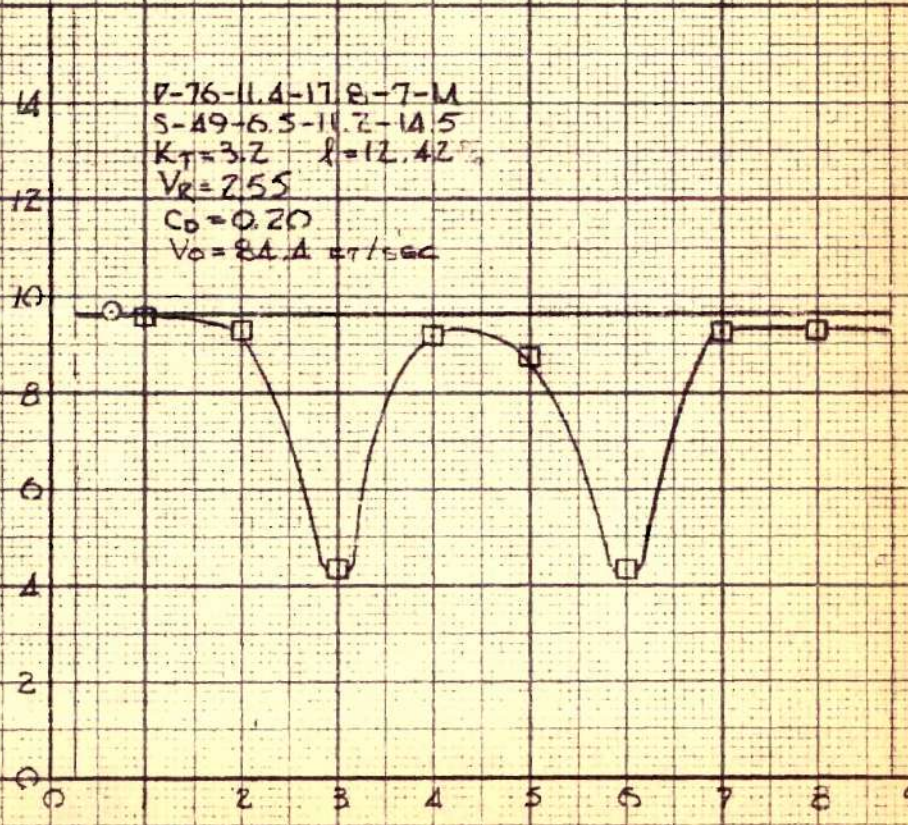

FIG. 45

TUNNEL STATION, FORE & AFT SECTIONS

TOTAL HEAD PRESSURES

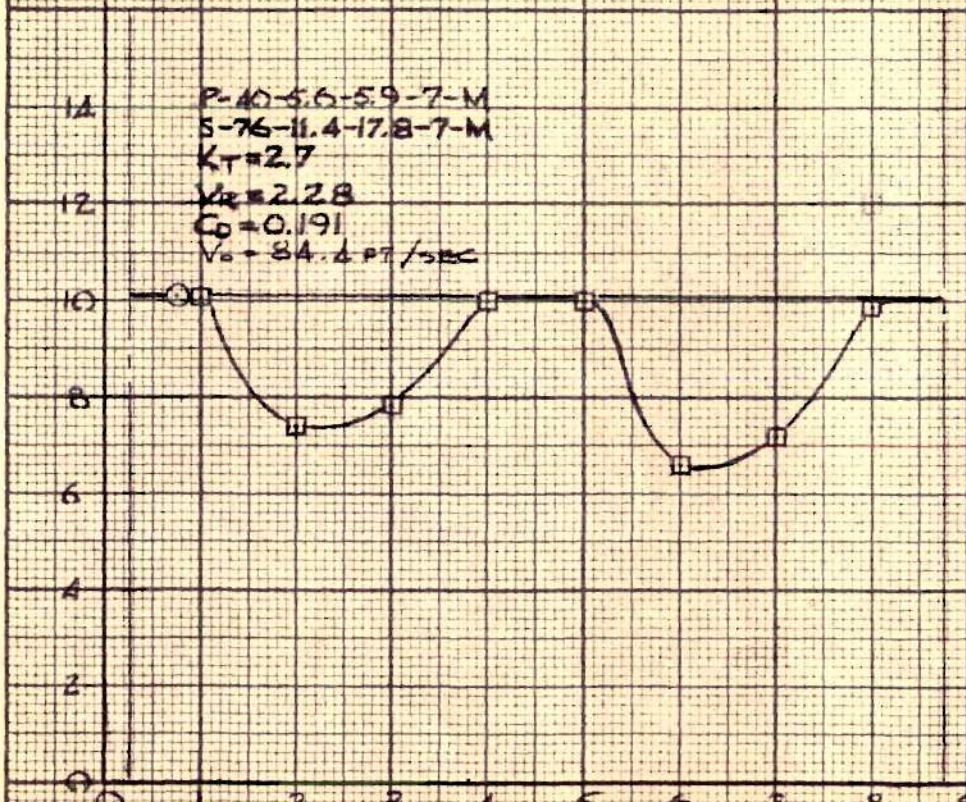

TUNNEL STATION, FORE & AFT SECTIONS

FIG. 46

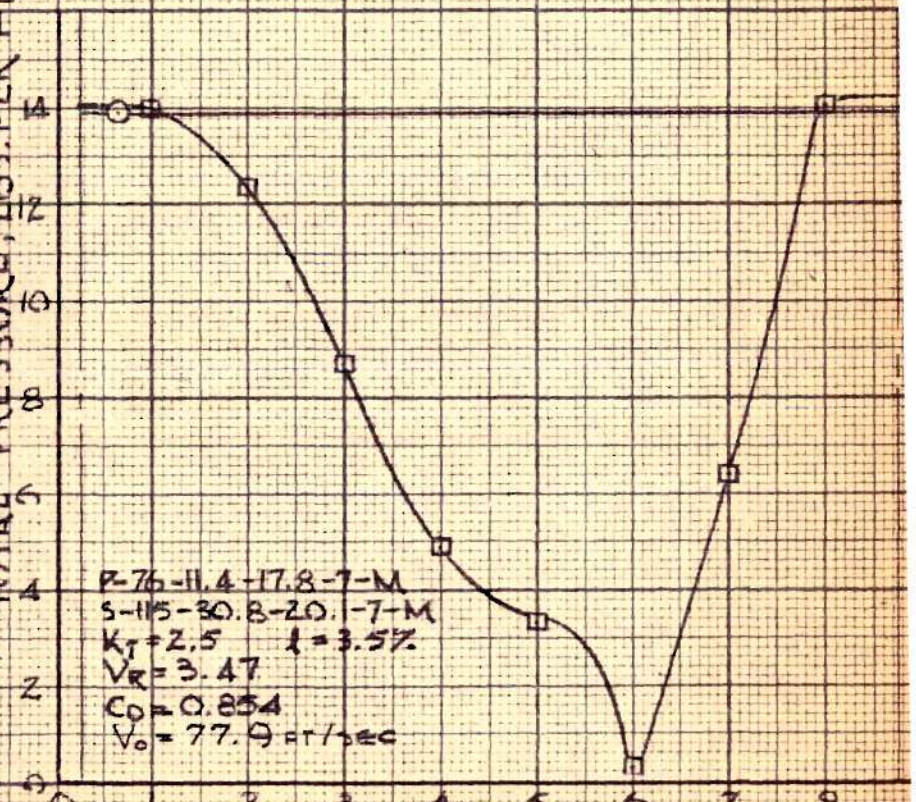

FIG. 47

TOTAL HEAD PRESSURES

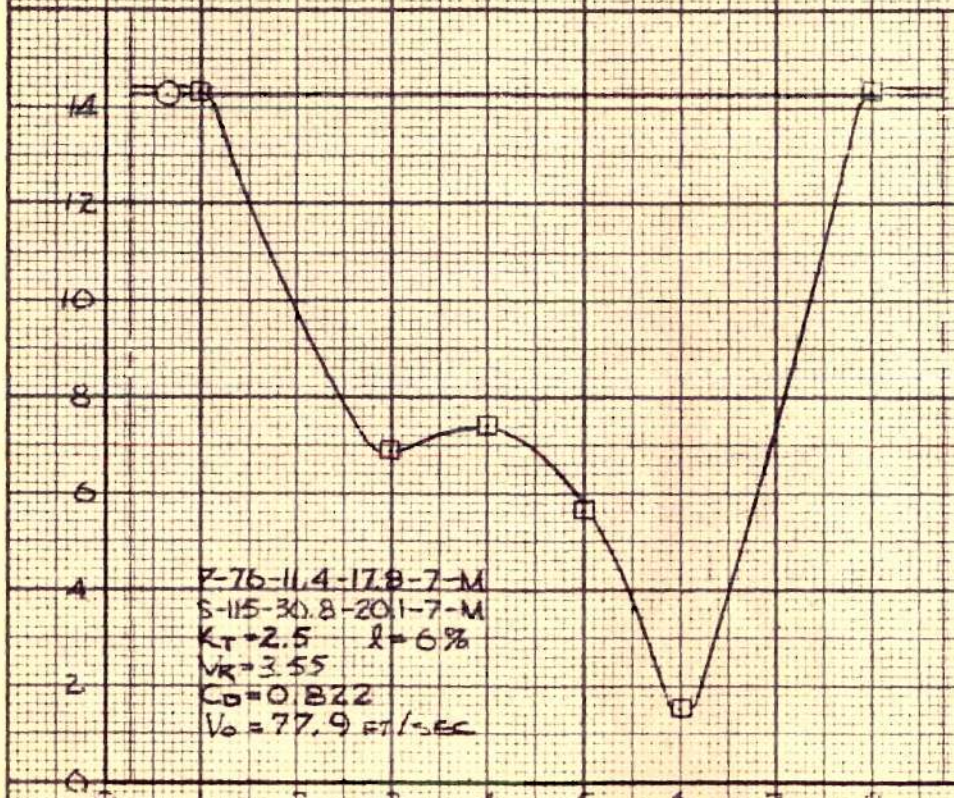

FIG. 48

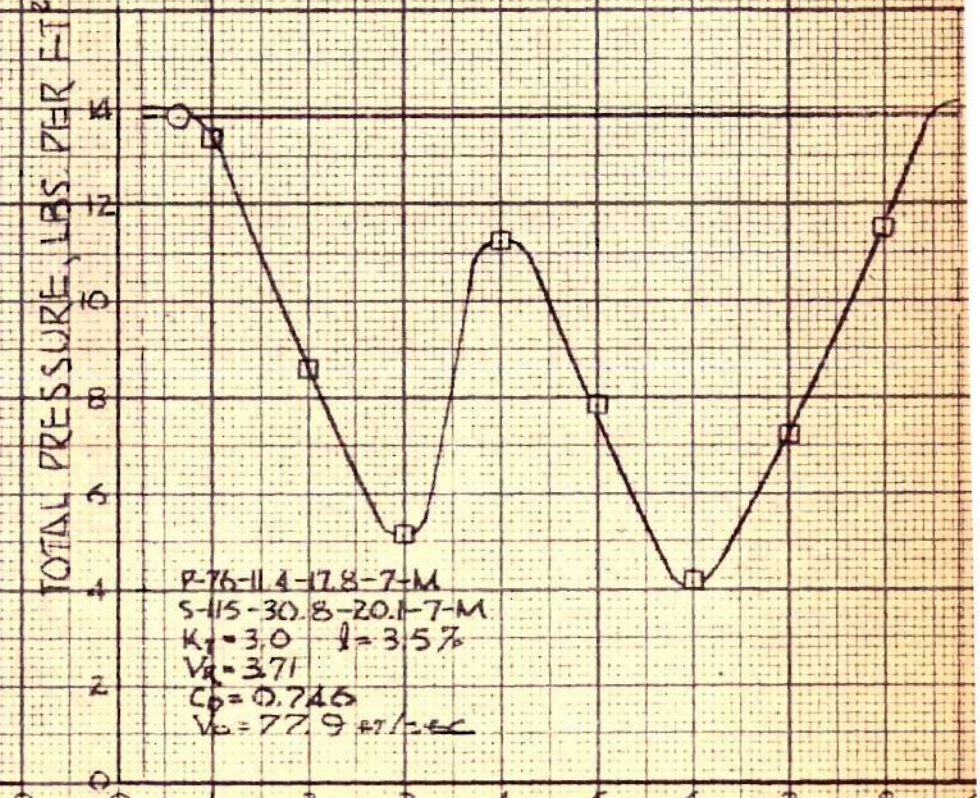

FIG. 49

TOTAL HEAD PRESSURES

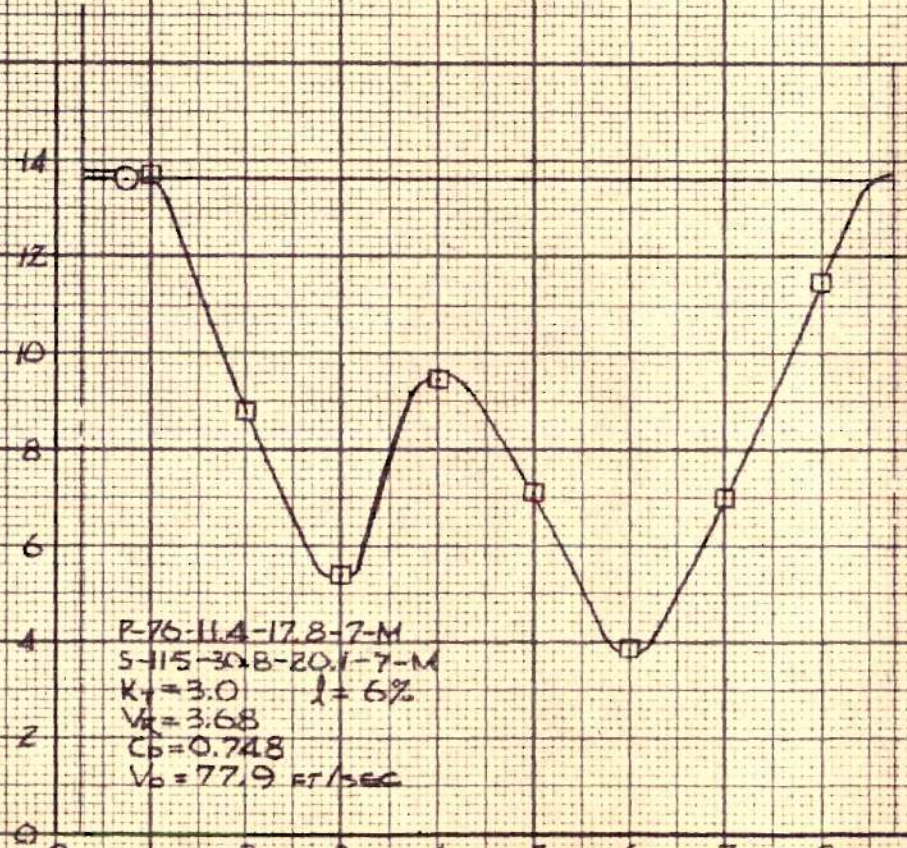

TOTAL PRESSURE, LBS./FT.^{2}

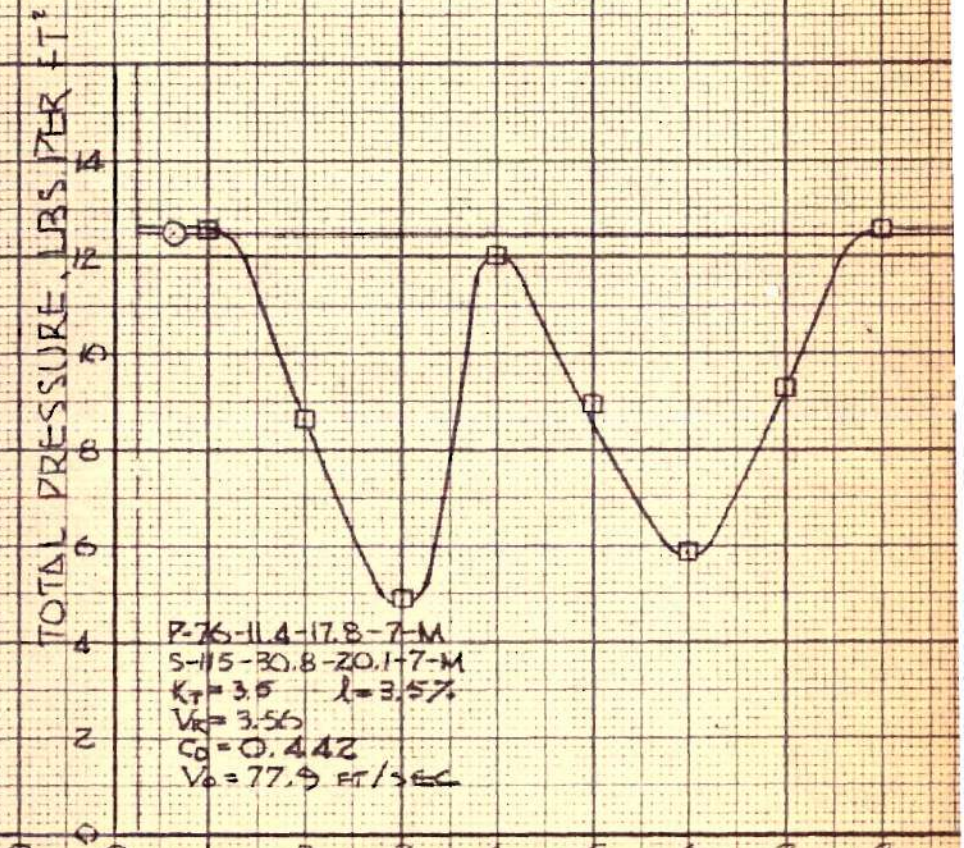

TUNNEL STATION, FORE & AFT SECTIONS

FIG. 50 FIG. 51

TOTAL HEAD PRESSURES

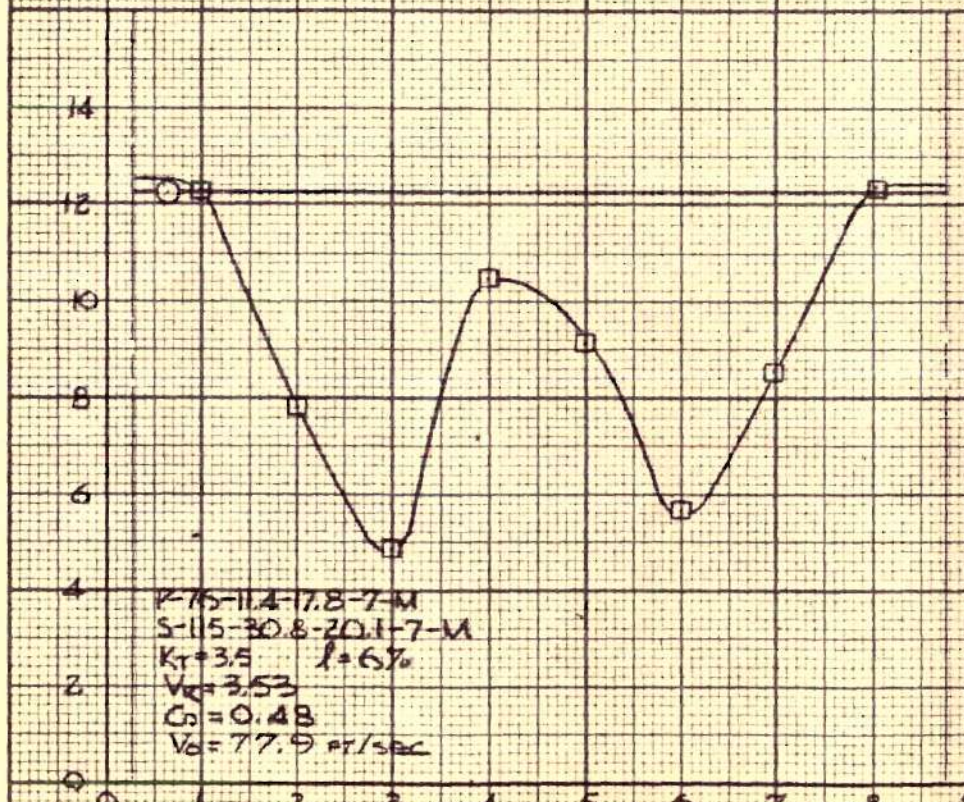

FIG. 52

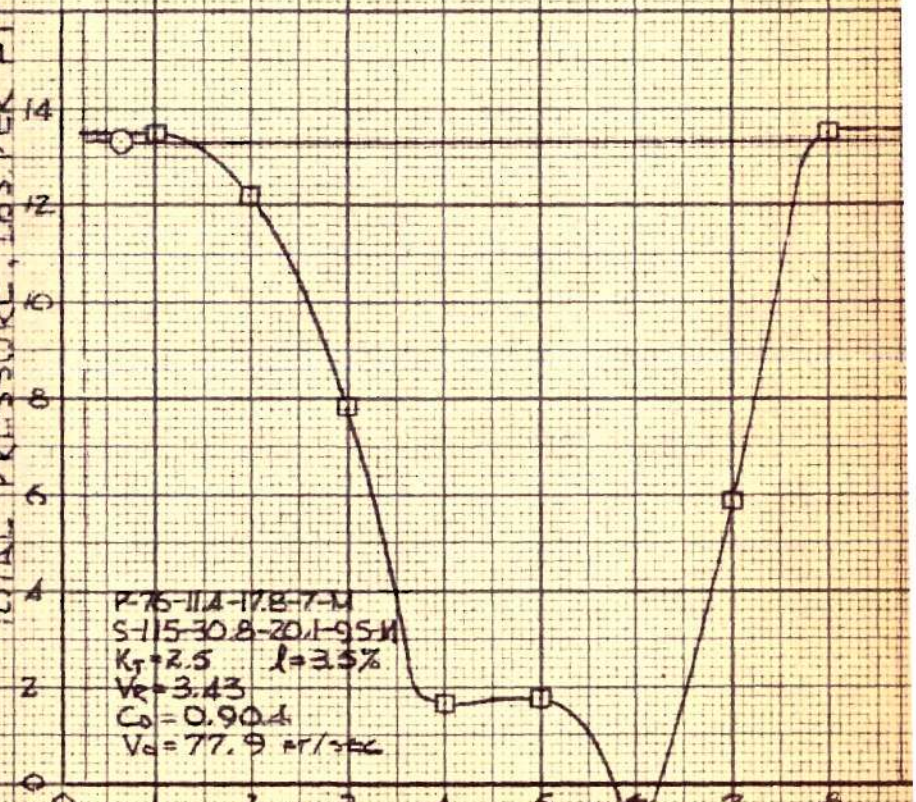

FIG. 53

TOTAL HEAD PRESSURES

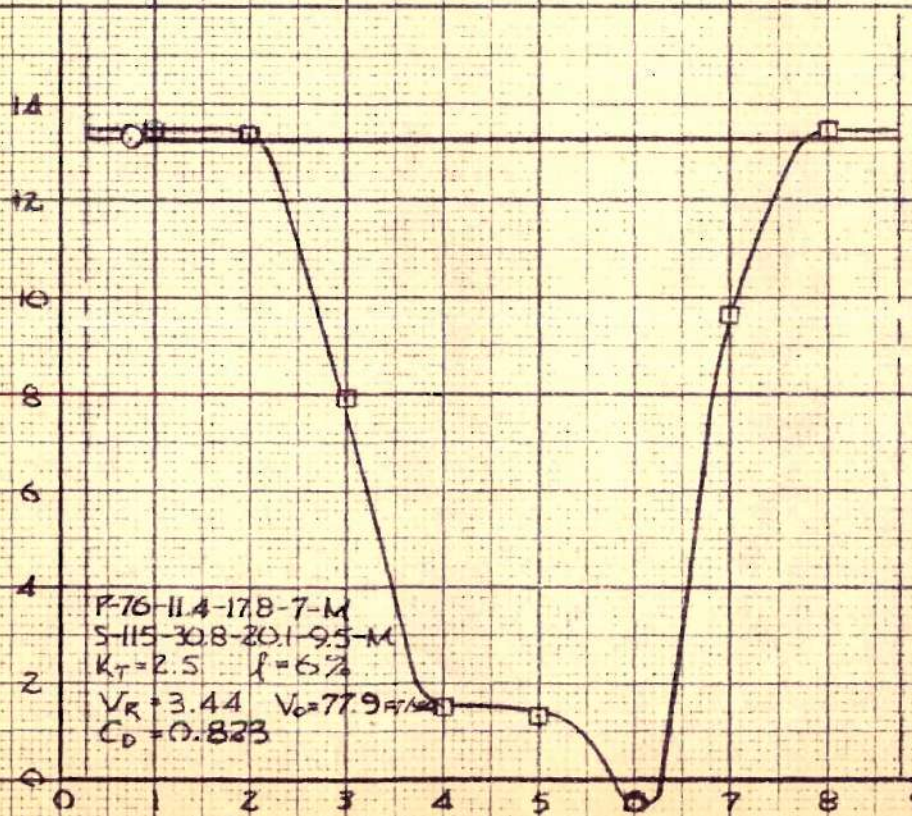

FIG. 54

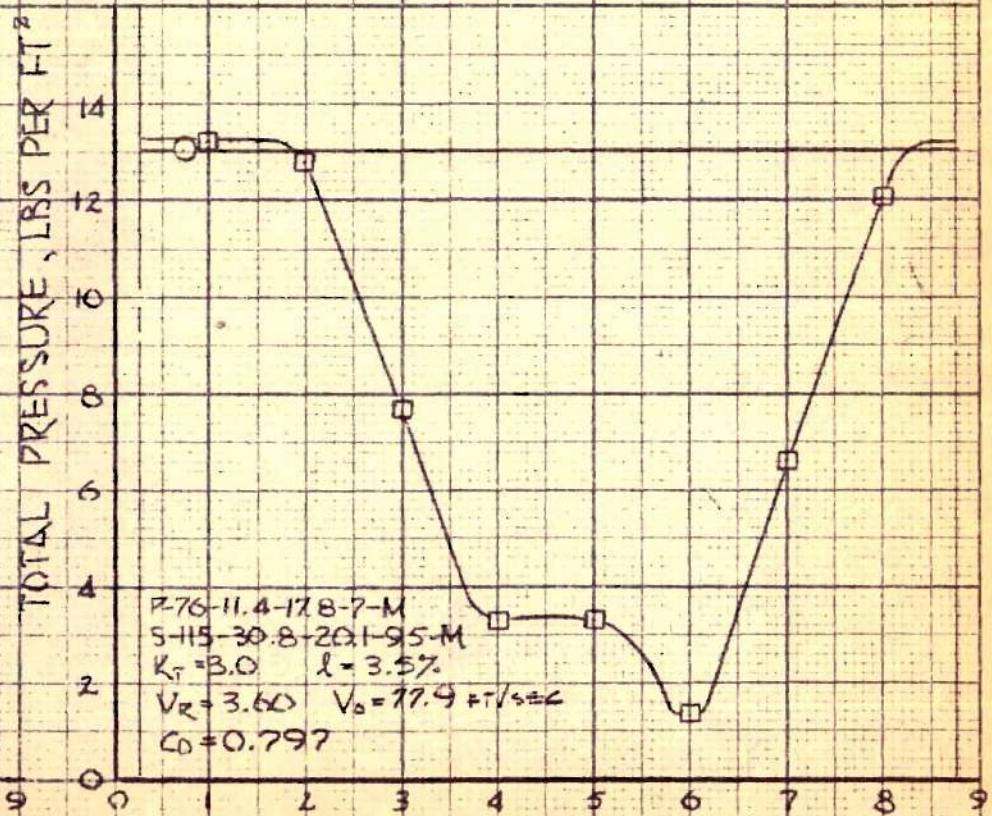

FIG. 55

TOTAL PRESSURE, LBS PER FT^2

TUNDEL STATION, FORE & AFT SECTIONS

TOTAL HEAD PRESSURES

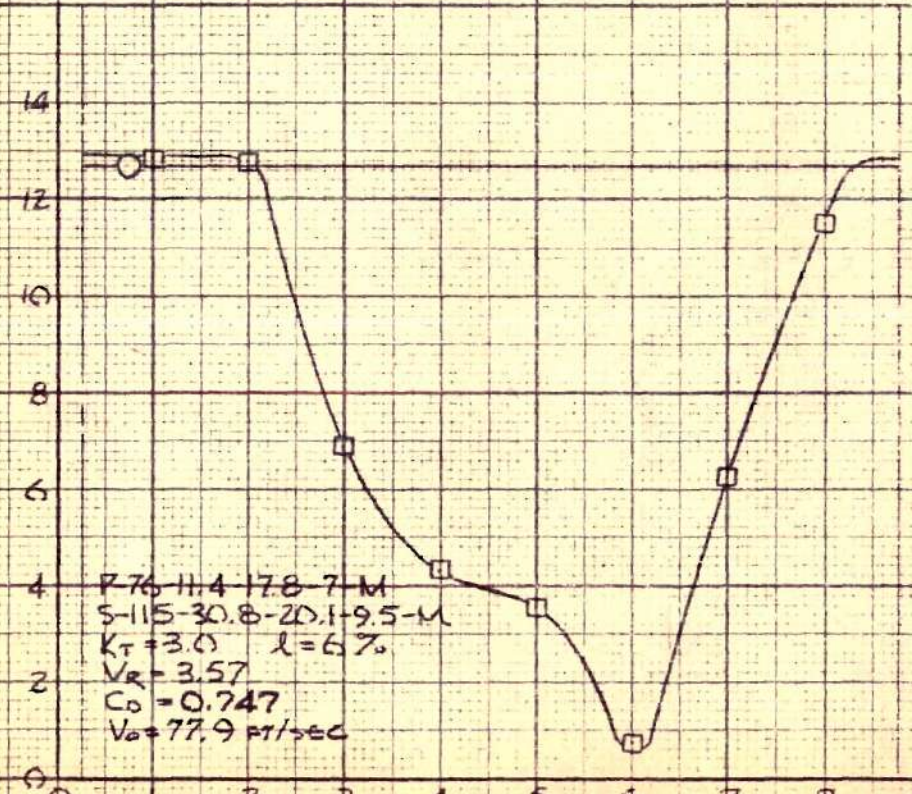

FIG. 56

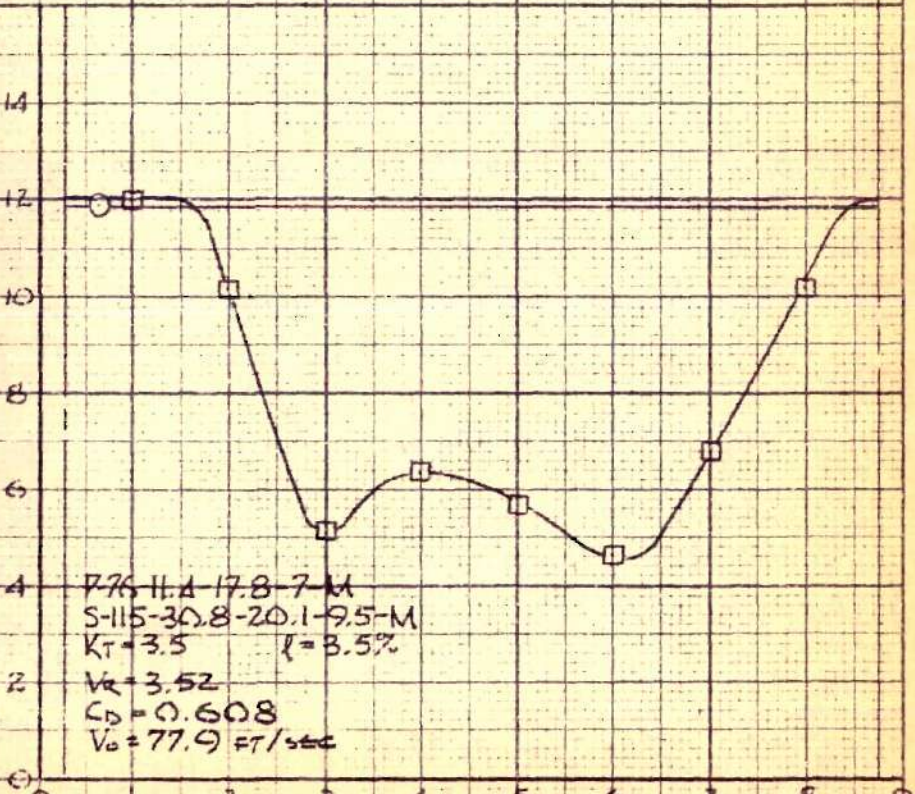

FIG. 57

TOTAL PRESSURE, LBS PER FT²

TUNNEL STATION, FORE & AFT SECTIONS

TOTAL HEAD PRESSURES

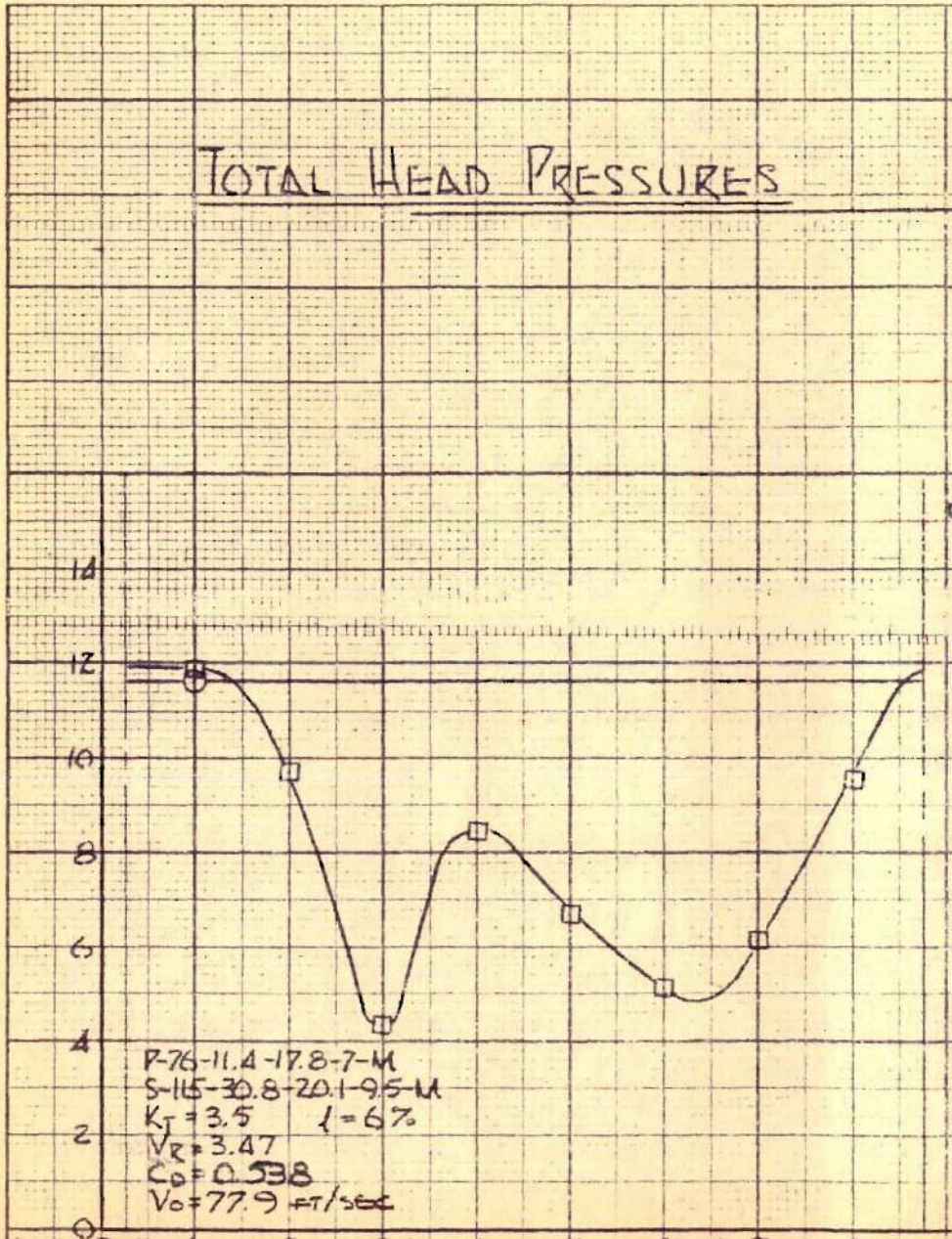

FIG. 58

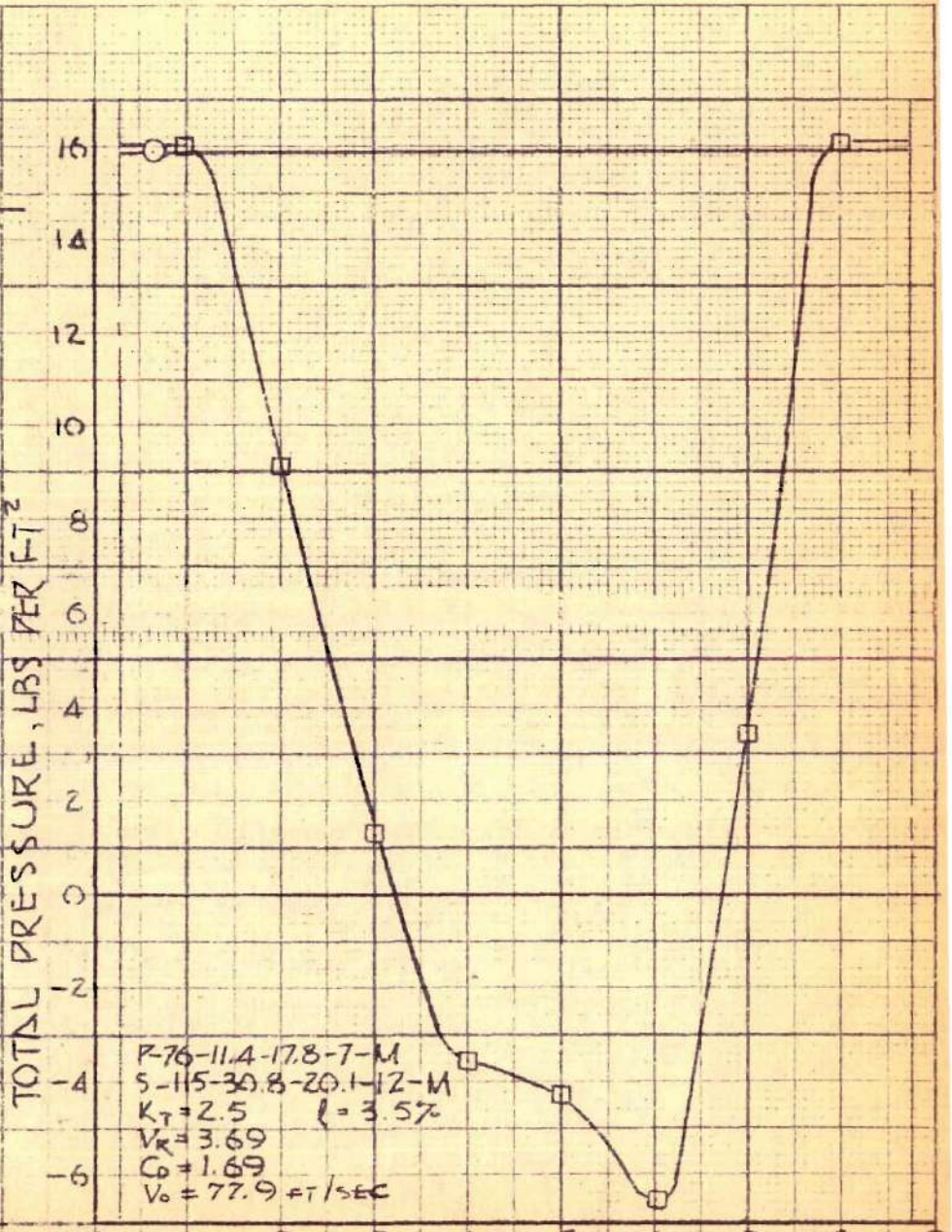

FIG. 59

TOTAL PRESSURE, LBS PER FT^2

TUNNEL STATION, FORE & AFT SECTIONS

TOTAL HEAD PRESSURES

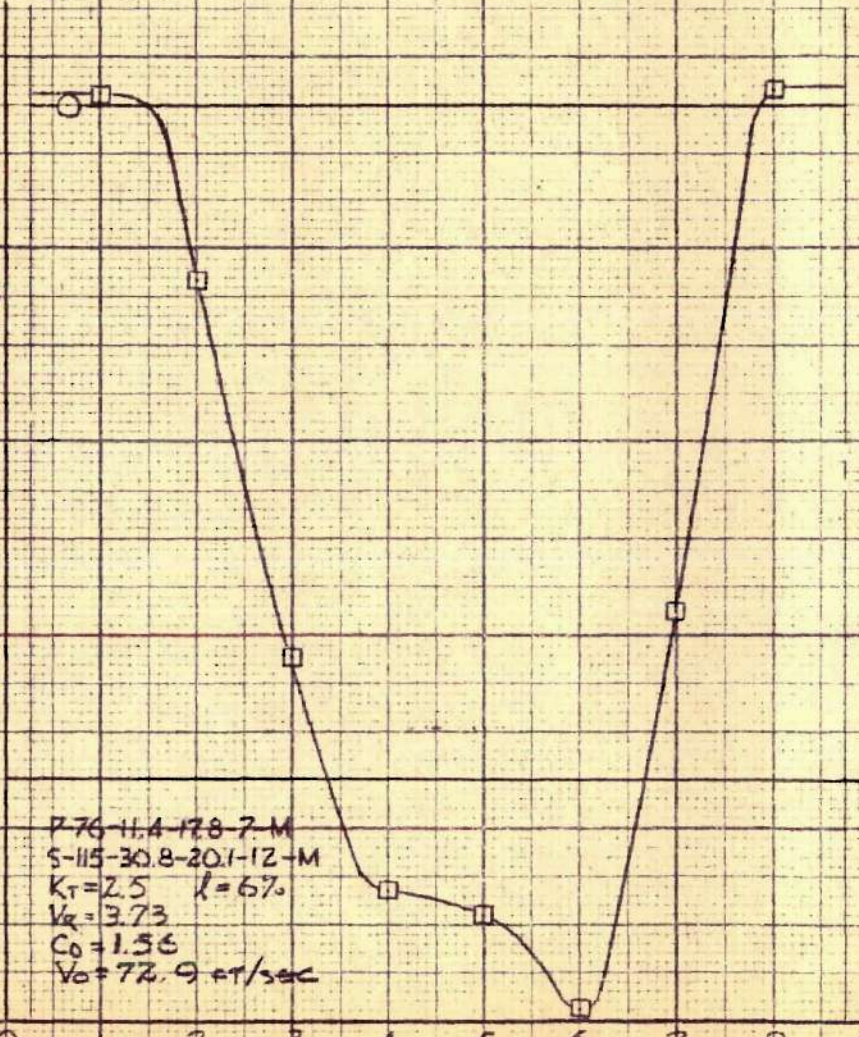

FIG. 60

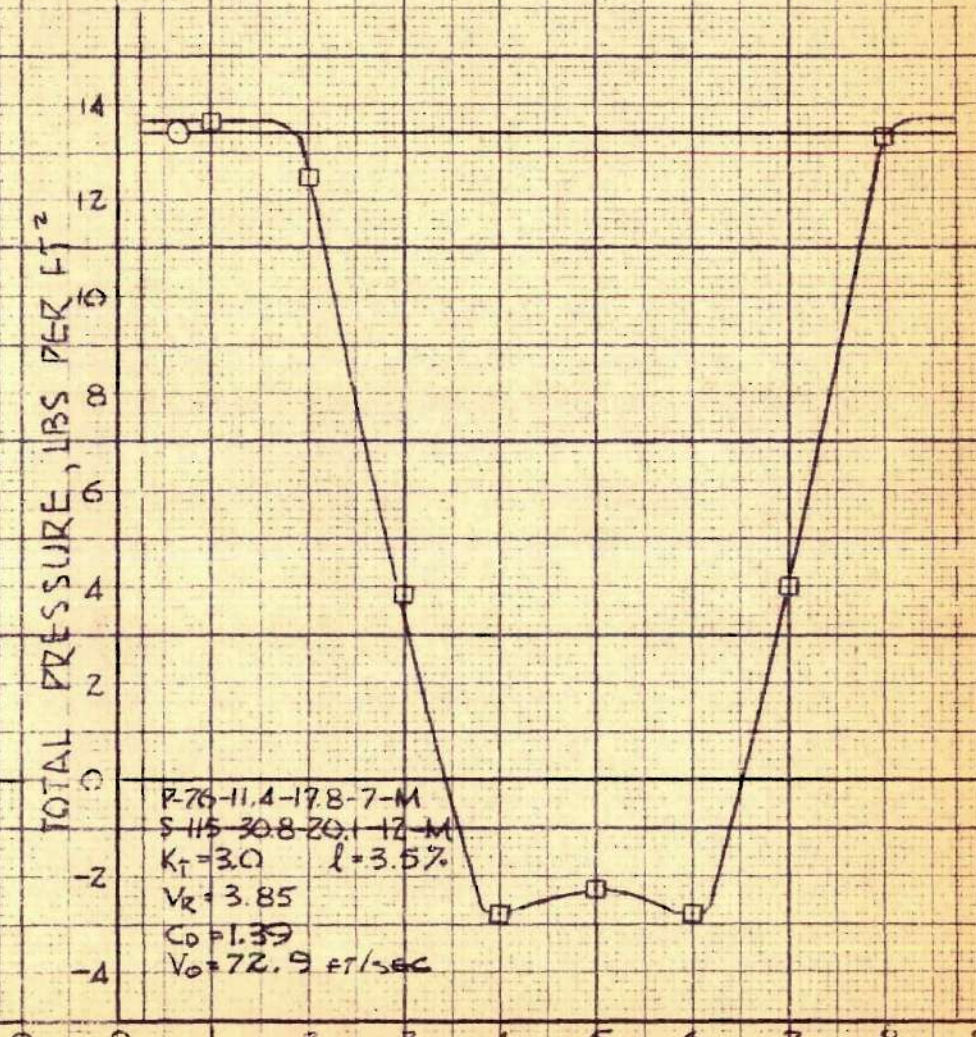

FIG. 61

TOTAL HEAD PRESSURES

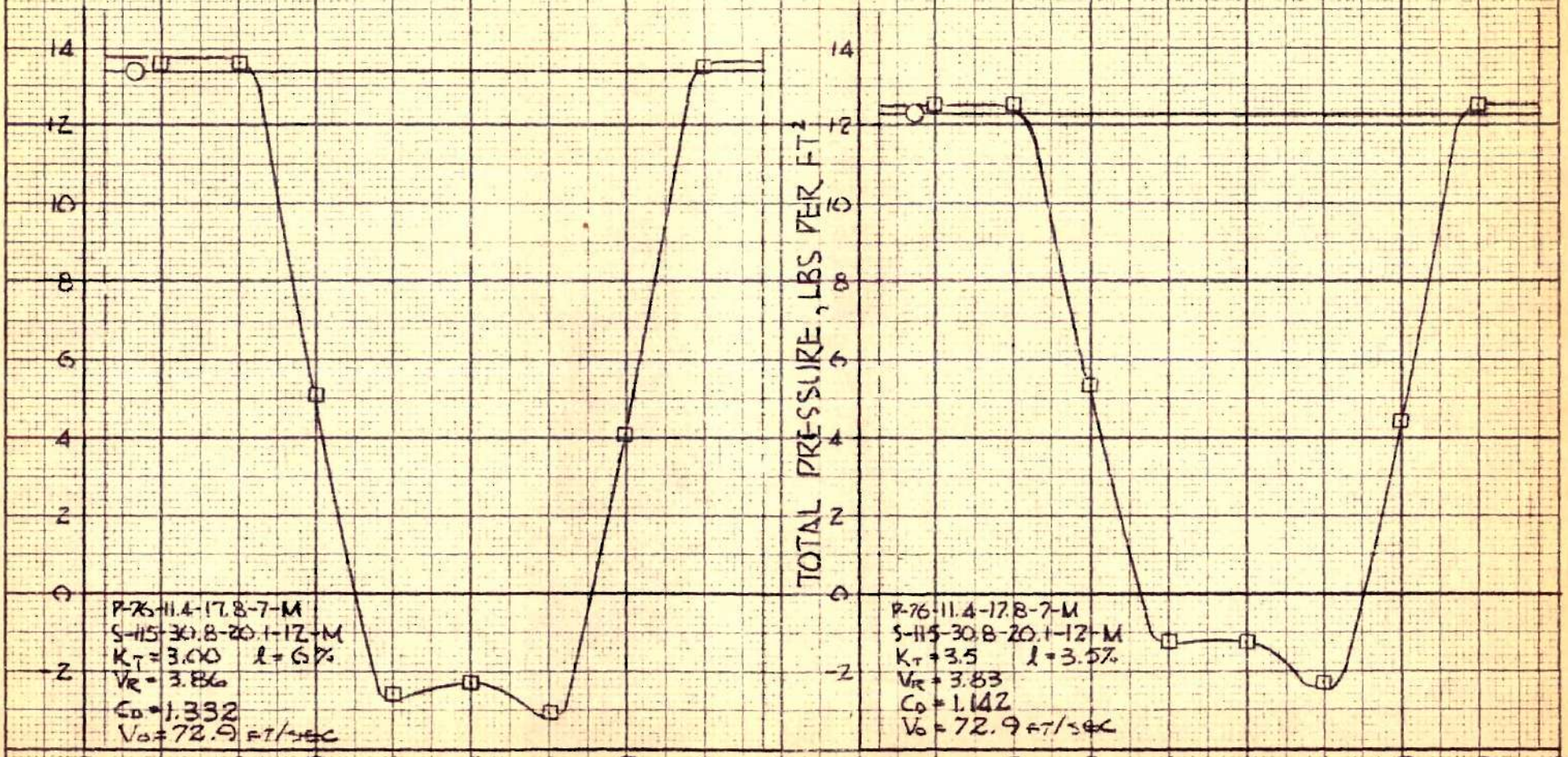

FIG. 62 FIG. 63

TOTAL HEAD PRESSURES

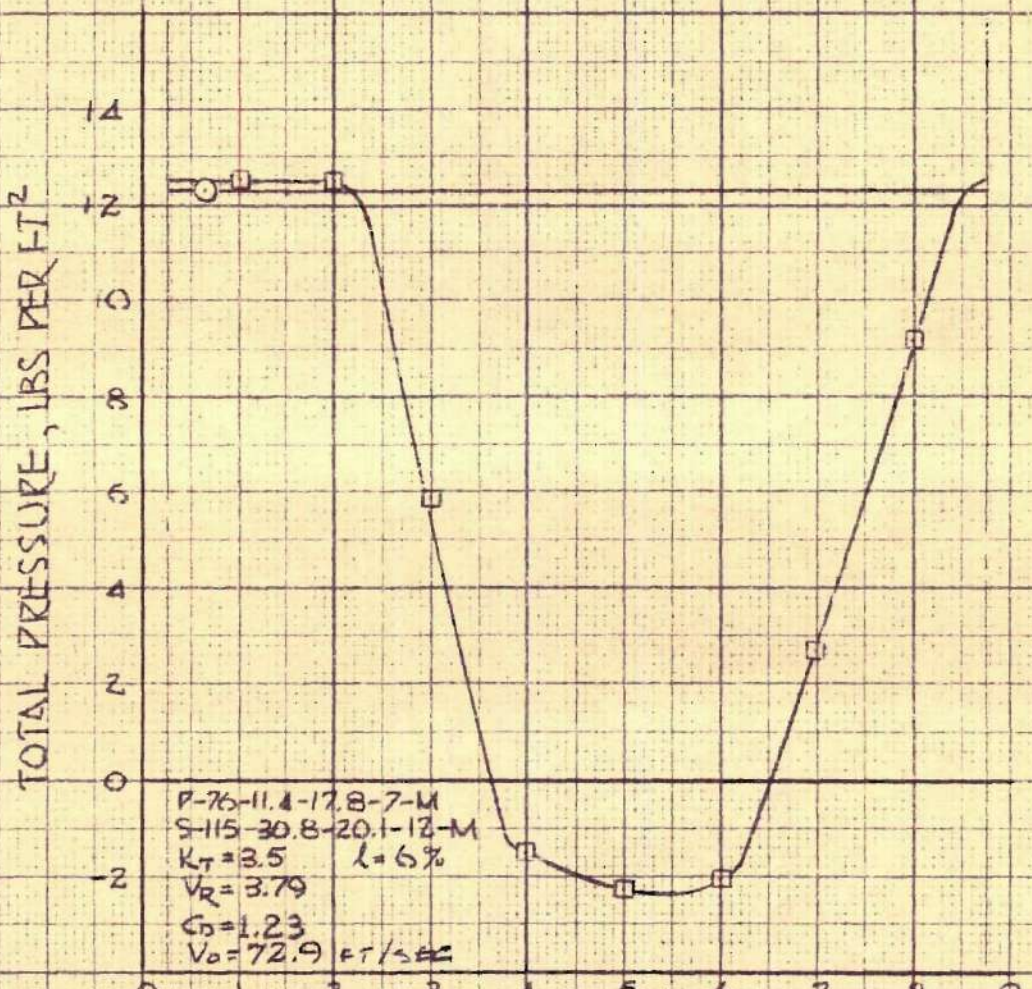

FIG. 64

TOTAL HEAD PRESSURES

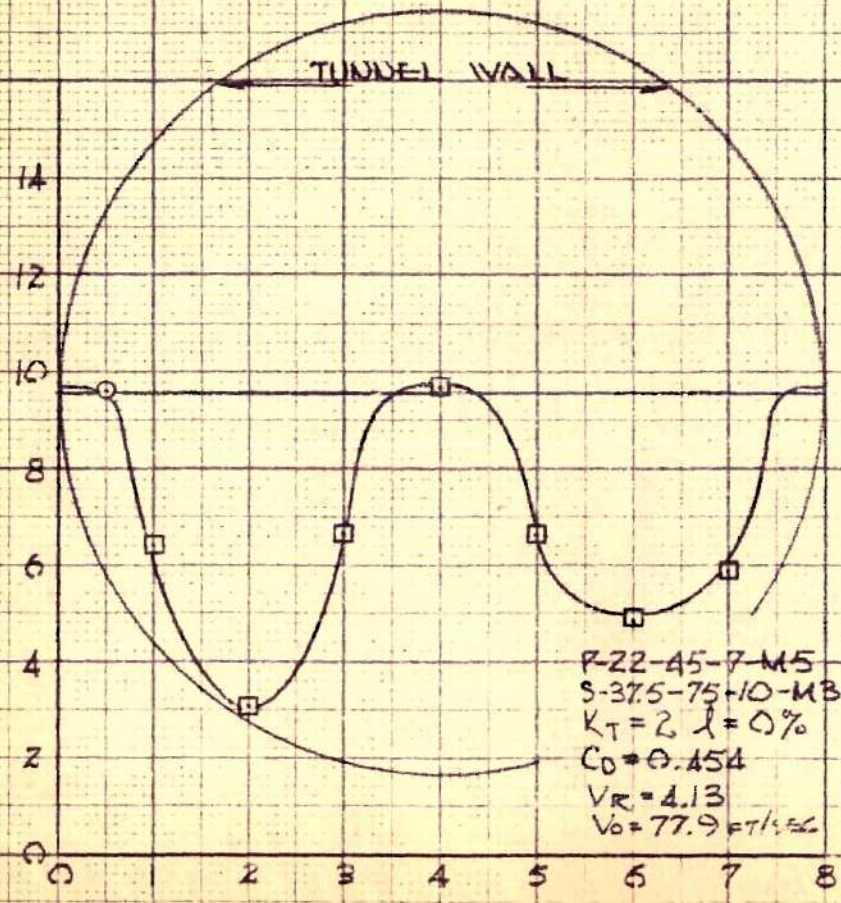

TUNNEL STATION, FORE & AFT SECTIONS

FIG. 65

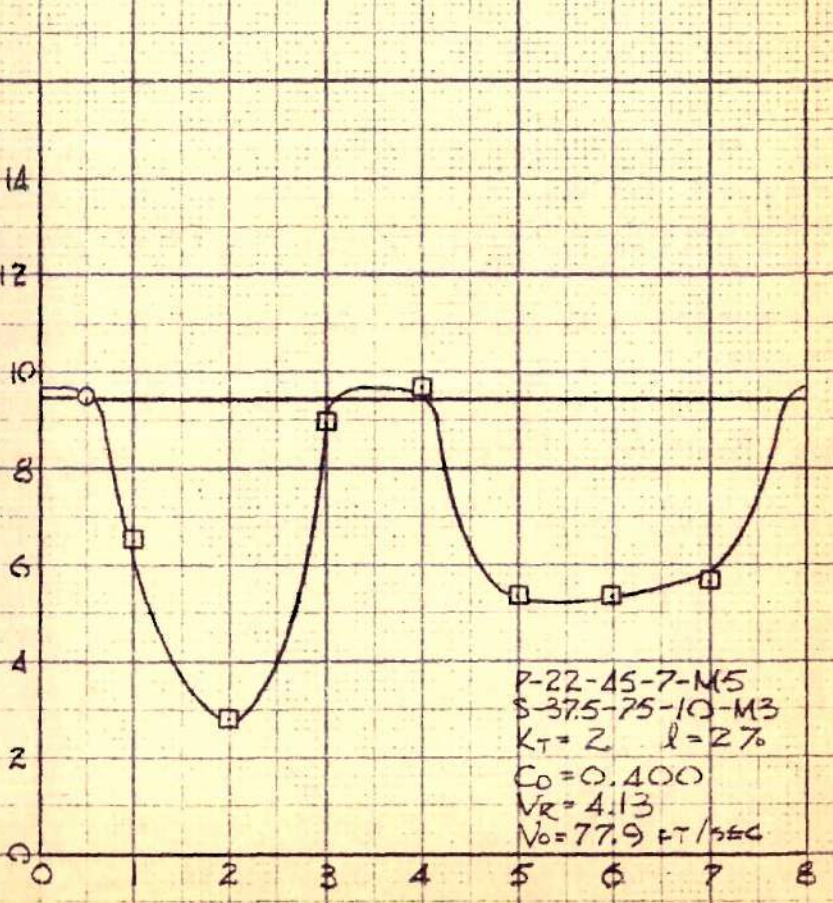

FIG. 66

TOTAL HEAD PRESSURES

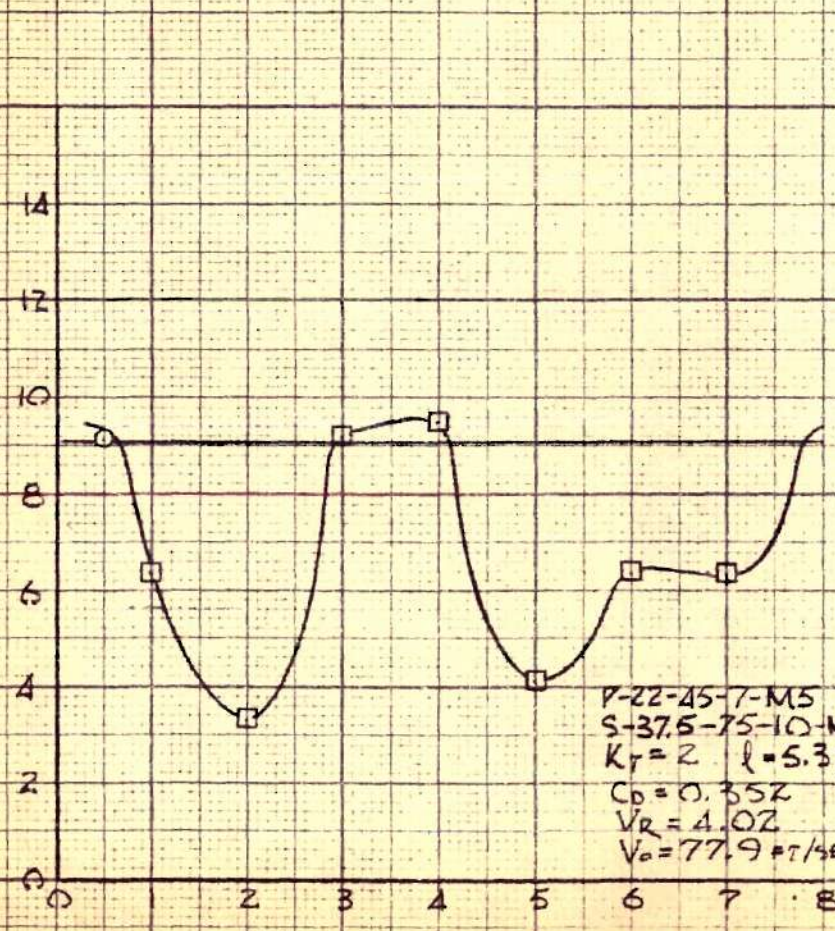

TUNNEL STATION, FORE & AFT SECTIONS

FIG. 67

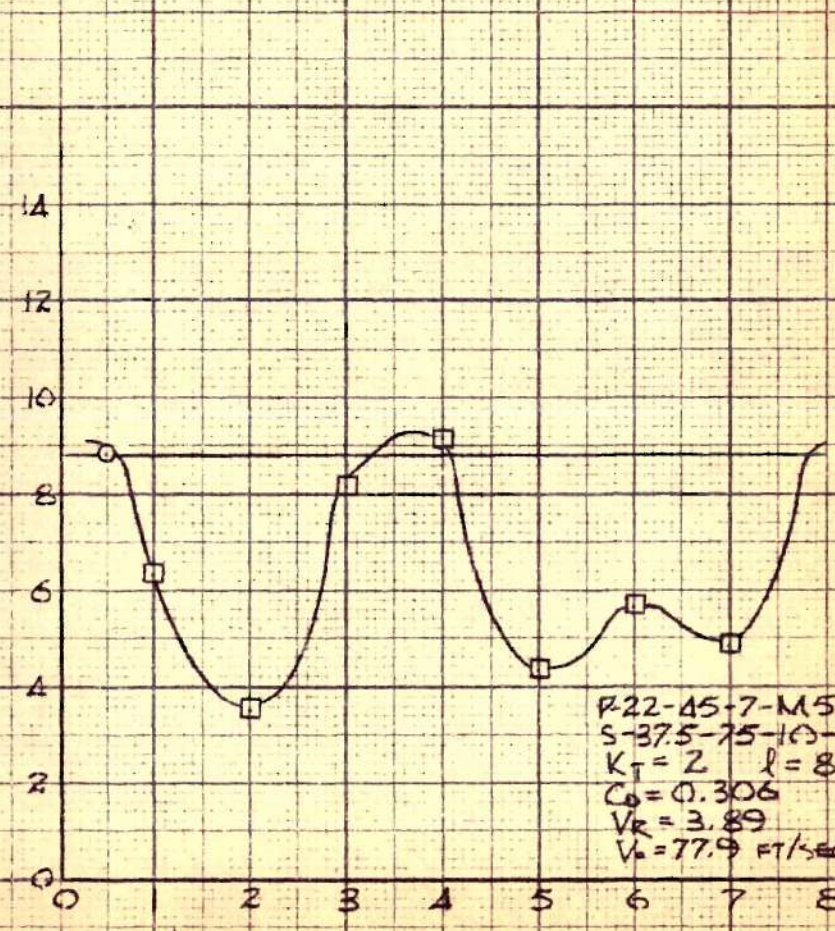

FIG. 68

TOTAL HEAD PRESSURES

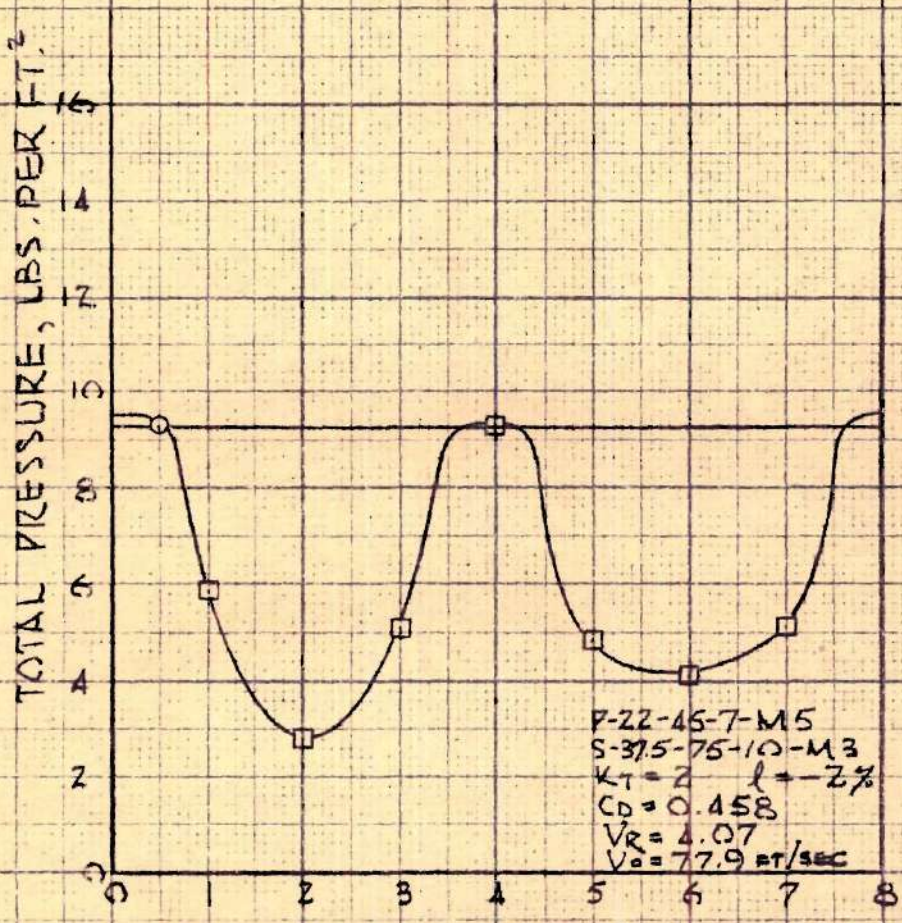

TUNNEL STATION, FORE & AFT SECTIONS

FIG. 69